TWO PHASE PIPE FLOWS IN FUEL TANK REFUELING

by

Deniz BOYACI

B.S., Mechanical Engineering, Istanbul Technical University, 2007

Submitted to the Institute for Graduate Studies in
Science and Engineering in partial fulfillment of
the requirements for the degree of
Master of Science

Graduate Program in Mechanical Engineering
Boğaziçi University
2009

ACKNOWLEDGEMENTS

I would like to express my sincere gratitude to Assoc. Prof. Hasan Bedir for his patience, support and knowledge throughout this research conducted in this study. Without his guidance and encourangement this thesis will not come to an end.

Comments and suggestions made by the committiee members Prof. Ahmet Erhan Aksoylu, Assoc. Prof. Kunt Atalık are greatly appreciated. Special thanks to Assist. Prof. Hakan Ertürk for providing me his laboratory and computer.

I am also grateful to Ford-Otosan for their financial support for this project. Special thanks goes for Bülent Yegenoglu for his technical contribution and partnership.

I am deeply indebt to my friends who helped me during my thesis at the Mechanical Engineering Department of Bogazici University.

Last but not least, i would like to acknowledge my family and my best friend. To my mother and father, thank you for giving me life for the first place, for your love, support and understanding through all of my life. For my brother and his wife, i am very grateful to both of you helping me all the time and making my life easier. Finally, special thanks to my best friend Burçin for her continued support and friendship even in my depressed mood during my thesis preparation.

ABSTRACT

TWO PHASE PIPE FLOWS IN FUEL TANK REFUELING

Automotive fuel tank refueling is modelled with FLUENT software which is a commercial CFD solver in fluid mechanics. Fuel tank components are modeled geometrically such as the fill pipe, vent pipe and tank dome. Additionally, the other important components are modelled as boundary conditions such as fuel nozzle and rollover valve. In FLUENT continuity, momentum, volume fraction and turbulence equations are solved. Gasoline and air are used as materials in the flow. The effect of pressure inside the tank dome to the flow, gasoline inlet velocity and fuel ratio in the fuel nozzle, different fuel nozzle angles, different fill pipe geometries are discussed in this thesis. In some cases premature nozzle shut-off is observed. It is seen that higher volume flow rate in the nozzle increased the tank dome pressure during the refueling process. Pressure value set at the top of the tank as a rollover valve led to more air to flow out through the top of the tank when it had lower values. It is also observed that when gasoline droplet sealed the vent pipe entrance due to the rising fuel level or the back pressure developed in the tank, pressure reached to a peak value in the tank.

ÖZET

BENZİN DEPOSUNUN DOLUMUNDAKİ ÇİFT FAZLI BORU AKIŞLARI

Bu çalışmada otomobil benzin deposunun dolumu bir akışkanlar mekaniği programı olan FLUENT ticari paket programı marifetiyle modellenmiştir. Benzin deposunu oluşturan bileşenlerden dolum borusu, çıkış borusu, benzin tankı geometrik olarak modellenmiş ve bunlara ek olarak benzin pompası ve rollover valfi de sınır şartı olarak modellenmiştir. FLUENT'te süreklilik, momentum, hacim oranı ve türbülans denklemleri çözülmüştür. Akışta malzeme olarak hava ve benzin kullanılmıştır. Benzin deposundaki basıncın akışa etkisi, benzin pompasından yollanan benzinin hızı ve benzin-hava oranı, farklı benzin pompası kullanım açıları, farklı dolum borusu geometrileri incelenmiştir. Bazı durumlarda da pompanın erkenden akışı durdurması durumu gözlenmiştir. Benzin pompasından çıkan benzinin hacimsel debisi arttıkça benzin tankı içindeki basınçların arttığı gözlenmiştir. Rollover valfi görevi gören benzin deposunun üzerindeki sınır basınç şartı düşük olduğunda daha fazla havanın o bölgeden çıktığı görülmüştür. Benzin tanecikleri tank içindeki yüksek basınçlardan ya da depo içindeki benzin yüksekliğinden dolayı vent borusu girişini kapattığında, depo içinde yüksek basınçlar oluştuğu gözlenmiştir.

TABLE OF CONTENTS

LIST OF FIGURES

LIST OF TABLES

LIST OF SYMBOLS / ABBREVIATIONS

C	Constant
$F_{\alpha q}$	Source term
F_j	Body force
G_k	Production of kinetic energy
k	Turbulent kinetic energy
$\hat{n}$	Surface normal
P	Pressure
R	Radius
t	Time
U	Average velocity
u	Free stream velocity
$\hat{\nu}$	Kinematic viscosity
α_i	Volume Fraction of the i^{th} fluid
β_ε	Effective inverse Prandtl number for the ε equation
β_k	Effective inverse Prandtl number for the k equation
ε	Turbulent dissipation rate
κ	Curvature
ς	Surface tension coefficient
ρ	Density
ϕ	Constant
μ	Dynamic viscosity
μ_{eff}	Effective dynamic viscosity
μ_t	Turbulent viscosity
η	Effectiveness factor

η_0 Constant μ_{eff}

CSF Continuum Surface Force

$RANS$ Reynolds Averaged Navier-Stokes ς

RNG Renormalization Group

VOF Volume of Fluid

1. INTRODUCTION

Fuel tank and its components are seen in Figure 1-1. Fuel tank system consists of fuel nozzle which starts and stops the flow, filler pipe, vent tube, fuel tank, rollover valve which delivers the fuel-air mixture to the carbon canister and fuel pump that delivers the fuel into the engine.

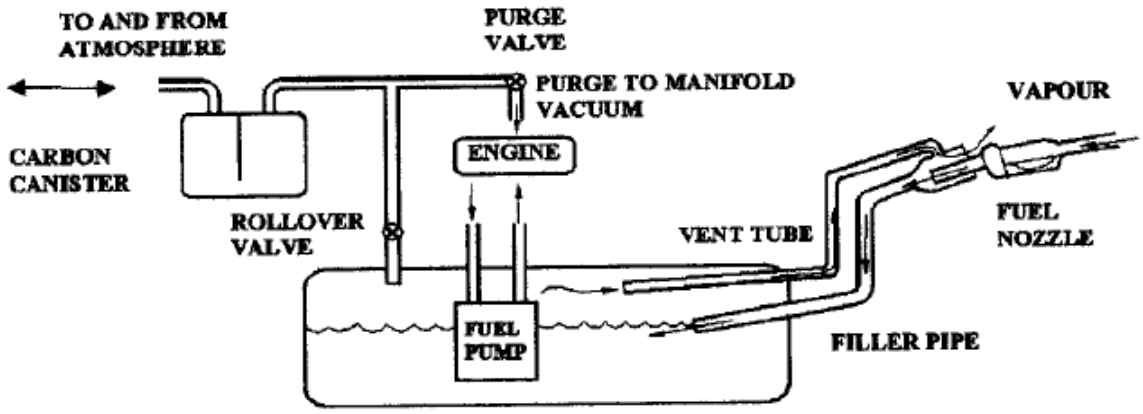

Figure 1-1. Fuel tank and its components [10]

In the dispensing nozzle, the fuel has air mixed with it as a consequence of the overfill prevention, automatic shut-off shown in figure 1-2. The nozzle uses several hidden components to shut itself off when the tank is full. There is a small hole near the end of the nozzle that becomes blocked by the liquid fuel as soon as the fill level reaches that hole. Blocking this hole with fuel is what shuts off the valve. There is actually a thin tube inside the main fuel delivery hose that operates this valve system. That tube runs from the hole in the nozzle to a vacuum pump inside the fuel-pumping unit. While the pump is dispensing fuel into a partially filled tank, air flows easily into the nozzle's hole and the pressure inside the thin tube remains close to atmospheric pressure. But when the level of fuel rises high enough, it essentially blocks the hole and the pressure inside the thin tube drops. This pressure drop is what triggers the valve and stops the fuel flow.

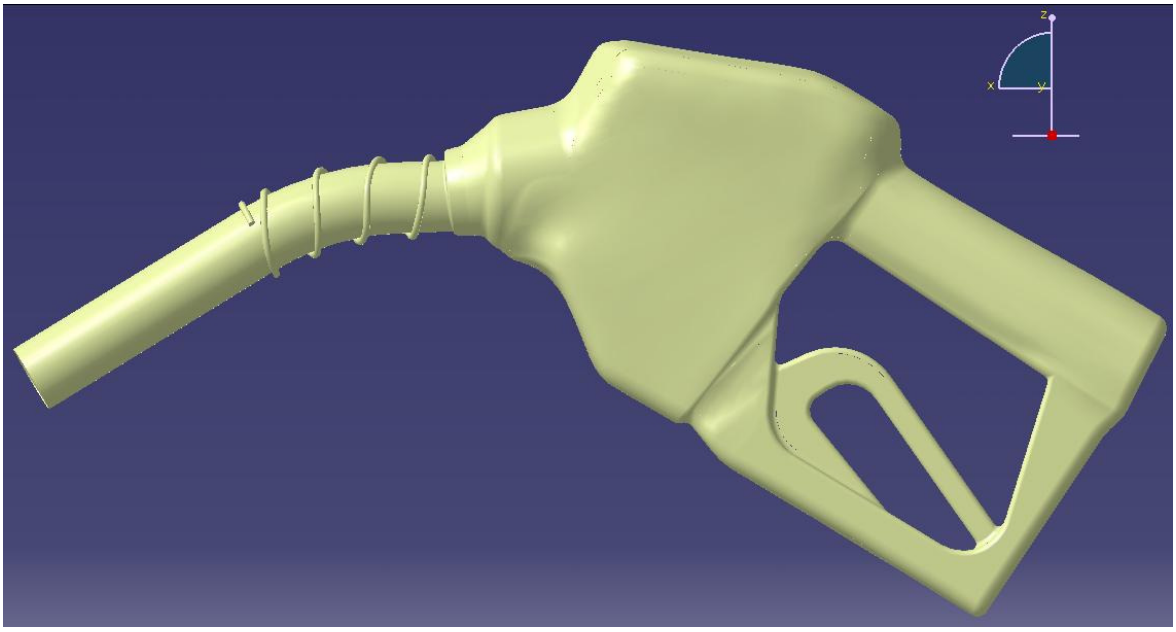

Figure 1-2. Catlow dispensing nozzle

Depending (a) upon the particular filler pipe design, (b) the amount of fuel already in the fuel tank and (c) the design of the vapor release system, the fuel may flow as a flooded conduit or it may flow as a non-flooded conduit with an open surface. Also, subject to the specification of the particular fuel being handled (vapor pressure, etc.) and its temperature (both absolute and relative to the ambient temperature of the environment at the time of filling), a portion of the fuel may also change phase and evaporate [1].

The first study about the auotomotive fuel filler pipe was done by Stoneman [1], and it had a leading role for the other people working on this issue. The output of this project was a computational fluid dynamic model of the losses in the filler pipe and the typical pressure versus time graph during tank filling was first represented in this study.

Another research was done by Thompson [2], which is focused on mostly the phase III during which nozzle shut-off occurs, characterized by a pressure rise of 0.25-0.50 m (of water) over approximately 1-2 seconds of time. In this project, details of various unit problems that were identified as relevant sub processes of the entire sequence of events leading to nozzle shut-off. This was done by a numerical code so called CRAFT. The sub processes examined in that study were speed-of-sound in a two-phase equilibrated mixture, flow field near tank dome prior to vent pipe sealing, compression of trapped air/vapor, wave propagation in a uniform cylinder with piston, effect of contraction, wave

propagation in a contracting cylinder with piston. This study was only give an insight into the complexities of unsteady wave processes that occur during fuel pumping, and frequently lead to premature fuel nozzle shut-off and does not represent the whole processes together.

The first comprehensive study was done by Mastroianni [3] in his master thesis project, which is an experimental investigation performed to determine how vent tube diameter, fuel Reid Vapor Pressure, and fill rate affect the occurrence of premature shut-off, spit-back and spill-back.

Banerjee and Isaac [4] investigated the back pressure builds up in the filler pipe and the effects of vent design on the air entrainment. And sum up that to reduce the backpressure, the vent pipe diameter can be increased. Also fuel tanks with larger length and width would reduce the rate of rise of the liquid level inside the tank, which would also reduce the pressure build up. Another interesting result was the fuel tank dimensions affect the pressure transients. It was discussed that to delay the pressure spike in the tank dome, the fuel tank should have larger length and width compared to height. This would delay the liquid surface to reach the opening to the vent pipe. Also, the vent pipe opening should be as close to the surface as possible.

After one year, Banerjee and Isaac [6] again investigated the two-phase filler pipe flow this time. They did experiments and computational fluid dynamics simulations. This study focused on how the air entrainment is changed with the filler pipe geometry and the fuel flow rate. They sum up that the rate of air entrainment indicates an increasing trend with increasing liquid flow rate, but it is not monotonic. Also they found that out-of-plane bends introduce strong swirl in the flow which enhances air entrainment.

In 2002, Allan G. Zhao [10], investigated a hybrid model, which is divided into a number of subsystems each with its own specific model. The interesting part of this study is that model considers the effect of tank expansion and that of the variation of the tank shape. Zhao concluded that the tank expansion during the period of fuel filling does not significantly affect the flow field. The tank expansion accounts for less than 4% of tank dome pressure difference. Additionally, the effect of tank shape on the pressure of gas phase inside the tank and on the multiphase flow movement was significant if the shape of

the tanks varied greatly. The key factor in the difference is the interface area between the liquid and gas phases.

Finally, a report about the simulation of automotive fuel tank filler pipe flows [8] stated that the total mass loss from the evaporation, phase change, or foam creation is only 0.15% up to 0.22%. It is also stated that the fuel evaporation during refueling is anything but unimportant and should be covered by a computational approach. In principle, it is possible to combine the volume-of-fluid approach with an evaporation algorithm. However, doing so requires at least the determination of a couple of more or less purely phenomenological parameters. Furthermore, the convergence behavior of the numerical approach is affected strongly, too. To conclude, this report indicated that computational fluid dynamics is not able to predict absolutely the refueling ability of an automotive fuel system, and only relative statements can be derived.

In Figure 1-3, a pressure time history is plotted, at first the pressure increases to a maximum (typically of order 1 kPa up to 4 kPa) and is then reduced as some vapor vents back to the nozzle and to the atmosphere through the valve and carbon canister. The tank pressure becomes mainly constant during the filling stage(phase II). As the fuel level rises to the vent, the tank pressure increases again (phase III). Finally, the increased tank pressure causes the fuel to accumulate within the filler pipe and a sensing mechanism at the fuel level shuts off the fuel flow. This shut-off mechanism or trip mechanism leads also to a certain amount of air entrainment even within the fuel nozzle due to its inherent Venturi-effect. It is possible that the shut-off mechanism of the fuel nozzle is triggered at an early stage of refueling due to flow reversal of flow jet reflection. Such a behavior is called premature shut-off and usually not acceptable for consumers [7].

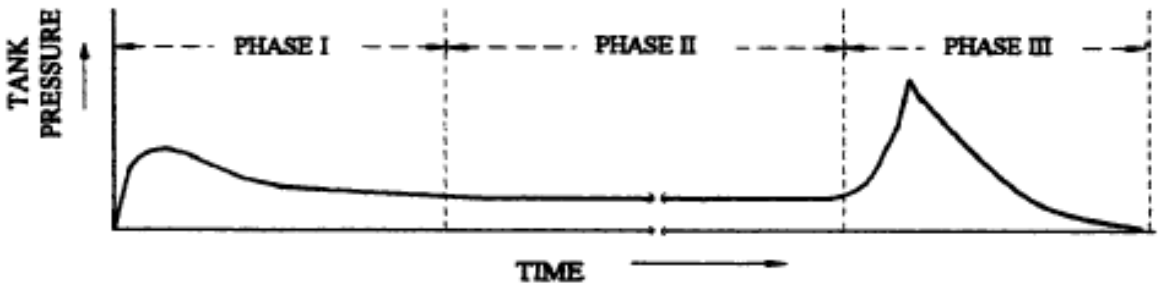

Figure 1-3. Pressure history during typical refueling event [10]

Because of the many parameters affecting it, the refueling process is very complicated. The main terms affecting the tank filling are premature nozzle shut-off, spill back, choking, tank and pipes geometry, propagations of waves, and fuel flow rates.

Premature shut-off which occurs in the nozzle due to the entrainment of fuel in the vent pipe creating compression waves ahead of it [4], also due to the pressure spike which occurs before the tank is full. Poor design of the filler pipe, which results in a misalignment of the fuel-dispensing nozzle relative to the filler pipe, any geometrical feature that tends to restrict the flow in the filler pipe (factors that would affect the restriction in the filler pipe are the radii of the bends and any reduction in area throughout the path in the filler pipe) can lead to premature nozzle shut-off [3].

Another factor is the spill back phenomena which is an undesired situation that affects the refueling process. It is some kind of outgoing fuel from the filling pipe which will be explained in more detail later.

Geometry of the tank system has a great influence on the refueling process. According to Mastroianni [3], when the vent area around the fuel nozzle reduces, it causes the fuel-dispensing nozzle to shut-off prematurely. The behavior of the flow changes according to the design of the vent pipe section. Additionally, the size of the tank dome and other fuel tank system particles affect the filling process.

Liquid fuel volume flow rate, fuel volatility and rollover valve diameter are also important parameters that affect refueling process. However, changes in the vent tube diameter, mass transfer coefficient, void fraction, and filler tube diameter causes any alteration in refueling[6].

Wave propagation, choking and fuel flow rate effects are also other parameters that will be discussed more detailed later.

1.1. Premature Nozzle Shut-off

Banerjee [3] made simulations to understand the premature shut-off, in which a vent pipe is attached on the top surface of the fuel tank. The pressure transients were

monitored at the inlet of the vent pipe for the last two seconds before the tank was completely filled with fuel. A pressure spike was observed as the liquid surface almost closed the pipe mouth. Initially the pressure was almost constant but as the liquid surface closed the vent mouth, the pressure decreased to a large negative value then subsequently increased to a large positive value. These large oscillations occured a few times. Subsequently, the pressure started increasing steadily. The behavior of the pressure transients is dependent on the dimensions of the fuel tank and the position of the vent pipe. In their model the vent pipe was located at the top surface of the fuel tank. But in other cases it may be projecting inside the tank. In that case the pressure spike would occur before the tank is full leading to premature nozzle shut-off.

The chain of events that lead to nozzle shut-off can be briefly summarized as:

i) As fuel is pumped, vapor/air is vented which forms a boundary layer on the vent pipe walls.

ii) Vapor path to vent pipe gets restricted, and, then sealed by rising fuel level in tank.

iii) Continued pumping of fuel leads to isentropic compression of vapor trapped in the tank dome.

iv) As trapped vapor is compressed, the subsequent pressure rise forces fuel and air/vapor into the vent pipe.

v) The steadily increasing driving pressure accelerates the liquid column inside the pipe which acts in a manner similar to an accelerating piston in an open cylinder (e.g. the interface is essentially impermeable).

vi) Compression waves ahead of the liquid in the gaseous part of the vent column and the vapor venting become unsteady.

vii) The presence of the boundary layer on the pipe wall acts to reduce the available flow area by an amount of equivalent to the boundary layer displacement thickness and the compression waves travel in an essentially contracting pipe flow.

viii) The contraction forces the compression waves to coalesce leading to a pressure rise at the vent pipe exit (unsteady, subsonic flow has the same characteristics as steady, supersonic flow) [2].

In addition choking in the rollover valve has the effect of increasing the maximum Phase I peak pressure that can lead to premature shut-off. Choking in the rollover valve, however, does not affect the tank pressure during Phase II of filling or the normal shut-off time.

1.2. Spill Back

Certain situations occur where the filling process is considered to be unsuccessful. Spill back is one such situation. Spill back can be broken up into two categories: spit-back and well back.

i) Spit Back: Spit back occurs when small droplets of fuel exit the filler tube entrance with the escaping gases [5].

ii) Well Back: Well back occurs when slugs of liquid escape the filler tube entrance due to the back-pressure developed in the vapor space of the fuel tank [3].

A malfunctioning fuel dispensing nozzle or a poor design of the filler pipe could cause fuel to spill or spit out of the filler neck. A fuel dispensing nozzle that does not shut-off automatically when the liquid level in the filler pipe has been sensed will cause spill-back. Also, if the fuel dispensing nozzle is mal-functioning such the response time taken to halt the liquid flow is too long, spill-back of fuel will occur. Additionally, there could be cases, at petrol stations, where the pumps used to dispense fuel from the underground storage tank to the vehicle are adjusted to a very high rate of flow. If the flow rate is too great the liquid level in the filler pipe can rise so fast that the delays between the sensing and actual shut-off causes overflow of fuel-spill-back. Spit-back may be caused by droplets of fuel becoming entrained in the air/vapor which enters the atmosphere from the filler tube. This is more evident during cases of generation of high fuel vapors [9].

Some other factors that affect vapor emission are the geometry of the nozzle-filler pipe fit, the characteristic of automatic nozzle shut-off, operating environment such as temperature and humidity, fuel dispense rates.

1.3. Geometric Effects

In a refueling process some air is entrained in the top portion of the filler neck, but a net outflow of air from the filler neck mouth occurs. This is due to the reverse flow of air from the tank. The displaced volume of air due to the rising liquid level can be vented off to the atmosphere either through the vent pipe or the filler neck mouth. The narrow diameter of the vent pipe offers a large resistance to the airflow. The mass outflow through it is less than the entire displaced volume in the tank because of this resistance. Therefore part of the air travels back through the inside air core of the filler pipe and flows out through the filler neck mouth.

The backpressure and vent design in the fuel tank has a large effect on the air entrainment. Hence to reduce backpressure, the vent pipe diameter can be increased. Also fuel tanks with larger length and width would reduce the rate of rise of the liquid level inside the tank, which would also reduce the pressure build up.

The fuel tank dimension also affects the pressure transients. To delay pressure spike, the fuel tank should have larger length and width compared to height. This would delay the liquid surface to reach the opening to the vent pipe. Also, the vent pipe opening should be as close to the surface as possible [3].

1.4. Wave Propagation

According to computational study done by Sinha [2], simulations indicate that air/vapor is compressed by rising fuel as the fuel rises in the tank and seals the entrance of vent pipe. Pressure increases and it forces fuel into the vent pipe and starts a standing wave in the fill pipe. Entrained fuel is accelerated up the vent pipe, leading to compression waves ahead of it. These waves coalesce to produce a pressure rise at the vent pipe exit. Shut off occurs when the standing wave impinges on the fuel dispenser sensing port.

Wave propagation studies clearly demonstrate that the details of the shut-off are strongly influenced by the composition of the fuel vapor and the level of liquid present. Also, the higher contractions provide an ability to sustain higher degrees of pressurization.

1.5. Flow Rates

In their experiments, Banerjee tested different flow rates were applied through a bended geometry [5]. Except for low flow rates at the filler pipe entrance, the flow is turbulent. The flow transitions to high turbulence at the bends because of the impact and break up of the liquid stream. The flow also acquires a swirl component due to asymmetric flow impacting the wall at the bends. At low flow rates there are large voids where the liquid free surfaces are clearly visible. At higher flow rates these voids becomes smaller and their boundaries become blurred. Also it is important to say that, the void fraction reduced with increase in flow rate as the liquid started filling more of the cross section.

In this project, fuel tank system was not completely modeled. The carbon canister part of the tank system was not modeled and the rollover valve was modeled as a pressure outlet boundary above the tank.

In this project flow from the nozzle is modeled with both 100 percent of fuel in most of the cases and 80 percent of fuel in some cases.

2. NUMERICAL PROCEDURE

2.1. Geometry and Grid generation

In this CFD study, GAMBIT was used as the pre-processor to generate complex three dimensional geometries and FLUENT was used as the processor to solve the problem. ENSIGHT and Tecplot programs were used as post-processing tools. GAMBIT is chosen because it is the recommended mesh generator for the FLUENT package software. Furthermore, it can be also run interactively to generate structured as well as unstructured grids and the resultant grid can be interactively viewed and optimized for the geometry and the flow problem in consideration.

For complex geometries, the most flexible type of grid is one which can fit an arbitrary solution domain boundary. In principle, such grids could be used with any discretization scheme, but they are best adapted to the finite volume approaches. The elements or control volumes may have any shape; nor is there a restriction on the number of neighbor elements or nodes. In practice, grids made of triangles or quadrilaterals in 2D, and tetrahedral or hexahedral in 3D are most often used [12]. This kind of flexibility gives the user to avoid highly skewed grid elements. The more highly skewed cells in a numerical model leads the more run times to convergence.

Because it is an easy way of meshing circular type geometries, Cooper tool [12] was used for meshing the pipe volumes in GAMBIT. The figure below shows the meshing scheme used in Cooper tool. When applying Cooper tool, each volume element is considered to be consisting of one or more logical cylinders, which are composed of two end caps and a barrel. Faces that comprise of the caps are called source faces, and the faces, which comprise of the barrel, are called non-source faces. In Figure 2.2 below, part (a) is the actual volume and part (b) is the logical cylinder. Hence while meshing using the Cooper tool, the source faces on one side of the geometry is meshed. The meshed source faces are then extruded along the non-source face and imprinted onto the other source face. The source face mesh can either be quadrilateral or triangular.

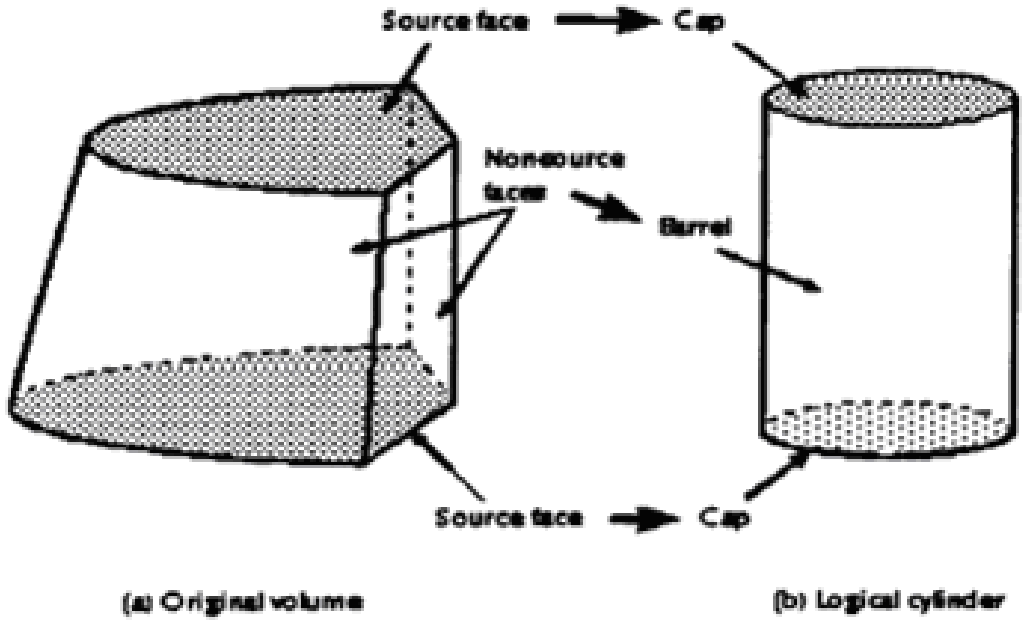

Figure 2-1. Scheme for cooper tool

In our geometry, the volume was divided into seven parts, because of the complexity. By the help of this, tank dome, fill pipe, vent pipe, and pressure outlet were meshed separately. Fill pipe and vent pipe was separated into three and meshed with Cooper tool because of the simplicity. The tank dome was divided into four parts because of the need of more accuracy near the upper part of the tank. There is a small hole in the middle of the upper part of the tank. It was meshed with Cooper tool. The zone near which the nozzle places in was meshed with tetrahedral elements because of the complexity of the geometry, however smaller grid size was used to obtain more accuracy. Hence non-uniform grids were used for all of the cases that were simulated. Quadrilateral and tetra/hybrid type of meshes were used in some part of the tank dome. A higher grid density was used in critical regions like fill pipe and vent pipe. As an example, out of a total number of 122000 grid points used in the whole model 80000 grid points were used for the fill pipe and the vent pipe. The geometry and a sample grid is shown in the figure below.

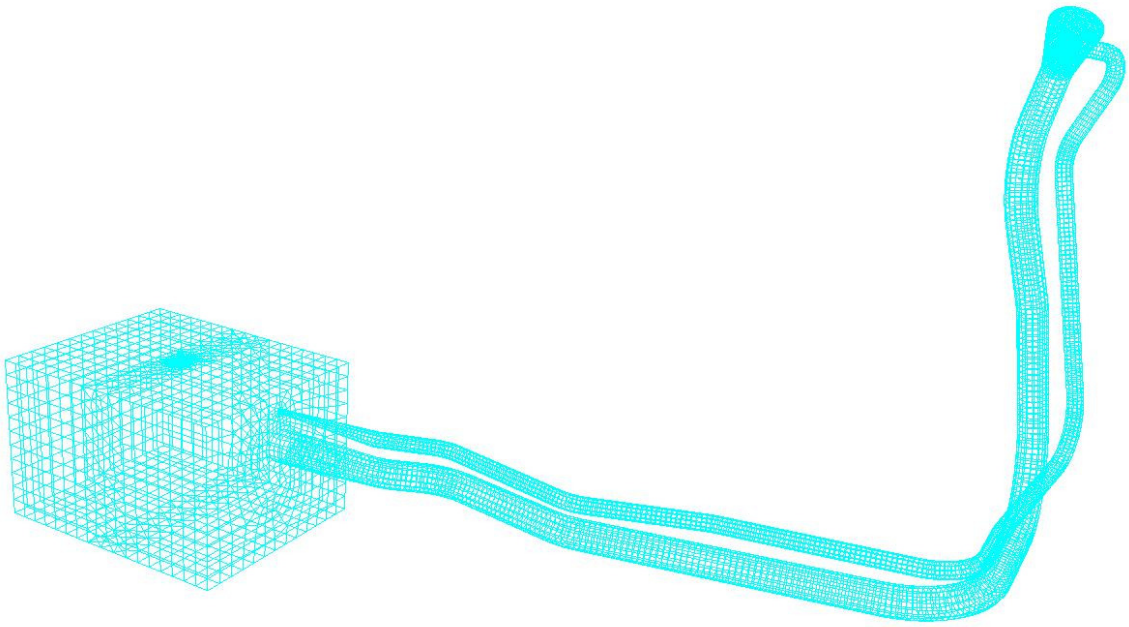

Figure 2-2. Mesh of the model

2.2. Multiphase Model

Flows with free surfaces are an especially difficult class of flows with moving boundaries. The position of the boundary is known only at the initial time; its location at later times has to be determined as part of the solution [13]. One of the most commonly used methods is the Fixed Grid Eulerian Method. This method is typically used for two or more fluids when the flow is relative to a fixed and non-deformable numerical grid. This property is especially advantageous for complex fluid configurations where time-to-time grid reconstruction may be difficult [12].

There are several numerical schemes for this method. One of them is Volume of Fluid (VOF) method which is a volume tracking method. It was developed by Nichols and Hirt [12]. VOF features an interface reconstruction with increased resolution combined with a modified interface advection. By using different techniques for solving a scalar marker transport equation, numerical diffusion and interface smearing are controlled.

The multiphase models available in FLUENT are VOF, Eulerian Model and Mixture Model. In FLUENT, VOF model tracks the interface between the phases by

solving a continuity equation for the volume fraction of the phases. For the q^{th} phase, this equation has the following form:

$$\frac{1}{\rho_q}\left[\frac{\partial}{\partial t}\left(\alpha_q.\rho_q\right)+\nabla.\left(\alpha_q.\rho_q.\vec{v_q}\right)\right]=S_{\alpha_q} \tag{2.1}$$

The volume fraction α_q can have the following values:

$\alpha_q = 0$ if the cell is empty of the q^{th} fluid.

$\alpha_q = 1$ if the cell is full of the q^{th} fluid

$0 < \alpha_q < 1$ if the cell is partially filled with the q^{th} fluid

For a two phase system, the volume fraction distribution is illustrated in Figure below.

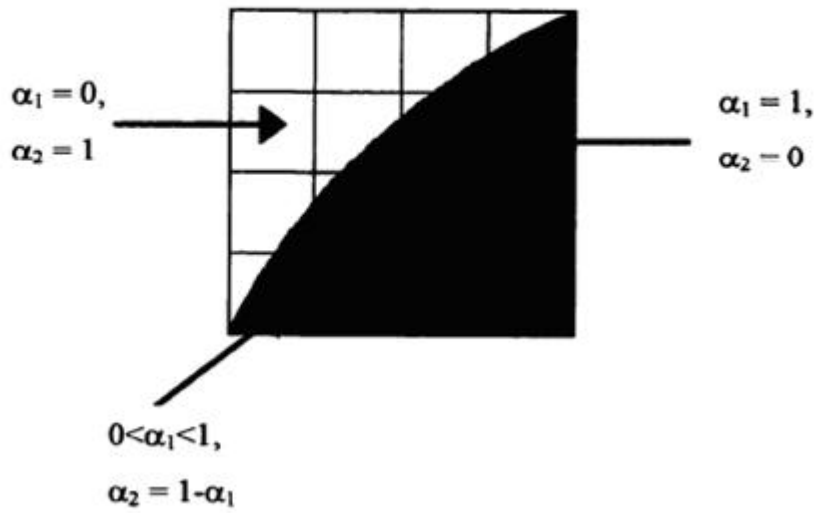

Figure 2-3. Volume fraction of q^{th} fluid for a two phase system in a computational domain

The VOF model in Fluent is incapable of handling inter-phase mass transfer. Therefore, the source term S_{α_q} in the equation above is zero. The volume fraction of the primary phase is not solved as it can be determined from the constraint:

$$\sum_{q=1}^{n}\alpha_q = 1 \tag{2.2}$$

A single momentum equation is solved throughout the computational domain and the resulting velocity is shared among the phases. The momentum equation is solved using the properties ρ and μ, which are calculated from the volume fractions of all phases. The momentum equation has the form:

$$\frac{\partial}{\partial t}\left(\rho\vec{v}\right)+\nabla.\left(\rho\vec{v}\vec{v}\right)=-\nabla p+\nabla.\left[\mu\left(\nabla\vec{v}+\nabla\vec{v}^{T}\right)\right]+\rho\vec{g}+\vec{F} \tag{2.3}$$

The properties appearing in the momentum equation are determined from the component phases in each control volume. In a two phase system, the volume fraction of the secondary phase can be used to determine the density as:

$$\rho=\alpha_2\rho_2+\left(1-\alpha_2\right)\rho_1 \tag{2.4}$$

All the other properties, like viscosity etc. are determined in a similar fashion. In case of turbulent flow a single set of transport equations is solved and the variable k and ε are shared by the phases throughout the phases.

In Equation 2.3, the source term F represents to body force due surface tension. Surface tension arises as a result of unbalanced intermolecular attractive forces at the surface. In FLUENT surface tension is modeled by using the continuum surface force (CSF) model by Brackbill et al. [12]. With this model, the addition of surface tension to the VOF calculation results in the source term F in the momentum equation. To understand the origin the source term, consider the special case where surface tension is constant along the surface, and only the forces along the normal to the surface are considered. It can be shown that the pressure drop across the surface depends upon the surface tension coefficient, ς and the surface curvature as measured by the two radii in the orthogonal directions, R_1 and R_2:

$$p_2-p_1=\varsigma\left(\frac{1}{R_1}+\frac{1}{R_2}\right) \tag{2.5}$$

where, p_1 and p_2 are the pressures in the two fluids on either side of the interface.

In FLUENT, the surface formulation using CSF model can be used only for two phase system. The surface curvature is computed from the local gradients in the surface normal at the interface. If the surface normal $\vec{n}$, defined as the gradient in α_2, the volume fraction of the secondary phase, then,

$$\vec{n} = \nabla \alpha_2 \tag{2.6}$$

The curvature, κ is defined in terms of the divergence of the unit normal, $\hat{n}$,

$$\kappa = \nabla . \hat{n} = \frac{1}{|n|}\left[\left(\frac{\vec{n}}{|n|}.\nabla\right)|n| - \left(\nabla . \vec{n}\right)\right] \tag{2.7}$$

where,

$$\hat{n} = \frac{\vec{n}}{|n|} \tag{2.8}$$

Surface tension can be written in terms of pressure jump across the interface. The force at the surface can be expressed as a volume force using the divergence theorem. It is this volume force that is the source term which is added to the momentum equation. It has the form:

$$F_{vol} = \sigma_{ij} \frac{\rho \kappa_i \nabla_{\alpha_i}}{\frac{1}{2}\left(\rho_i + \rho_j\right)} 2\varsigma\kappa(x)\alpha_2 \nabla \alpha_2 \tag{2.9}$$

The source term is added only to one side of the interface, i.e. the side on which volume fraction calculations are done.

As control volume approach is used in FLUENT, the convection and diffusion fluxes through the control volume faces are computed and balanced with the source terms within the control volume itself. There are four methods to determine the surface fluxes in VOF method: Geometric Reconstruction, Donor-Acceptor, Euler Explicit and Implicit methods. For the present work, geometric reconstruction scheme was used because it gives the sharpest interface between two phases. The figure below shows the actual interface shape and the interface represented by geometric reconstruction method. Geometric reconstruction method can only be used for a time dependent solution.

The geometric reconstruction scheme represents the interface between the fluids using a piecewise-linear approach. Geometric reconstruction method has been extended to unstructured grid from the work of Youngs[12]. It assumes that the interface between the two fluids have a linear slope within each cell and uses this linear shape for the calculation of the advection of fluid through the cell faces.

Geometric reconstruction scheme works in three steps. The first step in this scheme is calculating the position of the linear interface relative to the center of each partially filled cell, based on the information about the volume fraction and its derivatives in a cell. The second step is calculating the advection amount of the fluid through each face using the computed linear interface representation and information about the normal and tangential velocity distribution on the face. The third step is calculating the volume fraction in each cell using the balance of fluxes calculated during the previous time step.

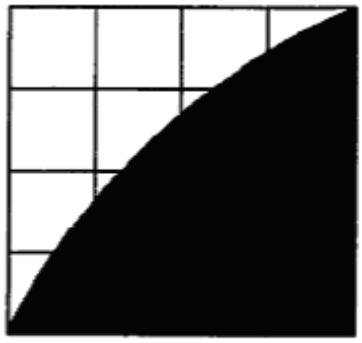

(a) Actual interface

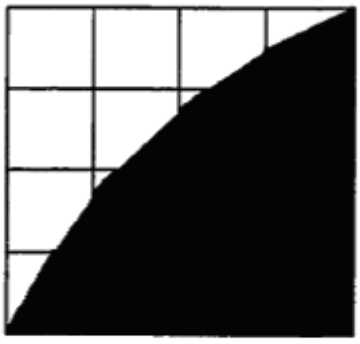

(b) Interface represented by geometric reconstruction scheme

Figure 2-4. Comparison of interface representation from geometric reconstruction scheme to the actual interface [12]

2.3. RNG k-ε Model

In turbulence modeling, a time-averaged Navier-Stokes equation is solved in such a way that small scale turbulent fluctuations do not have to be simulated. The equations thus obtained are called Reynolds Averaged Navier-Stokes (RANS) equations. Equation below is the time averaged RANS equation. In the RANS equation, the quantity $-\rho\overline{u_i' u_j'}$ is called Reynolds Stress Tensor, which is required to be modeled to obtain closure. A detailed discussion of the various turbulence modeling schemes is given by Wilcox [12].

$$\frac{\partial}{\partial t}\rho U_j + \frac{\partial}{\partial x_i}\rho U_i U_j = -\frac{\partial P}{\partial x_j} + \frac{\partial}{\partial x_i}\mu\left(\frac{\partial U_i}{\partial x_j} + \frac{\partial U_j}{\partial x_i}\right) + \frac{\partial}{\partial x_i}\left(-\rho\overline{u_i' u_j'}\right) + \rho g_j + F_j \qquad (2.10)$$

There is no single turbulence modeling scheme which is universally accepted as being superior to the rest. The choice of turbulence model is governed by considerations such as the physics encompassing the problem, established practice of a particular class of fluid flow, level of accuracy required, available computational resources and amount of time available for the simulation. FLUENT provides a number of turbulence models. Out of these, Renormalization Group Theory (RNG) $k-\varepsilon$ model by Yakhot and Orszag [12] was used in this study.

The Boussinesq approximation is used in standard and RNG $k-\varepsilon$ models. The advantage of this approach is the relative low computational cost associated with the computation of the turbulent viscosity, μ_t. The disadvantage of this approach is that it assumes μ_t to be an anisotropic scalar quantity, which is not strictly true.

For turbulence modelling, the RNG $k-\varepsilon$ model was derived using a rigorous statistical technique called the Renormalization Group Theory. It is similar in form to the standard $k-\varepsilon$ model, but includes the following refinements:

The RNG model has an additional term in the ε equation that significantly improves the accuracy for rapidly strained flows.

The effect of swirl on turbulence is included in the RNG model, enhancing accuracy for swirling flows.

The RNG theory provides an analytical formula for turbulent Prandtl numbers, while the standard $k-\varepsilon$ model uses only constants.

These features make the RNG model more suitable for a wider class of problems. The governing equations of RNG $k-\varepsilon$ models are:

2.3.1. Turbulent kinetic Energy

$$\frac{\partial}{\partial t}\rho k+\frac{\partial}{\partial x_i}\rho U_i k=\frac{\partial}{\partial x_i}\left(\beta_k \mu_{eff}\frac{\partial k}{\partial x_i}\right)-\rho\varepsilon+G_k \tag{2.11}$$

2.3.2. Dissipation Rate

$$\frac{\partial}{\partial t}\rho\varepsilon+\frac{\partial}{\partial x_i}\rho U_i\varepsilon=\frac{\partial}{\partial x_i}\left(\beta_\varepsilon \mu_{eff}\frac{\partial \varepsilon}{\partial x_i}\right)+C_{1\varepsilon}\frac{\varepsilon}{k}G_k-\left(C_{2\varepsilon}\rho\frac{\varepsilon^2}{k}+R\right) \tag{2.12}$$

2.3.3. Turbulent Viscosity

$$\mu_t=\rho C_\mu\frac{k^2}{\varepsilon} \tag{2.13}$$

G_k represents the production of kinetic energy, and μ_{eff} is the effective viscosity

$$\mu_{eff}=\mu+\mu_t \tag{2.14}$$

The quantities β_k and β_ε are the effective inverse Prandtl numbers for the k and ε equations, respectively.

The scale elimination procedure in RNG theory results in a differential equation for turbulent viscosity:

$$d\left(\frac{\rho^2 k}{\sqrt{\varepsilon\mu}}\right)=1.72\frac{\hat{\nu}}{\sqrt{\hat{\nu}^3-1+C_\nu}} \tag{2.15}$$

where,

$$\hat{\nu}=\frac{\mu_{eff}}{\mu}$$
$$C_\nu\cong 100 \tag{2.16}$$

Equation 2.16 is integrated to obtain an accurate description of how the effective turbulent transport equation properties vary with effective Reynolds number, allowing the model to handle better low-Reynolds number and near wall flows.

In the high Reynolds number limit, Equation 2.13 gives the turbulent viscosity equation, with constant $C_\mu = 0.0845$ derived from the RNG theory.

The inverse effective Prandtl numbers β_k and β_ε are computed using the following formula derived analytically by RNG theory:

$$\left|\frac{\beta - 1.3929}{\beta_0 - 1.3929}\right|^{0.6321} \left|\frac{\beta + 2.3929}{\beta_0 + 2.3929}\right|^{0.3679} = \frac{\mu_{mol}}{\mu_{eff}} \tag{2.17}$$

where $\beta_0 = 1$. In the high Reynolds limit $\left(\frac{\mu_{mol}}{\mu_{eff}} << 1\right)$, $\beta_k = \beta_\varepsilon \approx 1.393$

The main difference between the RNG $k-\varepsilon$ model and the standard $k-\varepsilon$ model is the additional term in the dissipation rate equation. The term R in the above equation is of the form:

$$R = \frac{C_\mu \rho \eta^3 \left(1 - \eta/\eta_0\right)}{1 + \phi \eta^3} \tag{2.18}$$

where η is defined as,

$$\eta = \frac{k\sqrt{\Omega_{ij}\Omega_{ji}}}{\varepsilon} \tag{2.19}$$

The rest of the model constants are: $C_{1\varepsilon} = 1.42$, $C_{2\varepsilon} = 1.68$, $\eta_0 = 4.38$ *and* $\phi = 0.012$

2.4. Computational Methodology

FLUENT allows users to choose one of the two numerical methods:

i) Pressure-based solver

ii) Density-based solver

Historically speaking, the pressure-based approach was developed for low-speed incompressible flows, while the density-based approach was mainly used for high-speed compressible flows. However, recently both methods have been extended and reformulated to solve and operate for a wide range of flow conditions beyond their traditional or original intent [12].

In both methods the velocity field is obtained from the momentum equations. In the density-based approach, the continuity equation is used to obtain the density field while the pressure field is determined from the equation of state.

On the other hand, in the pressure-based approach, the pressure field is extracted by solving a pressure or pressure correction equation which is obtained by manipulating continuity and momentum equations.

Using either method, FLUENT will solve the governing integral equations for the conservation of mass and momentum, and (when appropriate) for energy and other scalars such as turbulence and chemical species. In both cases a control-volume-based technique is used that consists of:

a) Division of the domain into discrete control volumes using a computational grid.

b) Integration of the governing equations on the individual control volumes to construct algebraic equations for the discrete dependent variables ("unknowns") such as velocities, pressure, temperature, and conserved scalars.

c) Linearization of the discretized equations and solution of the resultant linear equation system to yield updated values of the dependent variables.

As the governing equations are non-linear and coupled, several iterations are required to obtain a converged solution. A segregated solver, where the governing equations are solved sequentially, was used to perform the iterations. This is due to the restriction that FLUENT imposes on the choice of the solver with VOF multiphase model. Using this approach, the governing equations are solved sequentially. A single iteration consists of the steps outlined below:

1) Fluid properties such as density, viscosity and turbulent viscosity are updated, based on the current solution. (If the calculation has just begun, the fluid properties will be updated based on the initialized solution).

2) The u, v and w momentum equations (equation 2.3) are each solved in turn using current values for pressure and face mass fluxes, in order to update the velocity field.

3) Since the velocities obtained in Step 1 may not satisfy the continuity equation locally, an equation for the pressure correction is derived from the continuity equation and the linearized momentum equations. This pressure correction equation is then solved to obtain the necessary corrections to the pressure and velocity fields and the face mass fluxes such that continuity is satisfied.

4) Appropriate scalar equations such as turbulence, species, etc. are solved (equation 2.11 and 2.12) using the previously updated values of other variables.

5) A check for convergence of the equation set is made.

These steps are continued till convergence is achieved. An overview of the segregated solver is shown in Figure below [12].

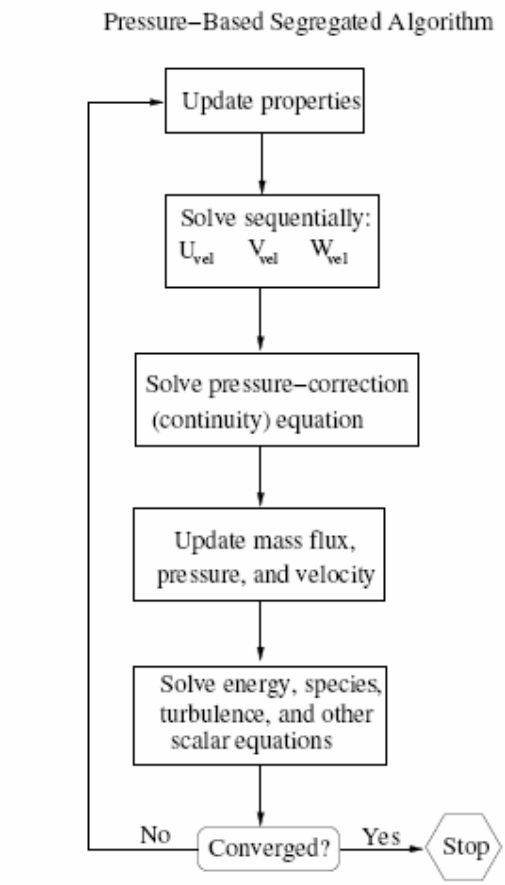

Figure 2-5. Scheme for pressure-based segregated algorithm

3. RESULTS AND DISCUSSION

Different inlet and boundary conditions were applied to understand the behaviour of the flow in the fill pipe and vent pipe during the complicated refueling process. In the entire cases a time step size of 0.0005 seconds was applied and convergence criteria was 0.0002 for the continuity equation; 0.0001 for the x-velocity, y-velocity, z-velocity; 0.001 for the kinetic turbulence energy and dissipation equations. Grid dependency was checked before the iterations which is explained in detail in Appendix A. Runtime for a case with higher velocity is about 15 days in workstations which has quad-core 2GHz processor and 4 GB of RAM. Different velocity inlet, pressure outlet conditions were applied and fuel-air ratio was changed to see how the behavior of the changes affect during the refueling process. The tank has 8 liters capacity and in all of the cases the tank was empty at the start-up.

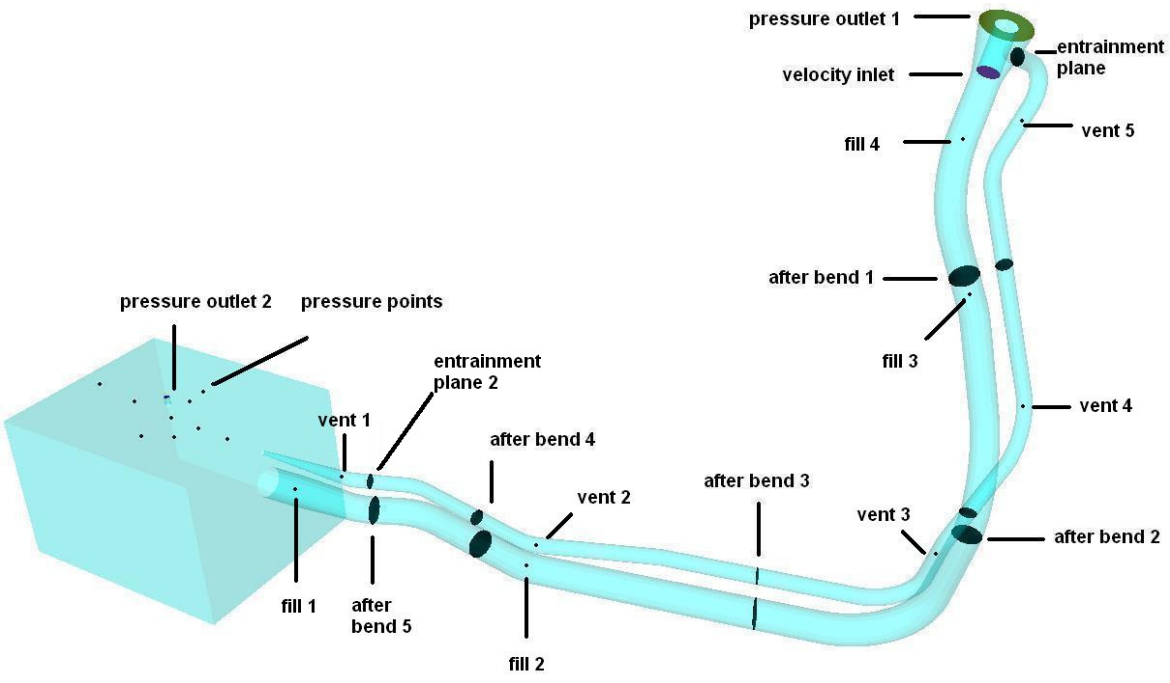

Figure 3-1. Pressure plot points and surfaces representation on the tank system

As a matter of simplicity, a simple illustration of the fill pipe system is given above which shows the locations where the boundary and initial conditions were applied and monitor points and surfaces that were used in the results and discussion section. For the

pressure contour and velocity magnitude plots, five different cross sections were utilized through the pipe and nine different points which are near to the upper surface of the tank were monitored in the tank. At some different points static and dynamic pressures were monitored throughout the fill pipe and vent pipe as well.

In the table below there is a list of cases run in this thesis. Over a hundred different cases were examined throughout the preparation of this thesis, however only thirteen of them will be discussed here. Cases were examined according to their volume flow rates at the velocity inlet, pressure outlet values at pressure outlet 1 and pressure outlet 2 boundaries, fuel-air ratio flowing out from the nozzle, shape of fill pipes and angle of the nozzles with the fill neck. The case 1 is tried at first, which is the base case of the thesis and has a volume flow rate of 60 liters / minute and zero pressure values are given at pressure outlet 1 and pressure outlet 2 and the total mesh size is 118784 elements. After that, case 2 was tried, which only differs from the base case in volume flow rate. Case 3 was examined to see the pressure boundary effect of to the refueling process. Nozzle entrance in the fill pipe was changed and given a little degree of angle at the fill pipe entrance and gasoline impinges to the wall at the start-up for case 5. Case 6 was examined which has a different fuel-air ratio with the base case. In case 6, the flow at the nozzle outlet has 80 percent of gasoline and 20 percent of air. Case 8 was similar to case 5 but with a different velocity inlet. Case 10 is a fictitious situation, for which the pressure outlet 1 is changed to a wall boundary, because in a real refueling process pressure outlet 1 is always opened to atmosphere. Although this condition was unrealistic, this was a good exercise to compare the results with other cases. Cases 11 and 14 were examined with different boundary conditions, for theses cases the fill pipe geometry is changed so that it has a radius reduction in the middle. Case 15 was run to check mesh independency. Finally, cases 22, 23 and 24 were examined to understand the wall boundary effect at pressure outlet 2.

Table 3-1. Table for the all of the cases

NUMBER	MESH SIZE	Volume Flow Rate (lt/min)	pressure outlet 1 (Pa)	pressure outlet 2 (Pa)	DESCRIPTION
CASE 1	118784	60	0	0	base case
CASE 2	118784	30	0	0	base case, different flow rate
CASE 3	118784	60	0	1000	base case, different p2 outlet value
CASE 5	118485	60	0	0	different nozzle angle
CASE 6	118784	60	0	0	different fuel ratio
CASE 8	118485	30	0	1000	different nozzle angle
CASE 10	118784	60	wall	0	base case, wall boundary at p1 outlet
CASE 11	131289	60	0	0	different fill pipe geometry
CASE 14	131289	60	0	WALL	different fill pipe, wall boundary at p2 outlet
CASE 15	146970	60	0	0	Meshing dependecy checked with base case
CASE 22	118784	60	0	WALL	base case, wall boundary at p2 outlet
CASE 23	118784	30	0	WALL	base case, wall boundary at p2 outlet
CASE 24	118784	90	0	WALL	base case, wall boundary at p2 outlet

In the thesis not all of the cases in the table are explained separately. Case 1 which will be named as a base case from now on, and case 23 is discussed and examined separately, for the other cases a comparison of them with each other are given. Firstly, base case is examined, then velocity effects are discussed, after this section how the ambient pressure has an influence on the refueling process is illustrated. After that the question of in which situations mass flow into the system or out from the system is answered. Furthermore, entrainment which is an important situation for automotive refueling process is explained and discussed in detail. After this section, how fuel ratio affect the refueling is

discussed. At section 3.7, nozzle angle is changed and a comparison of the results with the base case is given. At section 3.8, pressure outlet 2 boundary condition is changed to a wall boundary and its effects are discussed. Finally, at section 3.9, the studies are done with different fill pipe and the results are given. At the end, a general conclusion of this thesis is given.

3.1. Results and Discussion for the Base Case

Volume fractions of fuel and air on two perpendicular cross-sections of the tank are shown in figure 3.2 and figure 3.3 below at different times of the simulation. The total simulation time is 7.890 seconds. The pressure peak occurred at time 7.346 seconds and it is assumed that nozzle shut-off would have occurred at this time. But the refueling was not stopped until the 7.890 seconds.

In the figure 3-2 red color represents the fuel and blue color represents the air volume fraction. As the fuel enters the tank from the fill pipe below, air is vented from two venting locations. The first one is the vent pipe and the second is the small opening on the top surface of the tank (pressure outlet 2), the boundary condition at this location is defined as pressure outlet and the pressure value is set to zero gauge pressure for this case. Initially the fuel flows into the tank and hits the opposite face of the tank because of its high velocity. As the fuel level rises in time the fuel is pushed towards this face. At all times of the filling there are regions where fuel is diluted with air, both in the tank and inside the fill pipe. The vent opening on the tank top is free of any blockage during the entire simulation. On the other hand the vent pipe inlet is partially blocked by the fuel at when time t= 7.5 seconds (notice that this time is after the assumed nozzle shut-off). After this time the fuel partially blocks the vent tube and later it flows out of the tank from the vent line.

At time 2 and 4 seconds near the entrance of the tank dome, large air pockets are seen in the fill pipe, but after time 6 seconds smaller air bubbles are seen in the fill pipe.

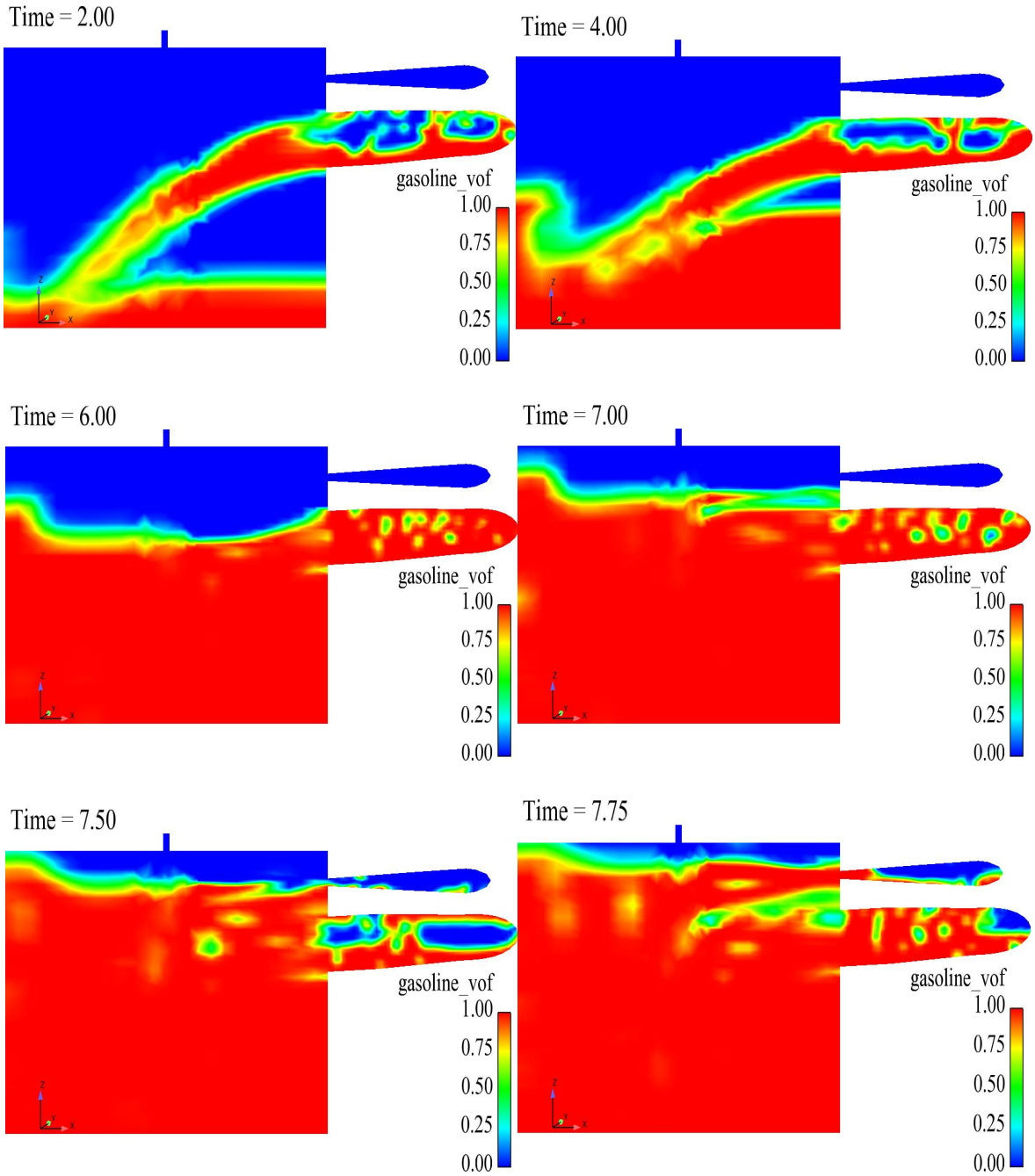

Figure 3-2. Fuel volume fraction on a cross-section in the tank dome at different times for the base case

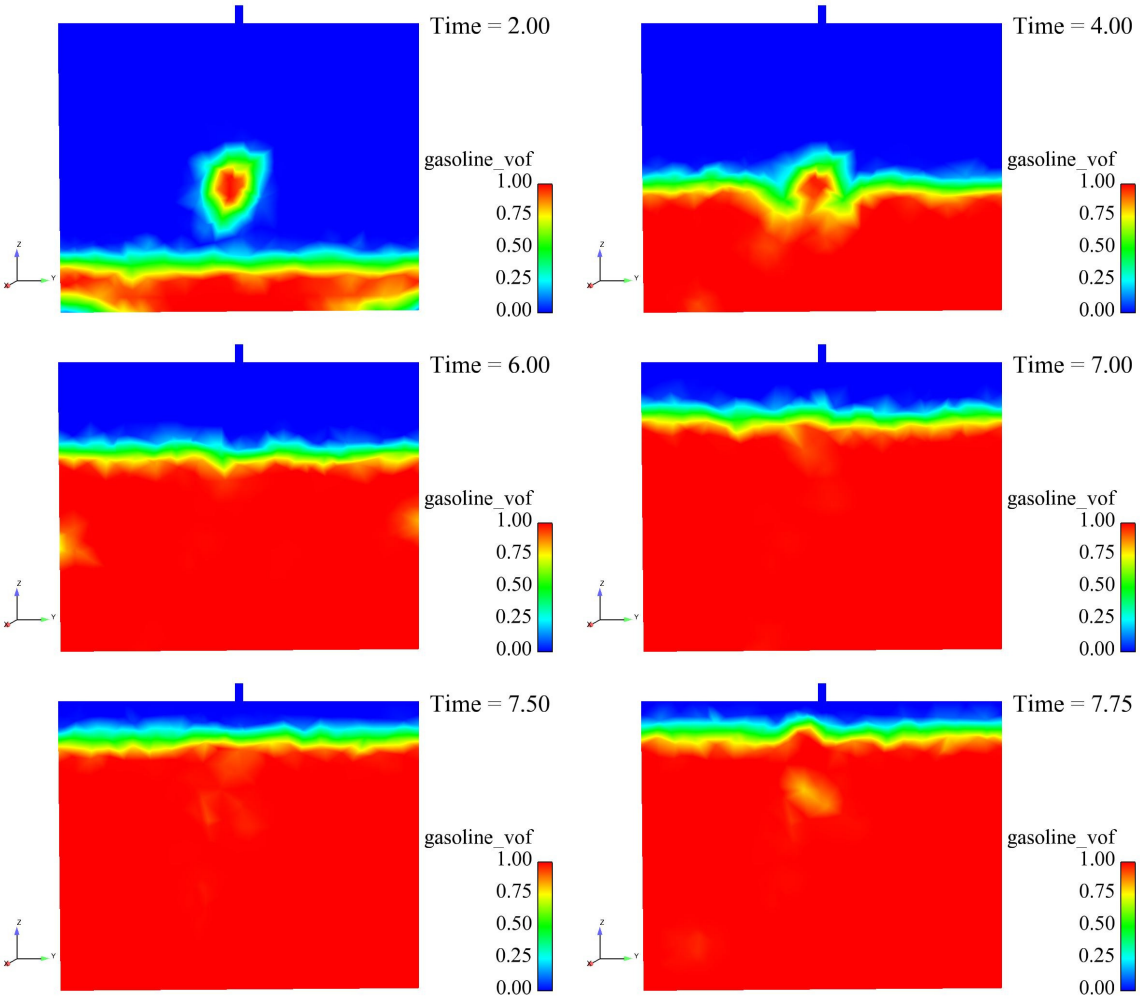

Figure 3-3. Fuel volume fraction on another cross-section of the tank at different times for the base case

For pressure measurements in the tank, nine different points near the upper part of the tank are chosen and average of them are calculated. Total, dynamic and static pressure values are monitored. Because of the smaller dynamic pressure values relative to the static pressure, total pressure do not differ significantly from the static pressure.

Time history of the tank static pressure is shown on figure 3-4 for this case. The static pressure increases in the beginning of the refueling, and then reduces to a stable value until the 7th second. The first peak occurs because of the vent system response [3]. The pressure is then reduced as some vapor vents back to the nozzle and to atmosphere through the top vent. At time 7.346 seconds the static pressure in the tank increases due to blockage of one of the vents, and after that the pressure value oscillates. In an actual filling this pressure rise is sensed by the nozzle and the fuel flow is stopped. In the simulations the

fuel flow is continued and the simulation is automatically stopped as a result of higher residuals in the continuity equation than the specified value.

Time history of tank dynamic pressure is shown on figure 3-5 for this case. The monitor points are very near to upper part of the tank and initially there is only air at this part of the tank. The dynamic pressure does not change until the 7.346 seconds significantly. After this time the dynamic pressure in the tank dome starts to increase. The dynamic pressure is proportional to the velocity squared and density. Since the fuel density is two orders of magnitude higher than that of air, whenever the fuel level in the tank reaches the monitored point of the pressure, both the density and the dynamic pressure increase.

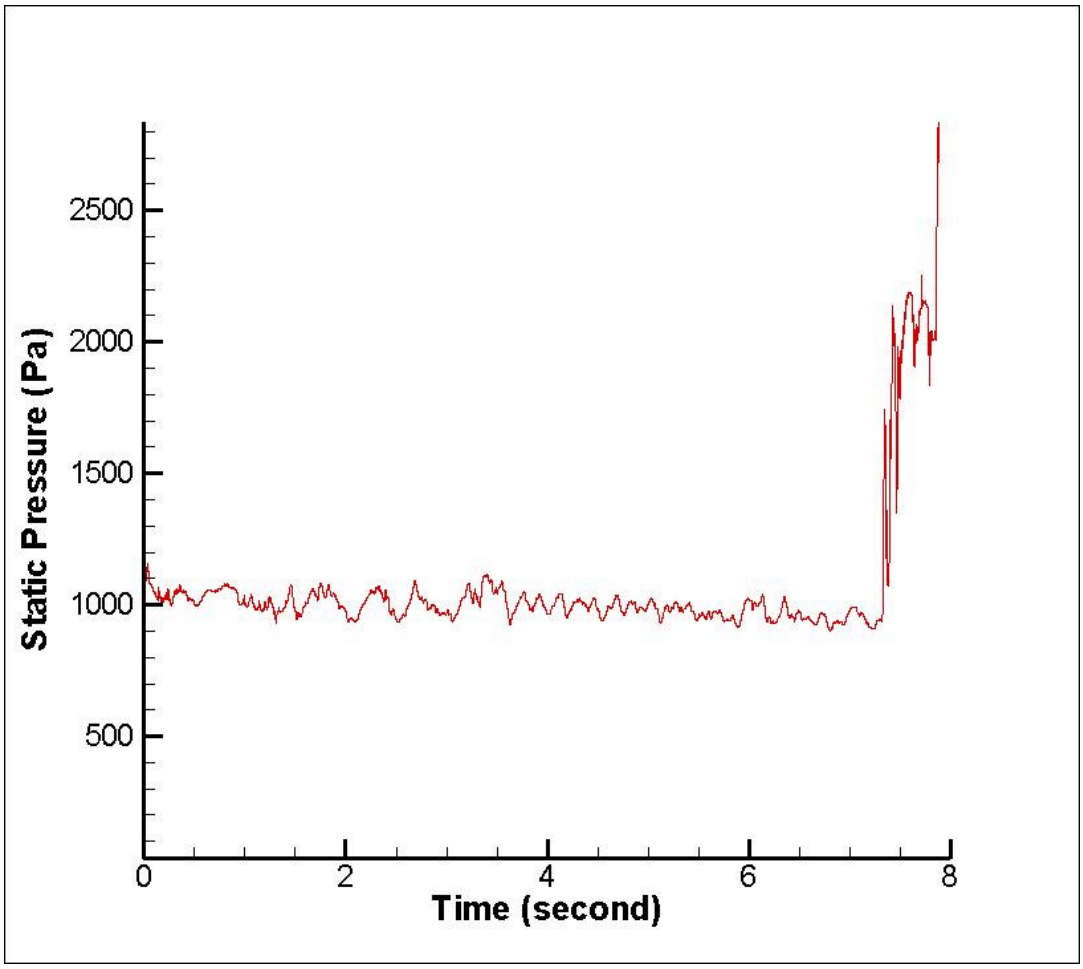

Figure 3-4. Static pressure change in the tank for the base case

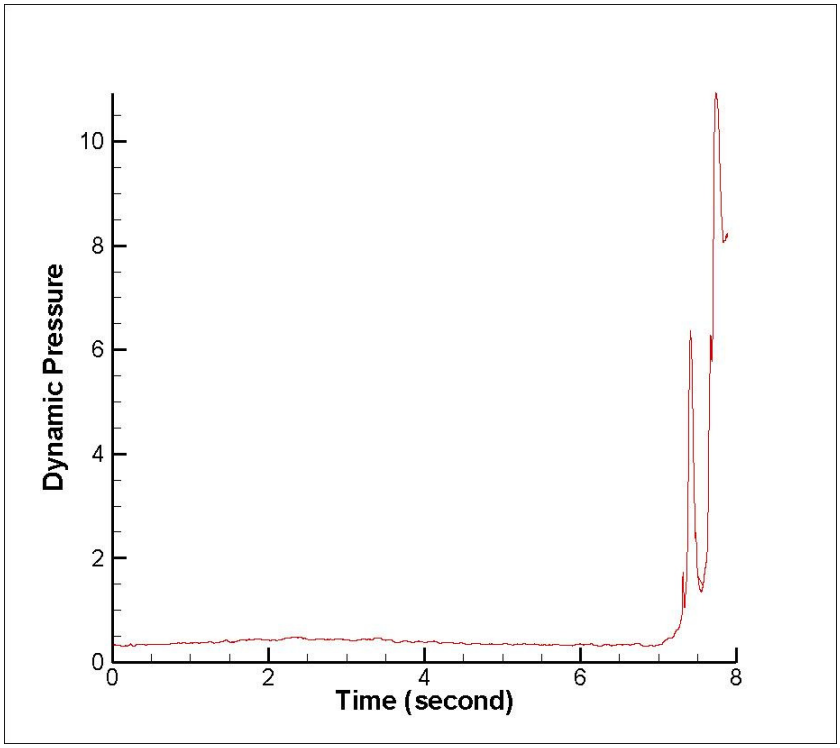

Figure 3-5. Dynamic pressure vs. time graph in the tank for the base case

Fuel volume fractions at some cross sections of the pipe at a time near the end of re-fuelling (t=7.75 second) are shown in Figure 3-6. At this time the total gasoline volume inside the tank is calculated to be 7.296 liters.

In figure 3.6, the smaller circle is the cross-section of the vent pipe and the larger one is the cross-section of the fill pipe. The cross section locations along the pipe are shown in figure 3-1, they are arranged to be after the bends and numbered starting from the nozzle inlet in the flow direction. In other means, the first figure represents the place after bend 1 and the last one represents the place after bend 5. When we look at the figures it is seen that at time 7.75, the area which gasoline covers changes at different locations through the fill pipe. For example, after bend 2 gasoline covers roughly two third of the area, however after bend 3 almost all of the area is covered with gasoline. It is seen that at the upper part of the pipe such as after bend 1 and after bend 2 gasoline coverage is not as much as the lower part of the pipe. The fuel does not cover the whole area of these cross-sections due to a lower nozzle diameter than the fill pipe diameter. But after bend 3 because of the low velocities, gasoline starts to accumulate. It is also interesting that after bend 5 the gasoline is going out of the tank through the vent pipe because of the high pressure in the tank with respect to the atmosphere.

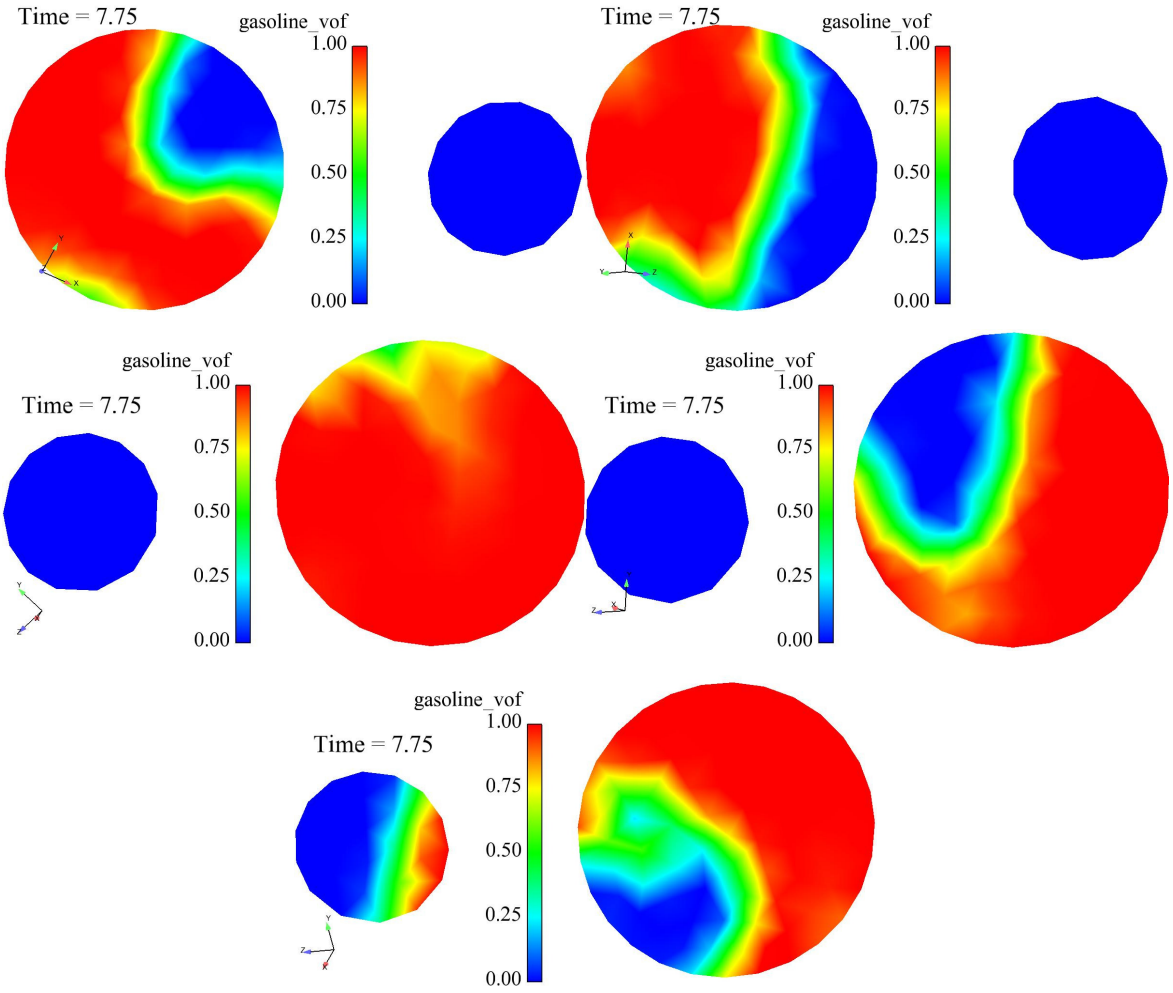

Figure 3-6. Fuel volume fractions at second 7.75 at fill and vent pipes (a) after bend 1 (b) after bend 2 (c) after bend 3 (d) after bend 4 (e) after bend 5 for the base case

In figure 3.7 contours of velocity magnitude are shown in the fill and vent pipe at time t=7.75 seconds at the same cross sections of the pipes in figure 3.6. The velocity boundary layer at the pipe wall is visible at all the cross sections. The high velocity spots in the fill pipe contours at the cross sections after bend 4 and 5 correspond to air packets in the pipe as can be seen from a comparison to the figure 3.7. In the upper part of the fill pipe such as after bend 1 and 2 gasoline has higher velocity magnitude than air because there is not an accumulation in these part of the pipe, however after bend 4 and 5 it is seen that gasoline velocity starts to decrease and air gets more speed than gasoline. When the fuel level in the tank dome is below the fill pipe level, fuel velocity is high. After the level of fuel inside the tank dome exceeds the level of the fill pipe, fuel velocity decreases due to

the back pressure of the accumulated fuel, whereas the velocity of the air bubbles increased due to the buoyancy effect.

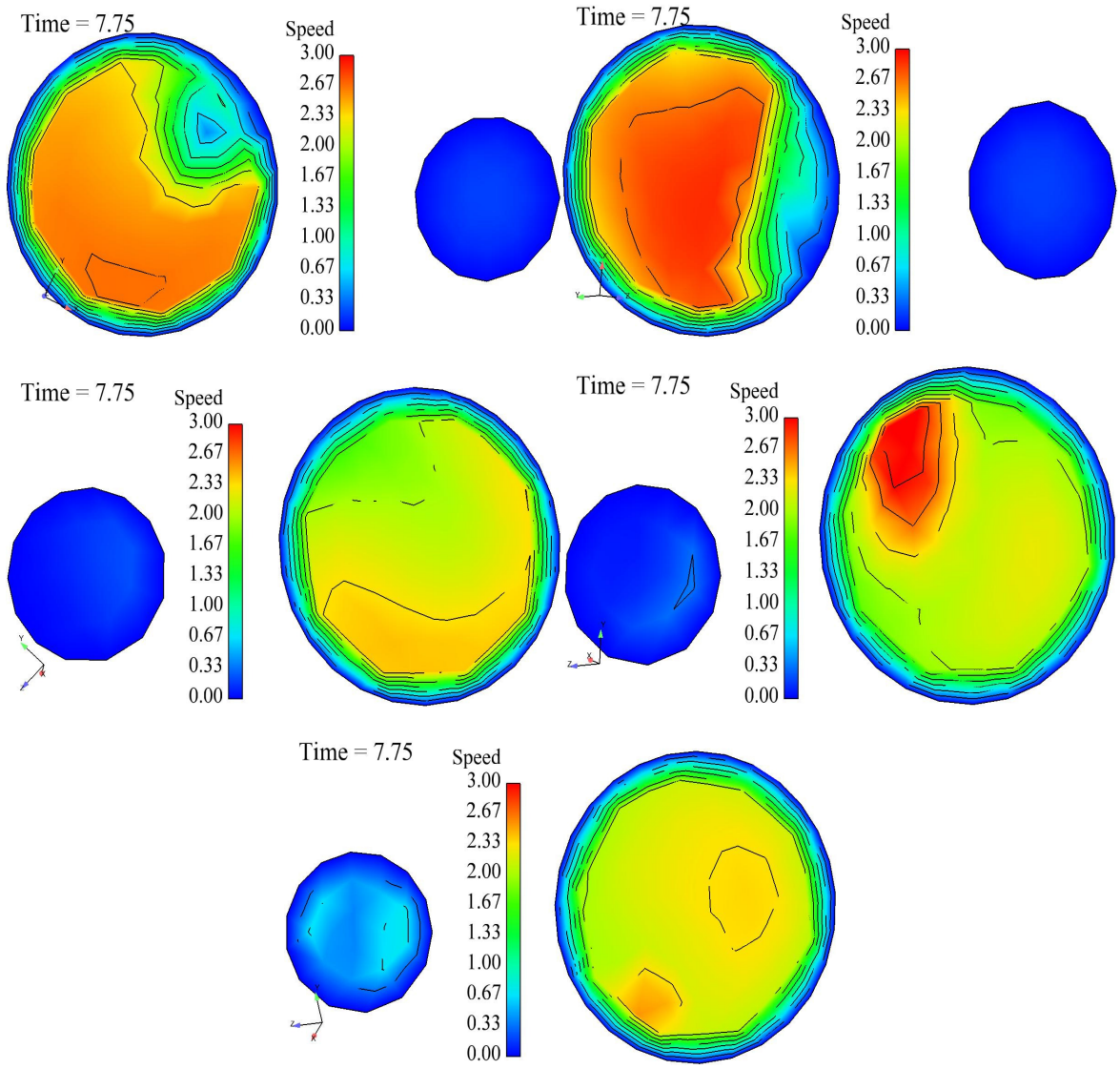

Figure 3-7. Velocity magnitude contours in different cross sections throughout the fill pipe and vent pipe at second 7.406 for the base case

Fuel volume fractions at the pipe cross sections after bend 5 at different times are shown in figure 3.8. Throughout the re-fuelling gasoline volume fraction changed in the fill at this location. In the vent pipe, at time t=7.89 seconds some fuel is visible.

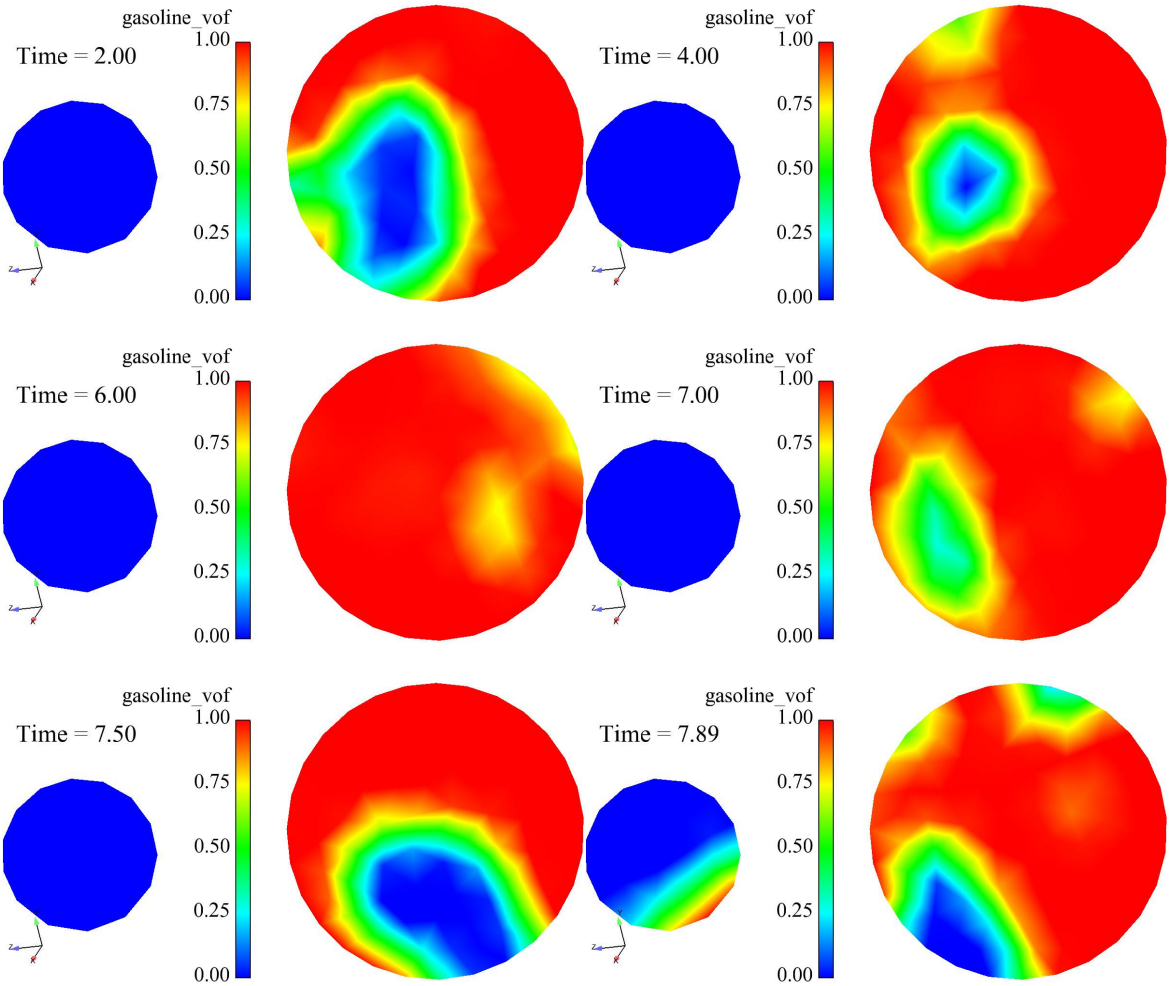

Figure 3-8. Fuel volume fraction at different times after bend 5 for the base case

Time history of the mass flow rate at the pressure outlet 1 and the pressure outlet 2 are shown in Figure 3.9. The red line shows the air flow rate at the pressure outlet 1 and the green one shows the air flow rate at the pressure outlet 2. Negative values denote a net mass out flow from the tank and positive values denote a net mass in flow to the tank. Most of the air is vented to the atmosphere from the pressure outlet 2. The vent pipe places a resistance to the air flow and the flow from the pressure outlet 1 is smaller. The flow from the pressure outlet 1 attains positive values as well at the very end of the re-fuelling. Notice that the tank pressure fluctuates at this time and locally the pressure at the boundary may become lower than the atmospheric value leading to mass intake from the boundary. The effect of increased pressure and pressure fluctuations are also visible in the pressure outlet 2 as well. The flow rate out of this vent also fluctuates at the end of the process but it

always remains at negative values since the tank pressure is always higher than the atmospheric one.

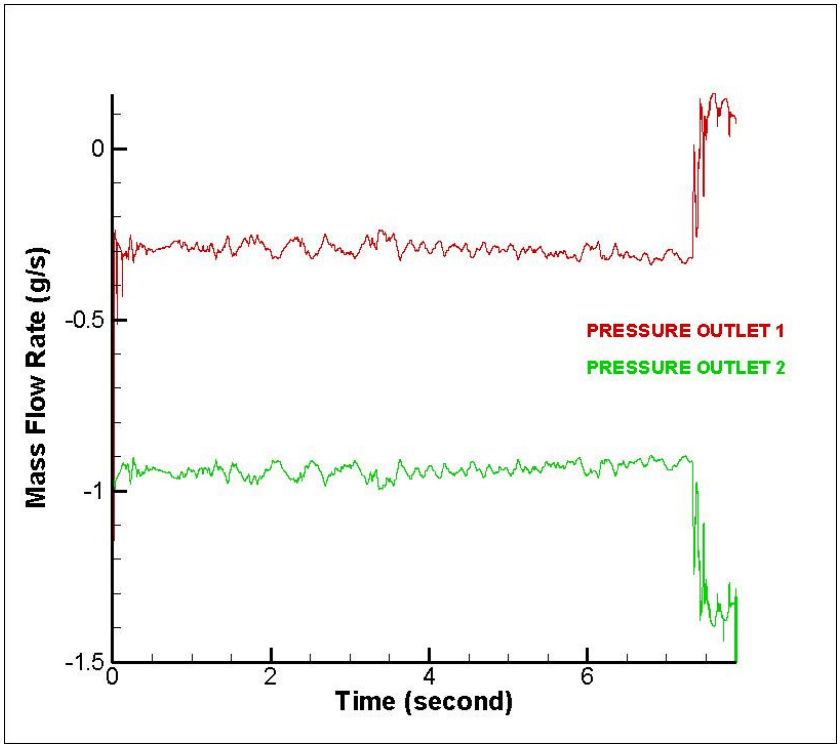

Figure 3-9. Mass flow rate of air at pressure outlet 1 and pressure outlet 2 for the base case

3.2. Flow Rate Effect

Figure 3.10 and figure 3.11 show the fuel volume fractions contours of case 2 at the same tank cross sections with the base case. In comparison to the base case, case 2 has half the fuel inlet velocity, hence the refueling process takes longer time and finishes at time t=15.875 seconds.

Because of the lower inlet velocity the fuel does not reach the opposite face of the tank, it is poured in the middle of the tank at time 2 seconds as seen in the first graph of the figure 3-10. The volume of the fill pipe covered by the fuel near the tank dome entrance is smaller in comparison to base case as well. At the earlier times of the re-fuelling process fuel is flowing as a liquid flow on the lower part of the fill pipe, and some fuel pockets are seen at the upper part of the fill pipe. As time passes the liquid fuel at the lower parts of the

pipe shows increasingly more and more air content because low mass flow inlet does not cover all of the fill pipe area. After the gasoline level in the tank dome reaches the entrance of the fill pipe level, air bubbles displacement due to buoyancy effects can be seen at time 13.5 second.

At time 13.5 second the gasoline droplet flowing through the vent pipe is first seen. A gasoline volume of 6,417 liters is calculated in the tank dome for this time. Gasoline droplet in the vent pipe is important to determine the nozzle shut-off time as discussed in the previous section. For the base case the first gasoline droplet is shown at time 7.346 in the vent pipe, and there is 6.911 liters of gasoline in the tank dome. Under these circumstances, it can be claimed that low fuel inlet velocity leads high refueling time but when nozzle shuts off itself there will be more gasoline in the tank dome.

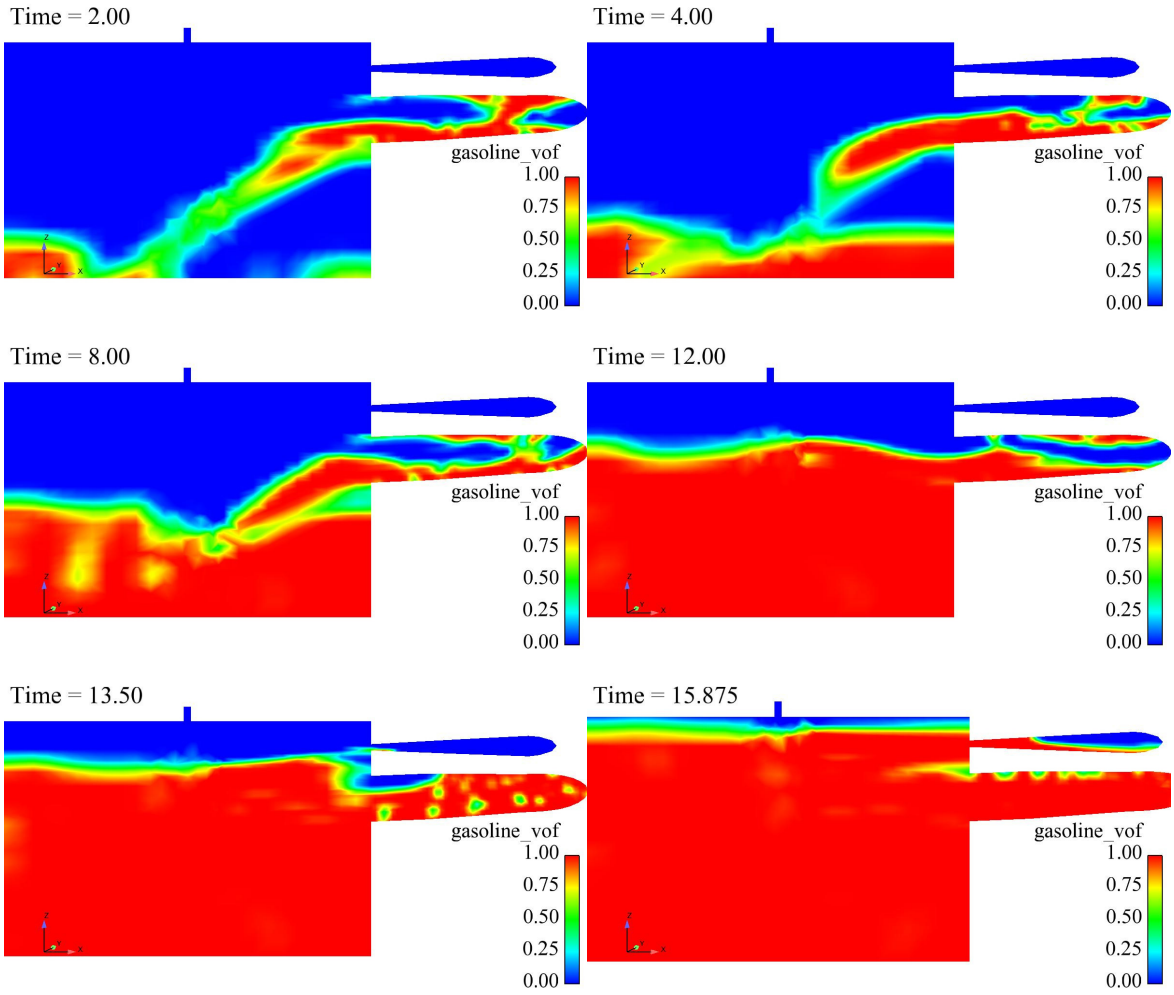

Figure 3-10. Fuel volume fraction on a cross-section in the tank dome at different times for case 2

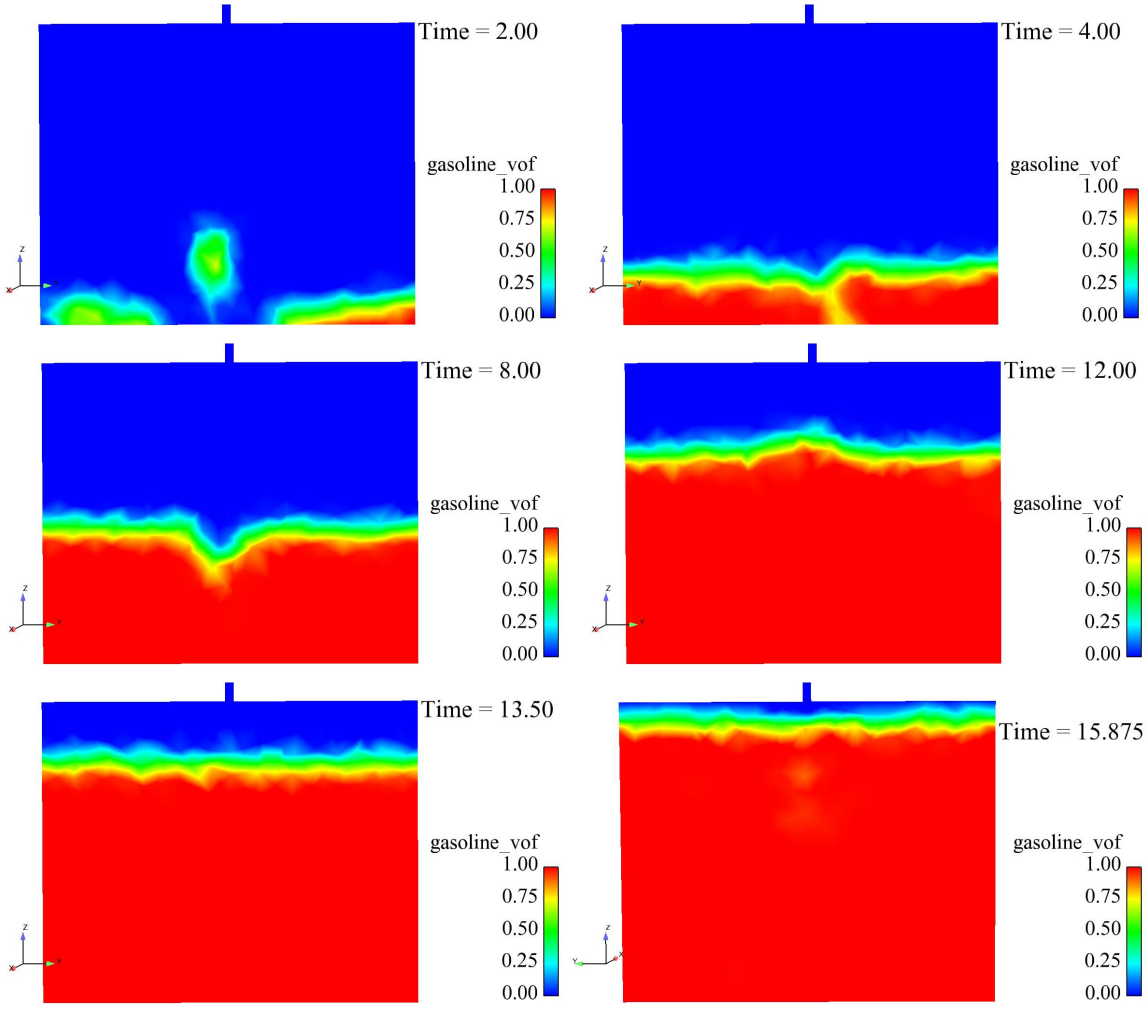

Figure 3-11. Fuel volume fraction on another cross-section in the tank dome at different times for case 2

Fuel and air volume fractions at various pipe cross sections at time t=15.23 seconds are shown in figure 3-12. At this time there is 7.298 liters of gasoline in the tank dome and this value is nearly the same as base case at time 7.75 seconds. It is understood from this facts that gasoline refueling time becomes approximately two times, as expected, of the base case when we applied half of the velocity inlet condition in case 2. At time 15.23 second for case 2, gasoline does not cover the whole area of the fill pipe because the nozzle inlet area is smaller than the flow area in the fill pipe. But speed of the gasoline is higher at this part of the fill pipe which can be seen in figure 3.13. When we approach the lower part of the fill pipe near the tank dome entrance gasoline flow-rate decreases and fill pipe is covered with full of gasoline after bend 4 and 5. Additionally, in the graph of after bend 4

there is a gasoline droplet flowing up to the vent pipe at time 15.23 seconds which shows that gasoline flow from the tank through the vent pipe has already started.

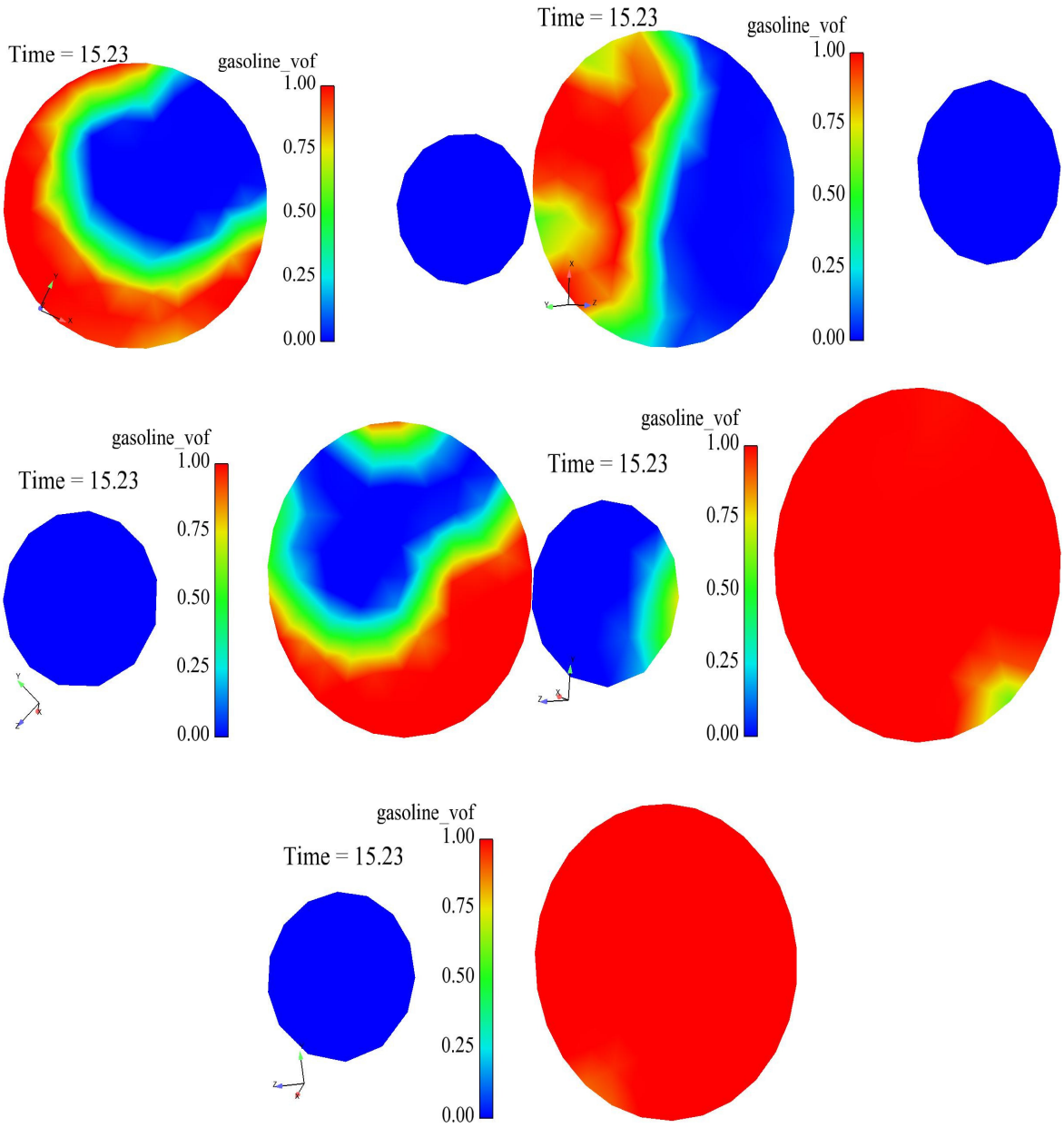

Figure 3-12. Fuel volume fractions at second 15.23 at fill and vent pipes (a) after bend 1 (b) after bend 2 (c) after bend 3 (d) after bend 4 (e) after bend 5 for case 2

Velocity magnitude contour plots at the same pipe cross sections are shown in figure 3-13. It is again seen that gasoline has higher speed than air in the pipes. Boundary layers are visible too as in the base case. The flow is turbulent throughout the fill pipe just like in the base case, whereas speed of gasoline in the fill pipe is lower than the base case.

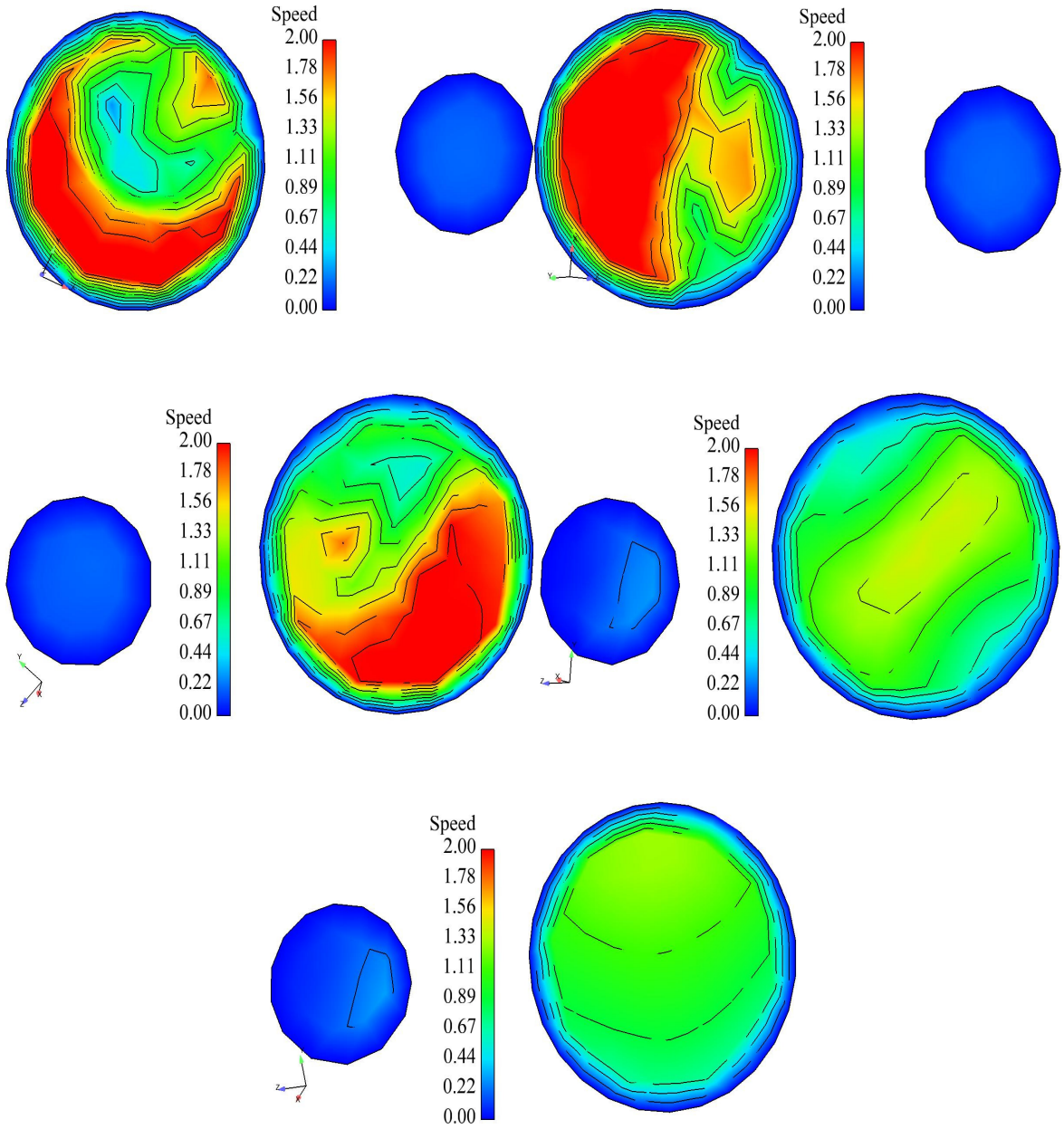

Figure 3-13. Velocity magnitude contours in different cross sections throughout the fill pipe and vent pipe at second 7.5 for case 2

Static pressure change in the tank dome is plotted in Figure 3-14. Pressure in the tank dome is lower than the base case during the whole refueling process because of the low velocity inlet conditions. The static pressure in the tank dome oscillates between 250 Pa and 400 Pa during the process. Static pressure in the tank dome reaches its peak point 1940 Pa at time 15.96 seconds. For the base case that peak point was as a value of 1742 Pa at time 7.346 seconds. For that reason, it can be said that low velocity in the filler pipe led to lower working pressure in the tank dome and the pressure peak was higher than base case.

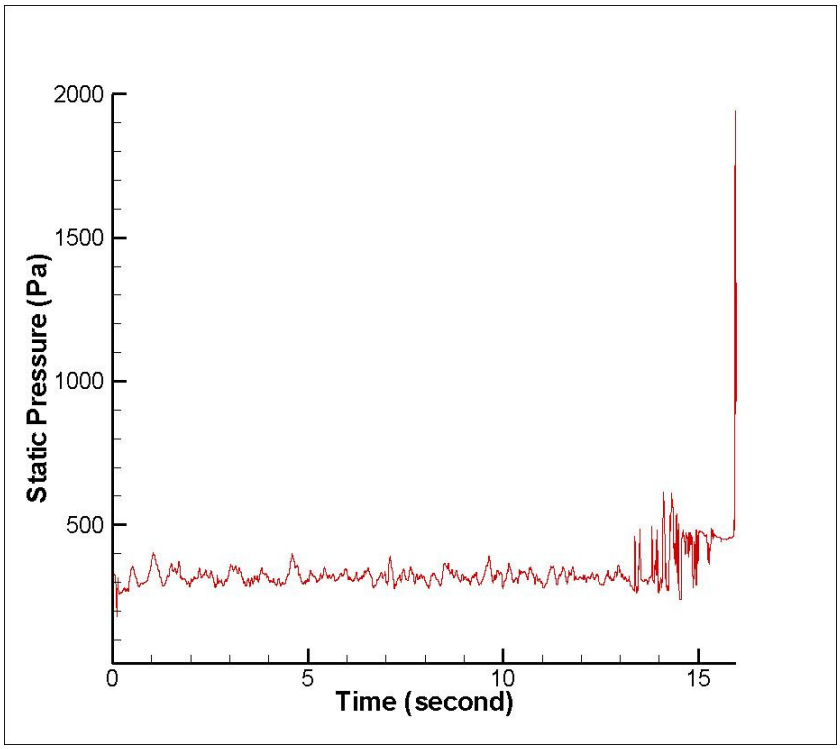

Figure 3-14. Static pressure change in the tank for case 2

3.3. Ambient Pressure Effect

To understand the effect of the ambient pressure in the tank dome case 3 was done. The difference of this case from the base case is higher pressure conditions applied in the pressure outlet 2. Pressure outlet 2 was set to 1 kPa (it was set to a value of 0 kPa in case 1). Fuel volume fraction during the refueling process can be seen below in figure 3-15. The cross section of the tank dome was taken in the middle of the tank as the previous cases. Pressure value at pressure outlet 2 did not alter the flow character significantly, both

bubbles and large slugs of air are seen in the tank entrance at fill pipe again as in the base case. But it should be said that when we compare the gasoline volume quantity in the tank dome it is always less in case 3. This difference is not so much but there is always a small difference between the base case and case 3. For example at time 6 seconds gasoline volume in the tank was 5.528 liters in case 3 however for base case this value was 5.546 liters. At time 7.5, gasoline volume in the tank dome was 7.034 liters for case 3 and for the base case it was 7.062 liters.

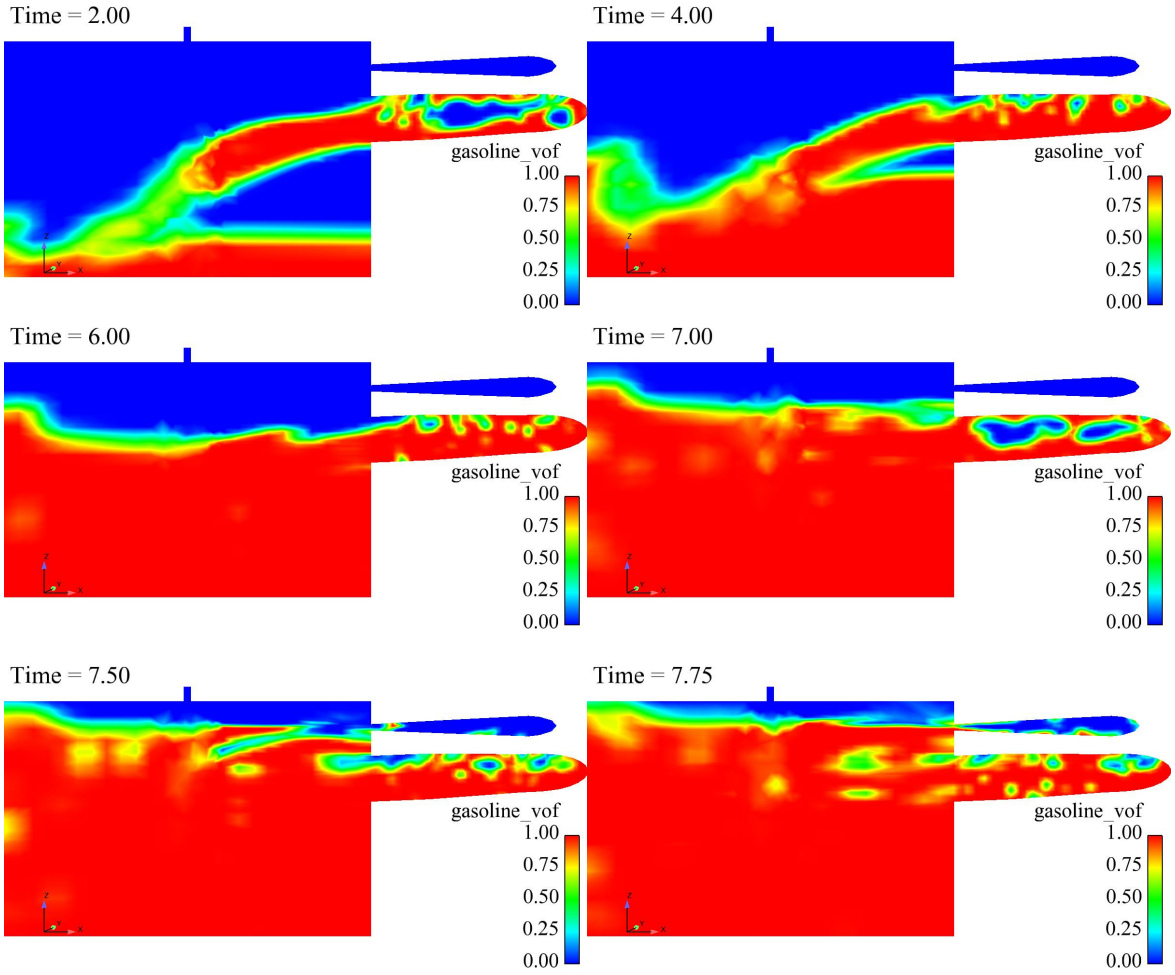

Figure 3-15. Fuel volume fraction on a cross-section in the tank dome at different times for case 3

Velocity magnitude contours at different cross-sections of the pipes are seen in figure 3-16 and they were plotted at time 7.75 seconds near the very end of the refueling

process. It is interesting to note that base case and case 3 only differ in the pressure outlet 2 boundary condition, however speed of gasoline is completely different at similar times. High pressure inside the tank dome made a resistance to the flow of gasoline fuel in the fill pipe and this reduced the total velocity magnitude of gasoline inside the filler pipe.

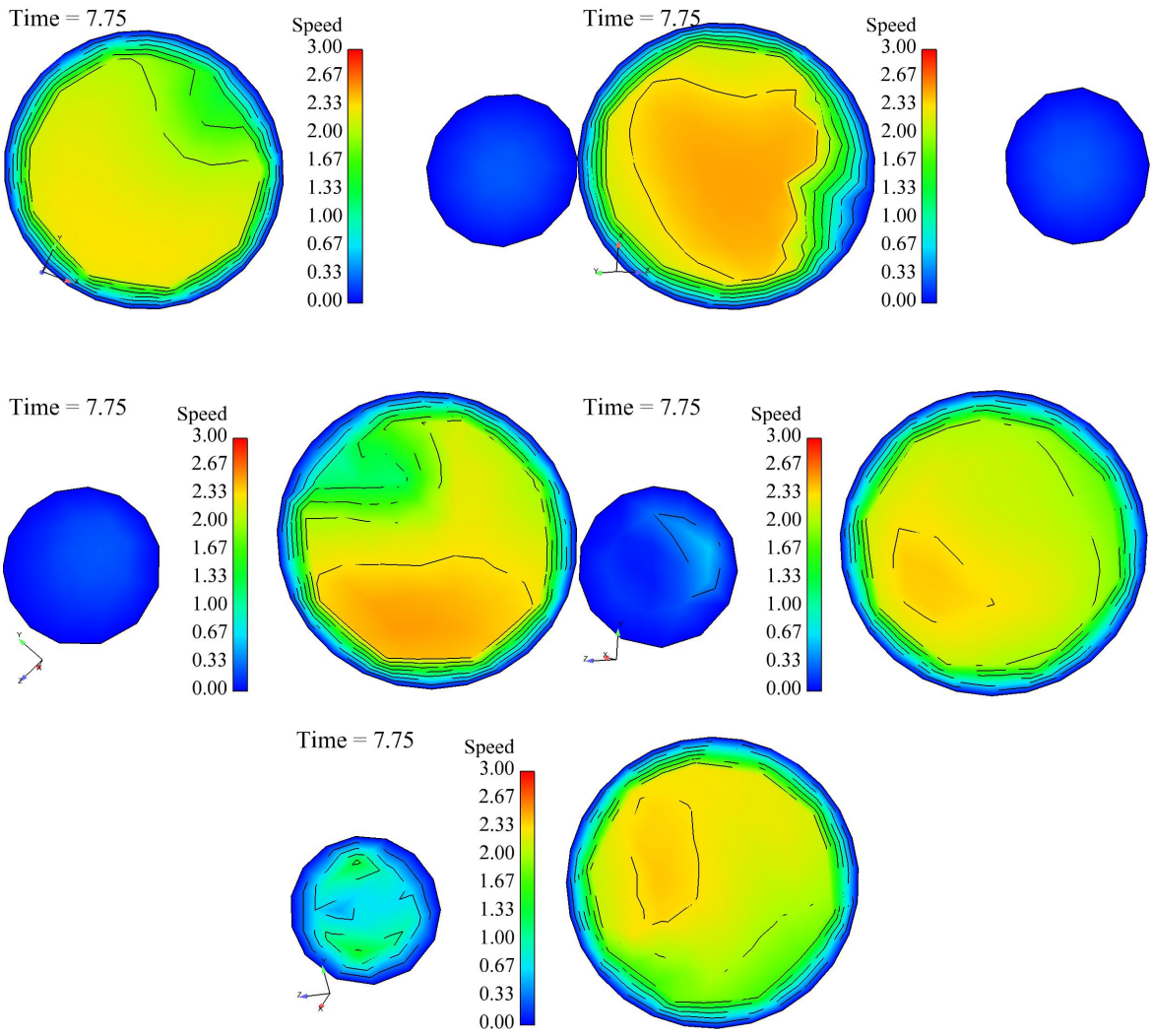

Figure 3-16. Fuel volume fractions at second 7.75 at fill and vent pipes (a) after bend 1 (b) after bend 2 (c) after bend 3 (d) after bend 4 (e) after bend 5 for case 3

Additionally, because of the resistance at pressure outlet 2 gasoline flow through the vent pipe starts earlier in case 3 and less amount of air is vented through the pressure outlet 2 as seen in the figure 3-17 below. The net outflow of air through pressure outlet 2 was nearly half of the base case for case 3. It is seen in the figure 3-17 that near the end of

the refueling, mass out flow increased suddenly at 7.32 seconds. This is because of the reduced vent area in the system forces air to flow out from the pressure outlet 2. At time 7.32 some gasoline particles partially closed the vent pipe area, and the total venting area reduced for the air. This resulted in more air flow through the pressure outlet 2. It can be also seen in figure 3-17 that this happened earlier for case 3. This means that gasoline flow through the vent pipe started earlier for case 3 than the base case.

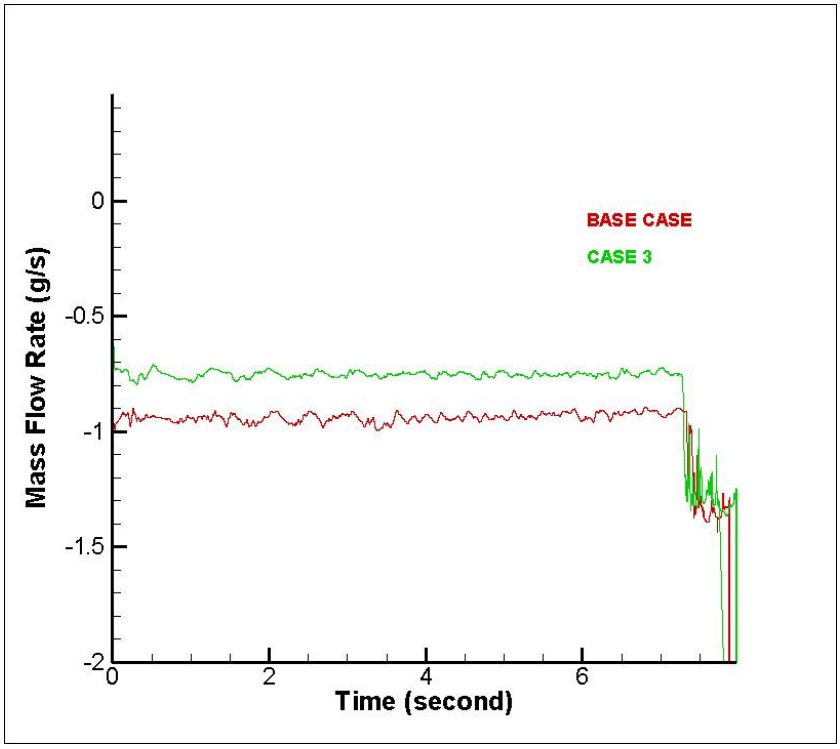

Figure 3-17. Mass flow rate of air from the pressure outlet 2

The static pressure time history is plotted in figure 3-18. Red line represents the results for the base case and green line represents the case 3. Static pressure values calculated for the case 3 are more than the base case for the most of the time. This is because of higher pressure boundary condition specified for case 3. Since the base case and case 3 have the same fuel inlet flow rates, pressure spike occurs similar times, but case 3 reached higher pressure peak than the base case.

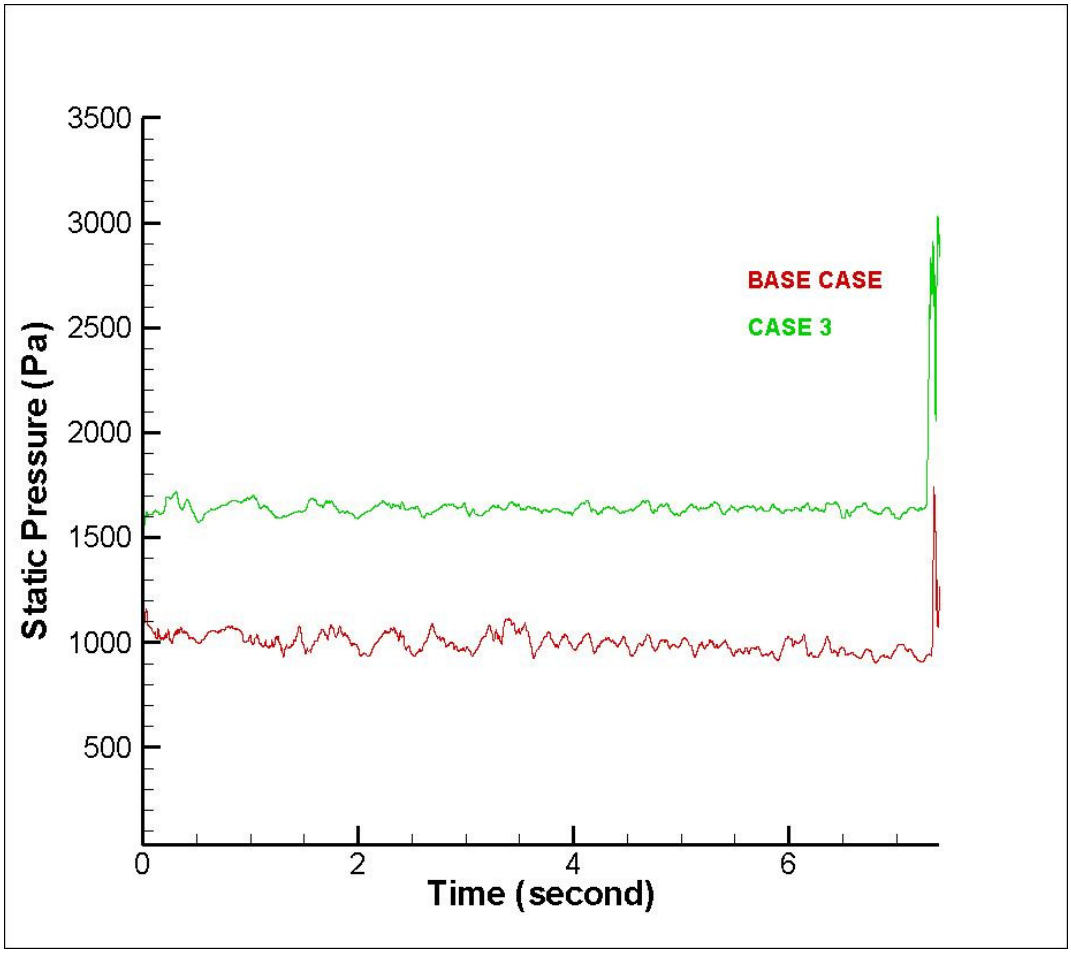

Figure 3-18. Static pressure change in the tank dome for case 1 and case 3

3.4. Effect of Mass in/out from the System

As a volume of fuel starts to flow in the fill pipe same volume of air flows out from the system through pressure outlet 1 or pressure outlet 2. At the outlets, depending on the local pressure difference between the atmosphere and the tank dome a net amount of air is flowing out from the system or flowing into the system. To understand the mass flow in or out from the system the base case 1, and cases 2, 3 and 10 are examined. Figure 3.19 shows the mass flow rate of air from the pressure outlet 1. Negative values of mass flow rate represent net outflow of air and the positive values represent net inflow of air from tank system through the pressure outlet 1.

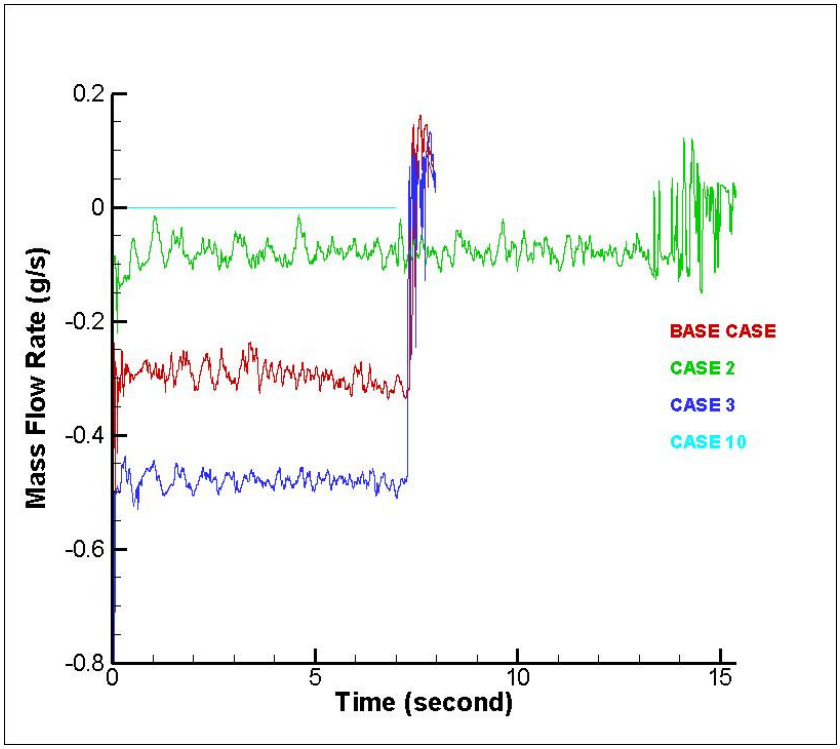

Figure 3-19. Mass flow rate from pressure outlet 1 for base case, case 2, case 3, and case 10

According to Figure 3.19, air is flowing out from the tank system for the base case up to the shut-off time (7.346). When we examine the results for case 2 which has a lower fuel inlet velocity than the base case, it is seen that air vented to the atmosphere diminishes due to lower pressure in the tank dome. However for case 3, the total amount of the air flowing out through the pressure outlet 1 increased due to higher tank dome total pressure. The higher pressure value specified at the pressure outlet 2 for case 3 prevents more air to escape from the pressure outlet 2 and air is canalized to escape through pressure outlet. In other words, mass flow rate of air is directly linked with the pressure boundary conditions that are applied at the outlets. Case 10, has a wall boundary condition applied at the same location where pressure outlet 1 is specified for the base case. The wall condition does not let any air flow. Hence the air flow through the pressure outlet 2 is increased as seen in Figure 3.20. Mass flow rate of air at pressure outlet 2 for case 10 has the maximum value over all of the cases we worked. For case 3 and the base case, mass flow rate of the air flowing out from the pressure outlet 2 reaches maximum values after second 7. When a fuel particle closes the vent mouth of the vent pipe exit, the total vent area is reduced and

more air flows out through pressure outlet 2. This is why mass flow rate values got maximum values after second 7.

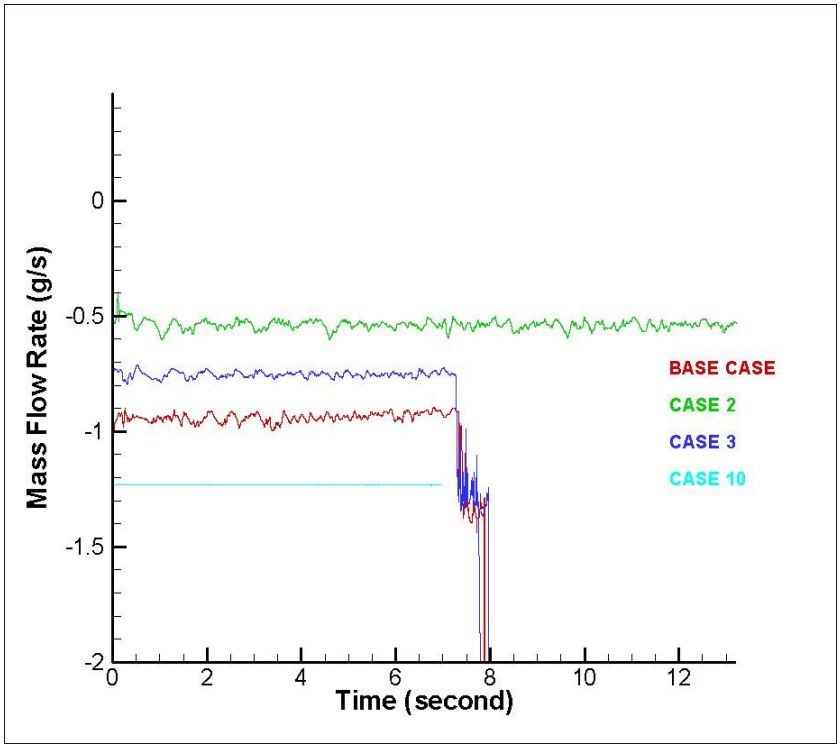

Figure 3-20. Mass flow rate of from pressure outlet 2 for case 1, case 2, case 3, and case 10

3.5. Entrainment Effect

Entrainment is defined here as the air drifted with the fuel flow. In the simulations, entrainment value is calculated as the surface integral of the flow rate according to the air phase volume fraction on the entrainment plane. We use the entrainment plane 1 as a reference plane through the refueling process to plot the results (see figure 3-1).

It can be seen in figure 3.21 that entrainment values were similar most of the time of the refueling process. As we know entrainment is proportional to the density, entrainment area and velocity values, density and entrainment area is fixed for that entrainment plane and only velocity changes affects the mass flow rate in that graph. The oscillation in the entrainment values especially for case 6 in figure 3-21 and case 10 in

figure 3-22 are because of large fluctuations in the velocity. Additionally, near the end of all cases entrainment values decreases suddenly. It can be explained as follows: when the fuel starts to flow out through the vent pipe, vent pipe flow area for air is reduced, and as we know entrainment is proportional to the flow area of the air, the entrainment value is reduced suddenly. It is interesting to note that when we compare the entrainment values for the base case and case 3, case 3 has higher entrainment values because of the pressure outlet 2 boundary condition. As we know, there are two ways for air-venting, when the refueling process is started. One is venting out to the atmosphere from the pressure outlet 2 and the other is re-circulating through the vent pipe. Because of the resistance at the pressure outlet 2, more air vented through the vent pipe and the entrainment values increased. When we look at the values for the base case and case 2, we see that case 2 has lower entrainment values than the base case because of the lower velocities at entrainment plane 1.

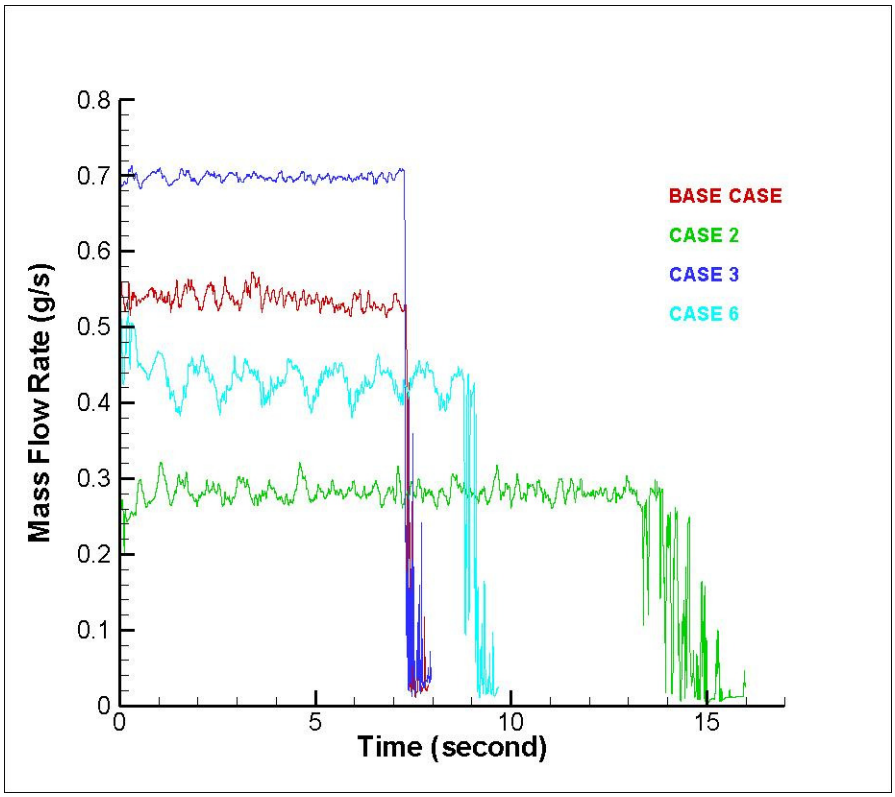

Figure 3-21. Entrainment values at entrainment plane 1 for different cases

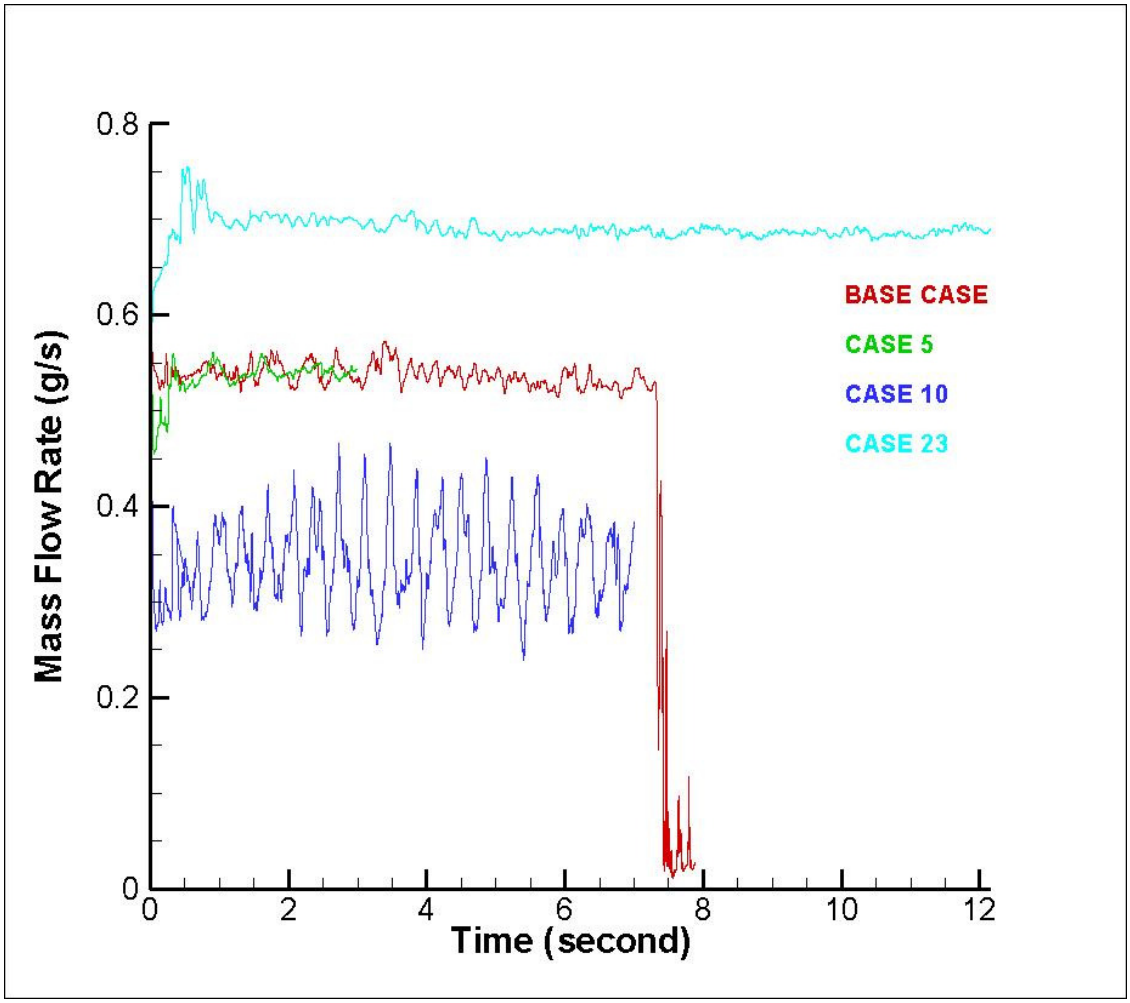

Figure 3-22. Entrainment values at entrainment plane 1 for different cases

In Figure 3-22 different entrainment values for different cases are plotted for the base case, cases 5, 10, and 23. Case 10 has lower entrainment values than the base case, because the tank system has only one opening to the atmosphere. All of the air flow out through pressure outlet 2 and we understood that lower recirculation happens in the fill and vent pipe. However case 23 has half of the velocity of the base case, it is interesting that case 23 has the largest entrainment values of all cases. There is only one way for the air in the tank dome and this way is through the vent pipe. For that reason, almost all of the air circulates in the vent pipe and it leads to the high entrainment values. It the entrainment plane. It is seen from a comparison of case 5 and the base case results in figure 3-22 that changing the nozzle angle does not have a significant effect on the entrainment values.

3.6. Fuel Ratio Effect

Case 6 is run to understand what happens when the fuel ratio of the nozzle is set to %80. In this case, air is added to the system through the fill pipe and the total refueling endured for 9.675 seconds, approximately 1.5 seconds more than the base case. The first peak of pressure occurs at time 8.823 seconds is assumed as the nozzle shut-off time however refueling process is not stopped and continued until 9.765 seconds. When the nozzle shuts-off, there is 6.7 liters of gasoline in the tank dome. It is slightly less than the base case (nozzle shut-off time 7.346 seconds, and 6.911 liters of gasoline in the tank dome). Additionally, at time 7 seconds, 5.25 liters of tank was filled with gasoline for case 6, which was 6.547 liters for base case. For that reason it can be said that low fuel ratio in the nozzle leads to late nozzle shut-off but gasoline volume quantity in the tank dome is lower than the case with the high fuel ratio.

Table 3-2. Gasoline volumes in the tank at specific times for the base case and case 6

time (second)	base case (lt)	Case 6 (lt)
7	6,547	5,250
7,346	6,911	5,528
8,823	7,417	6,700

When we look at the gasoline volume fractions at different times in the tank dome, the base case and case 6 were completely different. Case 6 has more air bubbles in the figure 3-23 and more air is seen at the inner core of the fill pipe, gasoline is attached to the inner walls of the fill pipe. Escape of gasoline droplets was not seen until 8.823 second of the flow which was first seen at second 7.346 in the base case.

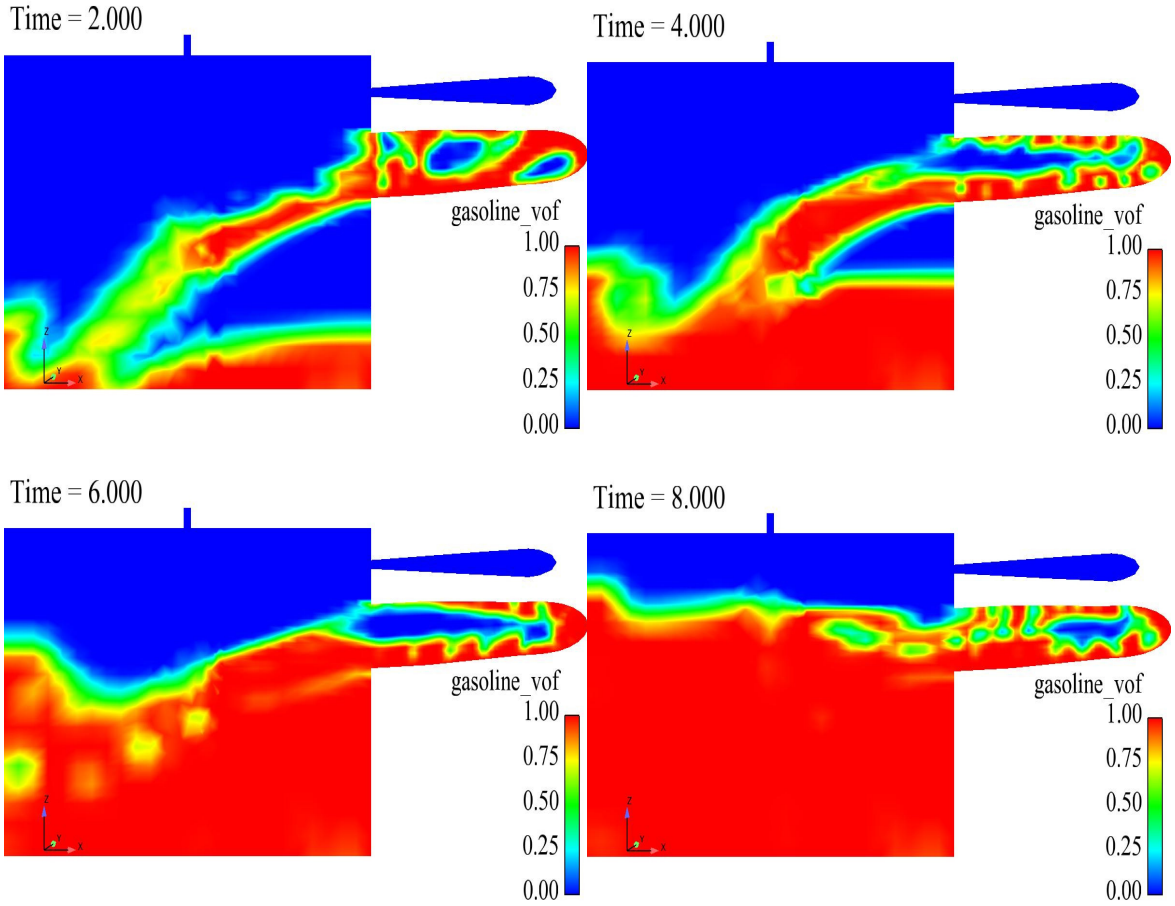

Figure 3-23. Volume fraction on a cross-section in the tank dome at different times for case 6

In figure 3-24, velocity magnitude contours for two different cases, for base case at the left and case 6 at the right side. Monitoring time is chosen in order to have a similar volume of gasoline in the tank dome. At time 8.625 for case 6 and time 7 for base case there is 6.547 liters of gasoline in the tank dome for both cases, for that reason time 7 second is chosen for the base case and 8.625 is chosen for case 6. When we compare the velocity magnitude values in the fill and vent pipes, the base case has higher velocity magnitudes at the vent pipe in all of the zones shown in figure 3-24. In the fill pipe velocity magnitudes is higher for case 6 than for the base case except for the first cross section. The smaller density of lower fuel ratio fluid is the reason for this increased speed.

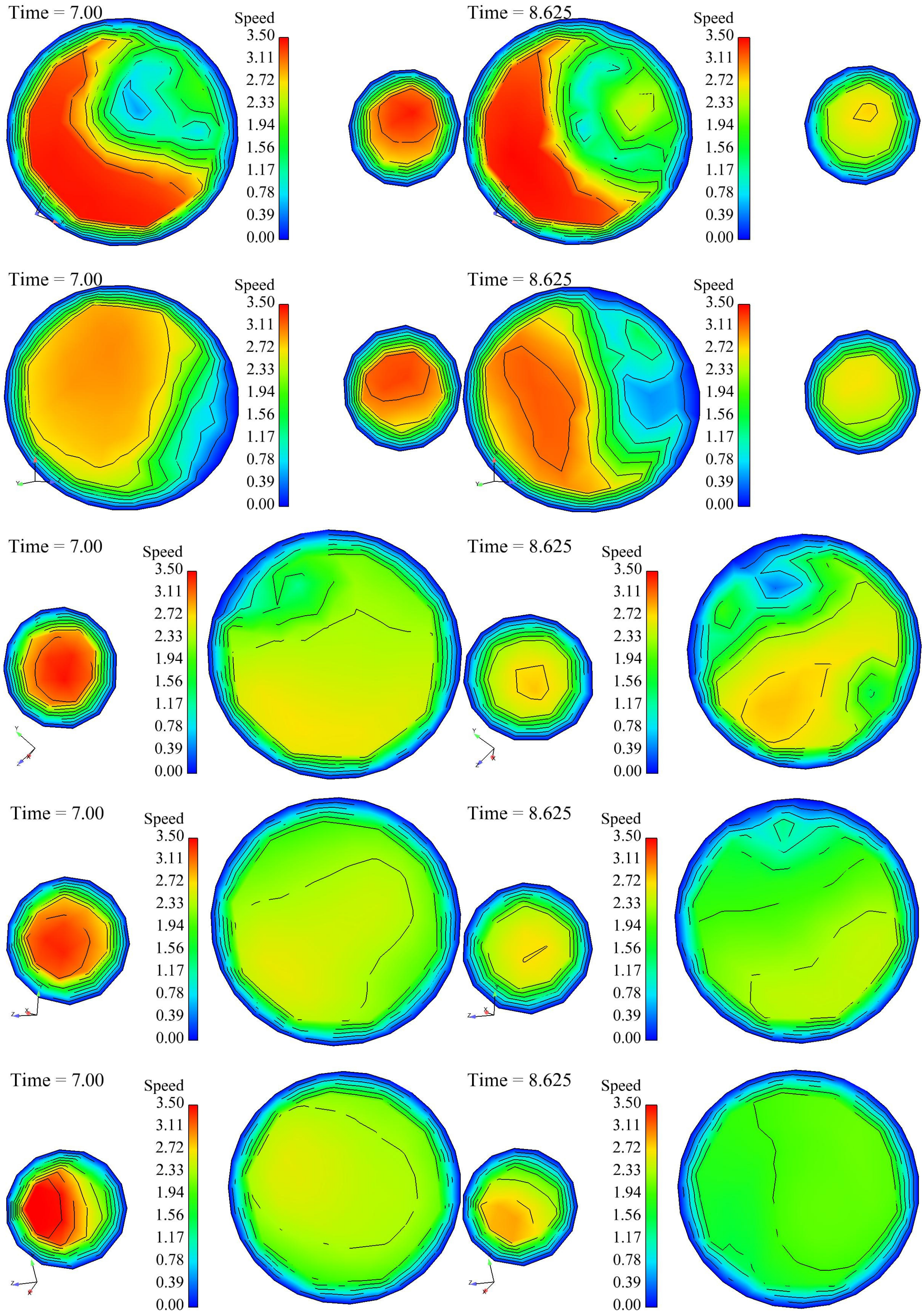

Figure 3-24. Speed for base case (left) and case 6 (right) after bend 1,2,3,4,5 respectively.

3.7. Refueling Process with Different Nozzle Angle

In USA there are over 20 different fuel nozzles in patrol stations. Different types of nozzles have different flow rates and different geometries and also have different sensitivities to pressure peaks to shut off the refueling process. In our CFD model the nozzle is defined as a velocity inlet boundary condition and nozzles which have different flow rates are examined in the previous sections.

In this section, case 5 and case 8 are examined for which the nozzle is placed with an angle into the fill pipe and the gasoline flowing from the nozzle hits the wall at the filler pipe neck as shown in Figure 3-25.

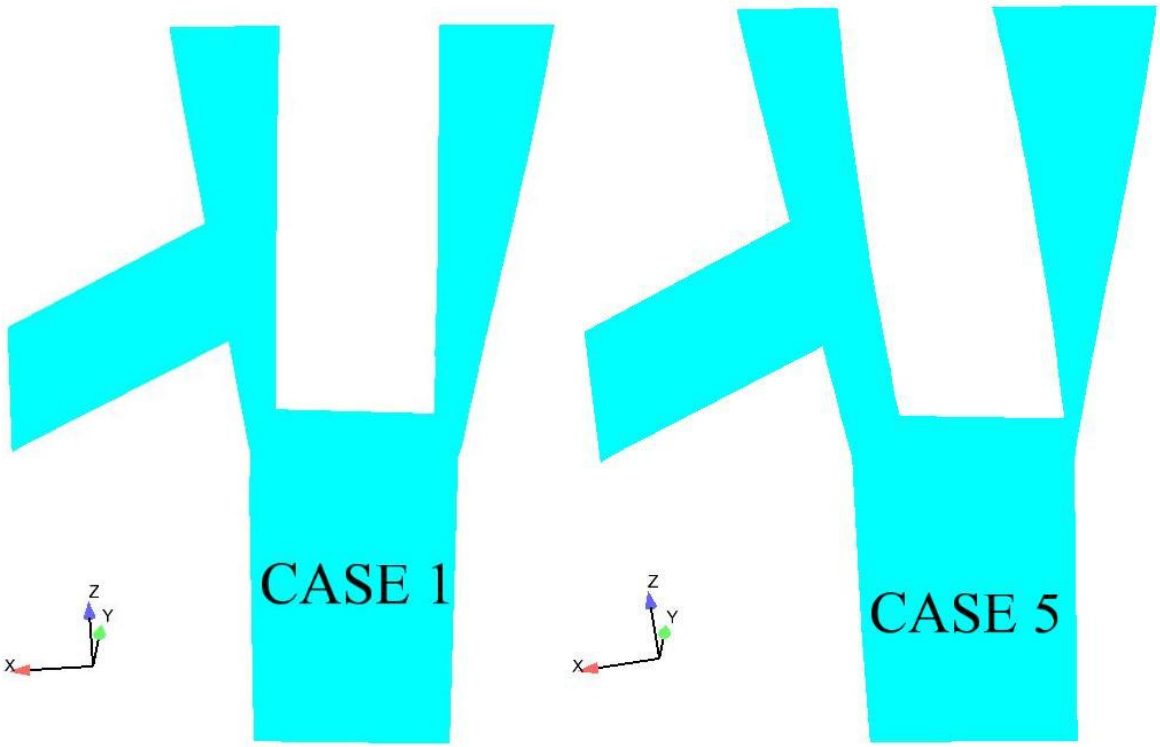

Figure 3-25. Different nozzle angles for case 1 and case 5

Gasoline volume fractions in the tank dome for case 5 are plotted in figure 3-26. Gasoline flows into the tank dome with air bubbles however when we compare the bubble sizes with the base case, case 5 has smaller air bubbles at time 2 second. Large air bubbles near the tank dome are not seen in the entrance at other times as well. It is because more

air is flowing out from the pressure outlet 1 than the base case. This leads less amount of air traveling in the system for case 5. It is seen at time 7.5 seconds, there are gasoline droplets flowing through the vent pipe which suggests that gasoline flow through the vent pipe is started earlier than this time. At time 7.21 seconds (not shown in the figure 3-26) first gasoline droplet is seen at the entrance of the vent pipe. This time is smaller than base case (7.346) in comparison.

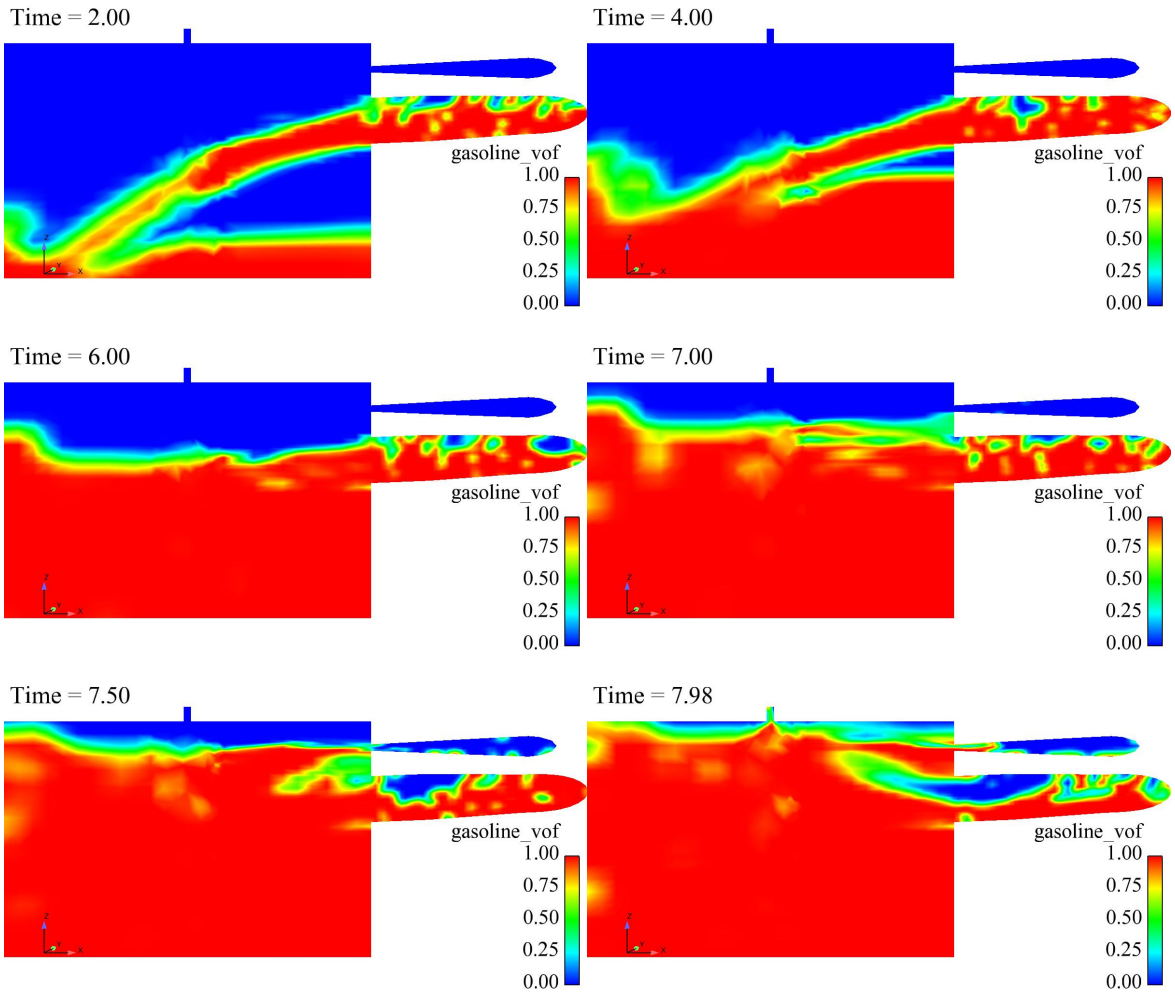

Figure 3-26. Fuel volume fraction on a cross-section in the tank dome at different times for case 5

There is one another thing to note that at time 7.98 second fuel tank is full with gasoline and some gasoline starts to flow from the pressure outlet 2 boundary. This situation is not realistic for the refueling process since gasoline flow would have stopped (due to increases pressure values) long before we reach 7.98 seconds. However it is a good practice to see the pressure limits of the refueling to avoid such a situation. As it can be

seen in figure 3-27 in the tank dome at time 7.98 second pressure value reached to 20000 Pa. By the help of this, it can be assumed that if a nozzle sensor does not close the fuel pumping until 20000 Pa, gasoline starts to flow out from the system, and it would be dangerous.

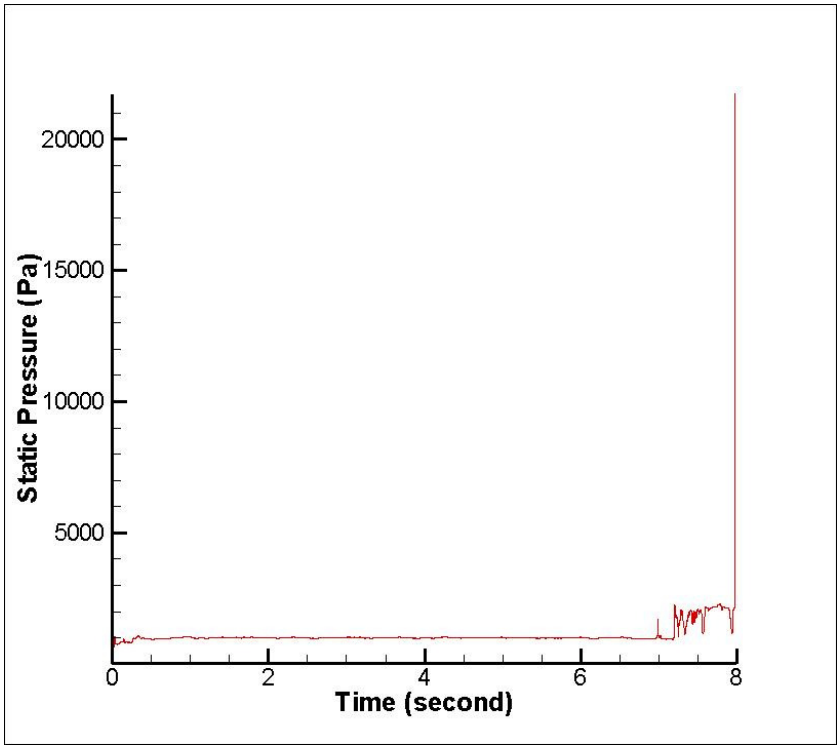

Figure 3-27. Static pressure change in the tank dome during the refueling process for case 5

Fuel volume fraction after the five bends in the fill pipe is seen in figure 3-28. After bend 1, fill pipe is fully covered with gasoline at time 7.75 second and after bend 2 the flow is in the left part of the fill pipe there is some part of air in the right side of the fill pipe. Gasoline is always in the lower part of the fill pipes after bend 2, bend 3, bend 4, and bend 5. After bend 3 a small gasoline droplet is seen in the vent pipe, it is not a suprising event because it is known that the gasoline flow through the vent pipe has already started at 7.21 second. It is seen that air and fuel flow separately in the fill pipe just like the case 4. However in case 2 fuel is sticked to the wall of the fill pipe and air is flowing inner core of the fill pipe, it is seen in case 5 that air and fuel is flowing separately.

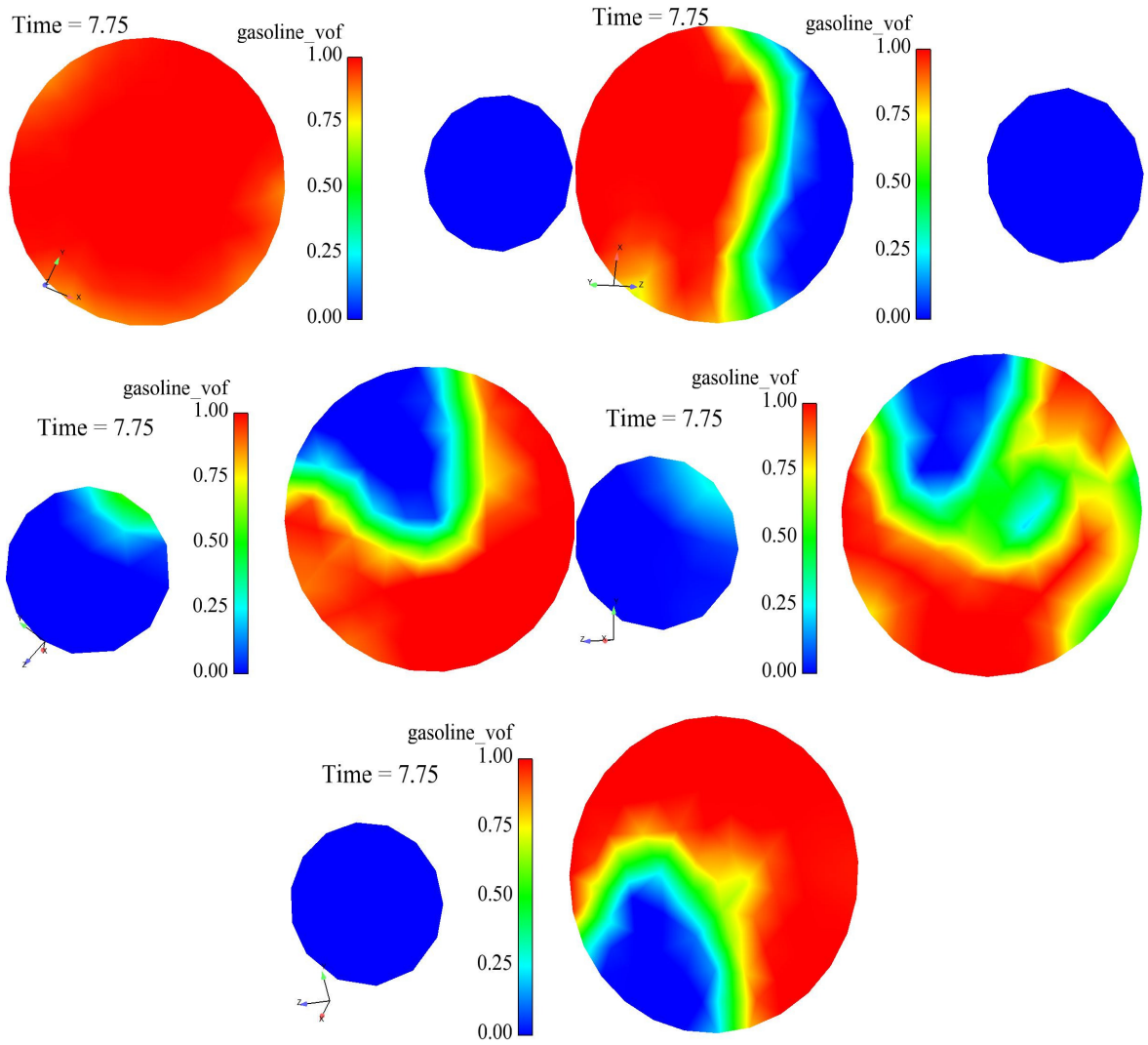

Figure 3-28. Fuel volume fractions at second 7.75 at fill and vent pipes (a) after bend 1 (b) after bend 2 (c) after bend 3 (d) after bend 4 (e) after bend 5 for case 5

Velocity magnitude contours which are plotted at the end of the refueling the tank at time 7.75 are shown in figure 3-29. When we compare the gasoline volume and velocity magnitude graphs it is obvious that in the fill pipe after all bends gasoline has more speed than air. Near the wall boundary there are zero velocity. At vent pipes velocity magnitude values seemed to be near zero value, it means that air flow in the vent pipe is nearly stopped because air in the tank dome is nearly finished and this small amount of air was being vented through pressure outlet 2.

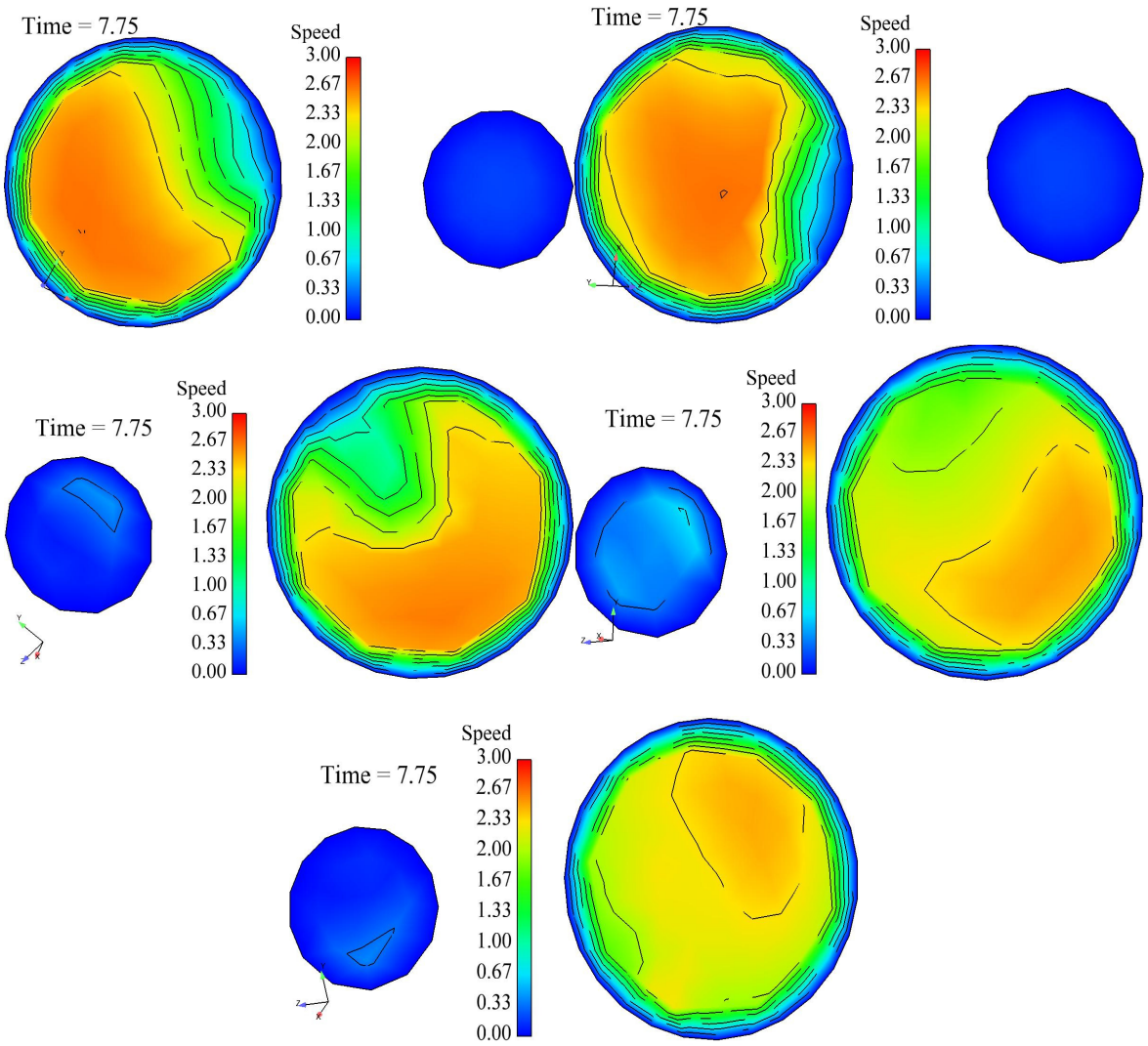

Figure 3-29. Velocity magnitude contours in different cross sections throughout the fill pipe and vent pipe at second 8.15 for case 5

Case 8 was tried but the simulation is aborted before the tank is filled with gasoline. As it can be seen in Figure 3-30, after a little time the case was started, fuel started to flow backwards to the pressure outlet 1. This is occurred because of the low velocity conditions in the different nozzle angle could not compensate the pressure difference with atmosphere to start to flow into the tank dome and the flow started to flow backwards. This kind of situations in real refueling processes is an undesirable condition and leads to premature fuel nozzle shut-off.

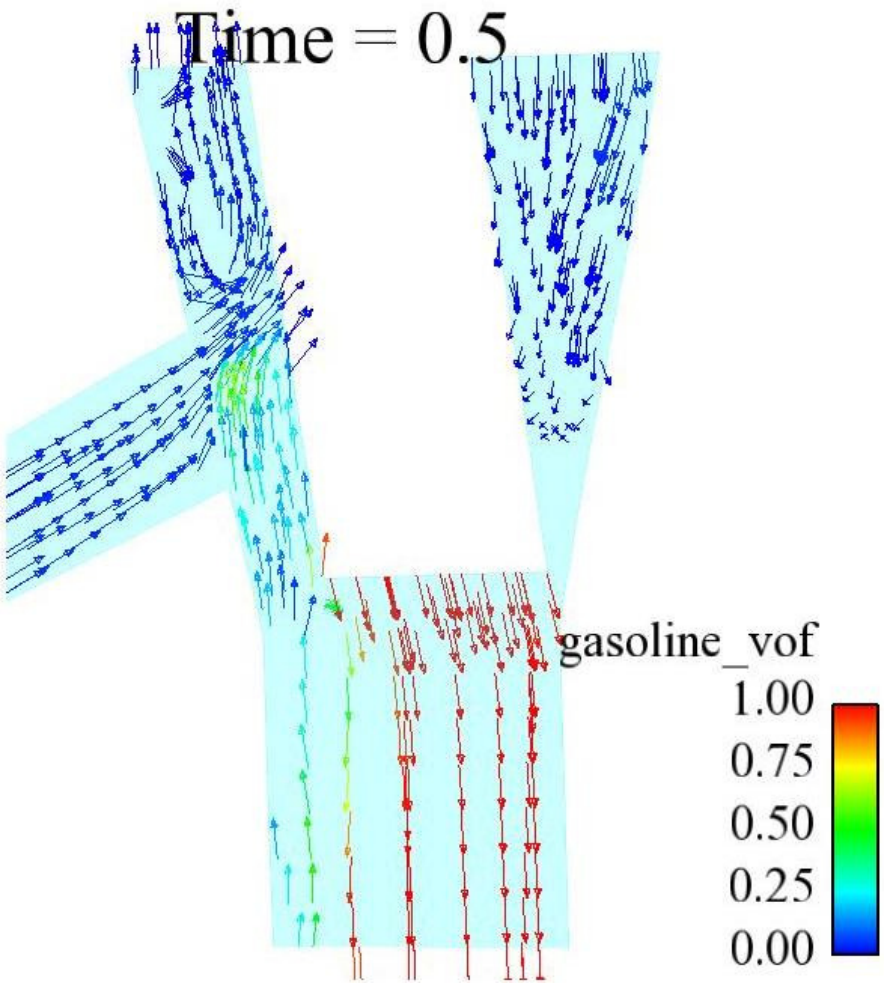

Figure 3-30. Velocity vectors near the nozzle at time 0.5 for case 8

3.8. Effect of Wall Boundary Condition at Pressure Outlet 2

Case 22 which has a wall boundary condition at pressure outlet 2 is explained in this section. For this case, the same mesh and model with case 2 were used except wall boundary condition is applied instead of a pressure condition at pressure outlet 2. The results were interesting, for different flow rates as 60 liters/min and 90 liters/min flow calculation diverged because of the continuity equation and the simulation is aborted before the tank is filled with gasoline. For these cases the static pressure values were quite high as can be seen in figure 3-31. However in 30 liters/min nozzle flow the refueling was done successfully and filled up with gasoline. At high flow rates such as 60 liters/min and

90 liters/min pressure in the tank dome increases and this high pressure does not let the gasoline to flow into the fill pipe and forces the flow to the upper part of the nozzle to the atmosphere. But in lower flow rates such as 30 liters/min, the total pressure rise in the tank dome is not as much as with the higher flow rates and the refueling is done successfully.

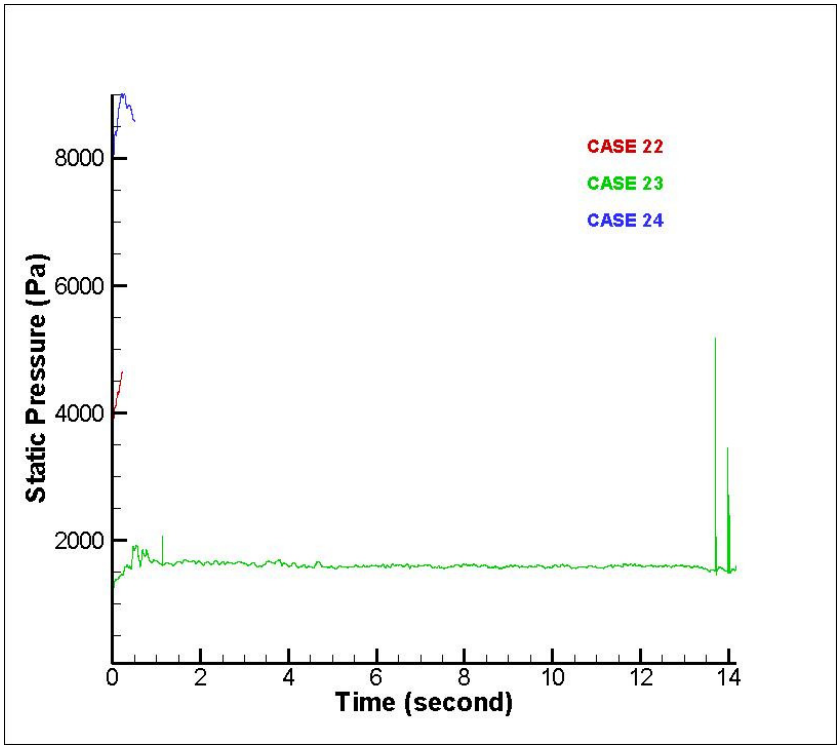

Figure 3-31. Static pressure change in the tank dome for case 22, case 23 and case 24

The successful case, case 23 was examined in this section. The complete refueling endured until the time 14.673 seconds, however the first pressure rise to a 5.2 kPa value happened at time 13.712 second which is assumed as nozzle shut-off time. Results are discussed with case 2 at specific times when the three quarters of the tank was full with gasoline (6 liters). At time 12.625 there was 6 liters of gasoline in the tank dome for case 2 and at time 12.88 there was also 6 liters of gasoline in the tank dome for case 23. In figure 3-32 fuel volume fraction of these cases are shown. Fuel level in the tank dome is the same however flow near the tank dome entrance in the fill pipe is completely different. Small air bubbles are seen at time 12.625 for case 2, in case 23 at time 12.88 large slugs of air are seen and they are separated from each other.

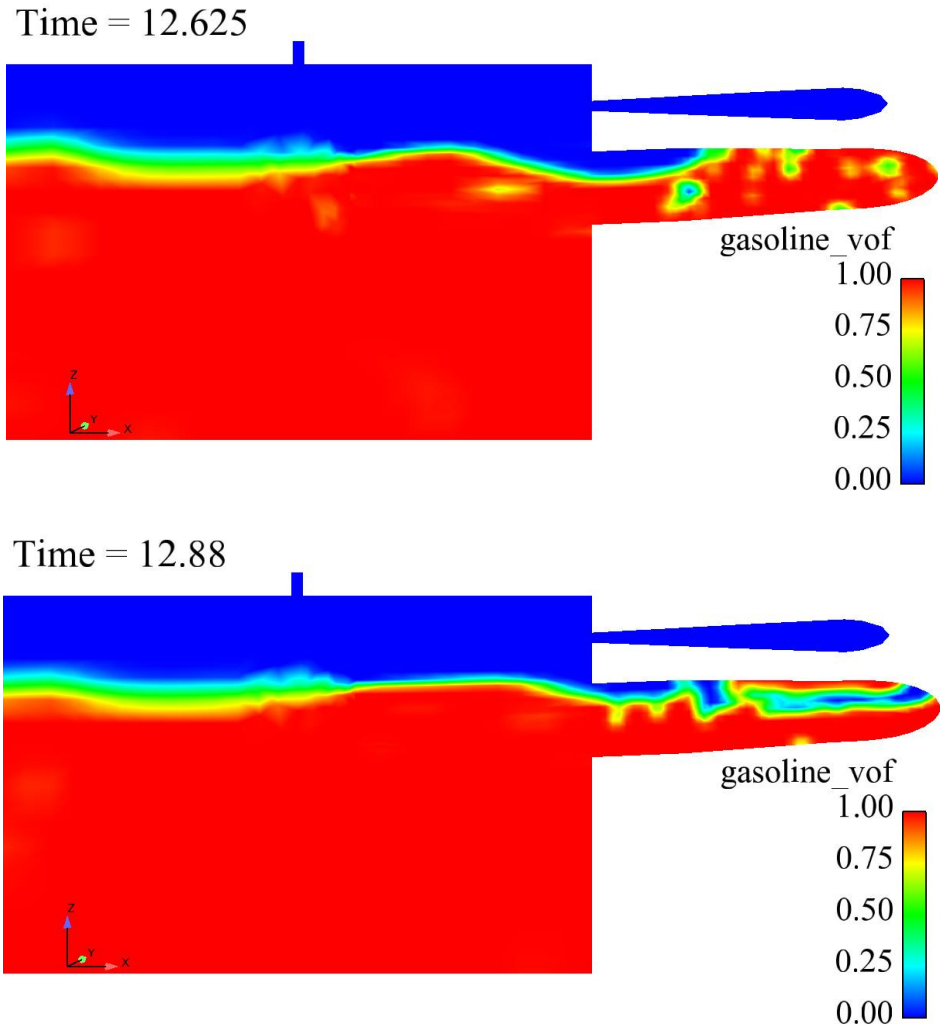

Figure 3-32. Fuel volume fraction on a cross-section in the tank dome at different times for case 2 and case 23

Velocity magnitude contours after different bends for case 2 and case 23 at the same times with the previous figure shown in figure 3.33. It is seen in figure that gasoline speed in the fill pipe is higher in case 2, on the contrary air speed in the vent pipe is lower in case 2 than case23. Lower velocities in the fill pipe can be explained with the wall boundary at pressure outlet 2 for case 23 which increased the tank dome pressure and also made resistance to flow inside the fill pipe. For the vent pipe, air speed is higher because there is only one discharge for the air inside the tank dome. Wall boundary at pressure outlet 2 is closed and it canalizes all of the air to the vent pipe.

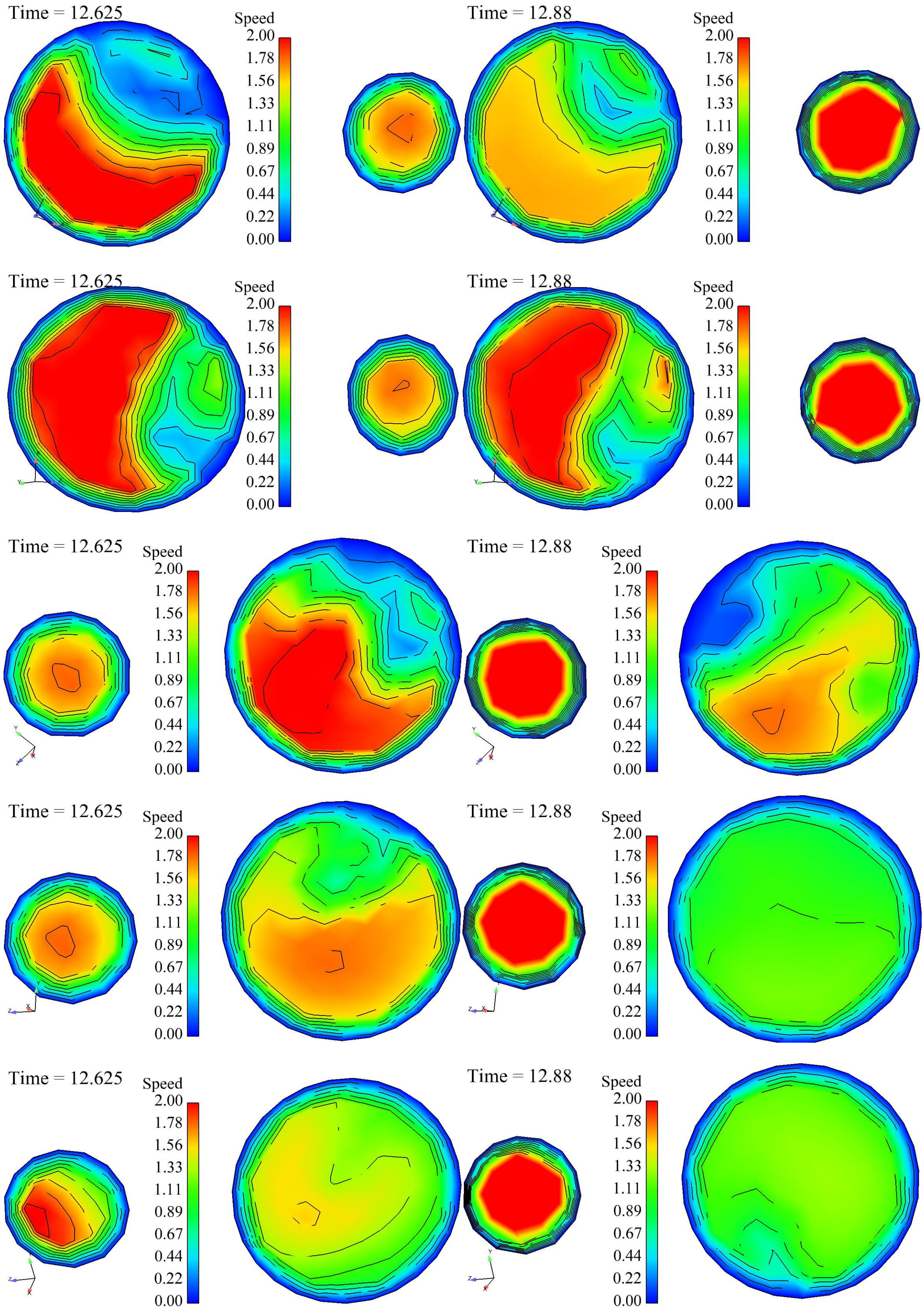

Figure 3-33. Velocity magnitude contours after bend 1,bend 2, bend 3, bend 4 and bend 5 for case 2(left) and case 23(right)

When we compare the tank dome pressures during the refueling of case 2 and case 23 because of the wall not letting the air to flow out from the tank into the atmosphere, case 23 has much higher pressure values, approximately four times of the pressure that we obtained in case 2. For case 23, the first pressure rise in the tank dome is more recognizable at time 0.473 seconds to a value 1.9 kPa, in case 2 there is not as significant pressure rise at the start of the refueling. Additionally, nozzle shut-off happens before in case 23 at time 13.712 seconds however in case 2 nozzle shut-off happened at time 15.96 seconds.

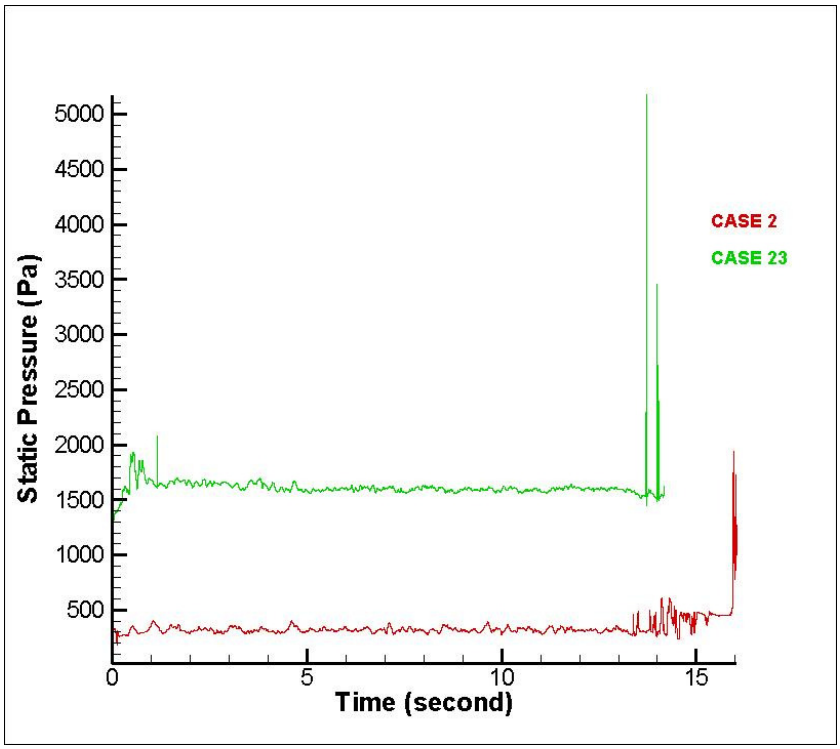

Figure 3-34. Static Pressure Change in the tank dome for case 2 and case 23

3.9. Effect of the Filler Pipe Geometry

In this section, another fill pipe is examined which has the same radius through its longitude, however there is a radius reduction zone in the fill pipe which is encountered in most of the automotive fill pipe applications. For that reason, case 11 is tried and fill pipe is modified and a radius reduction is added on the fill pipe as shown in the figure 3-35 below.

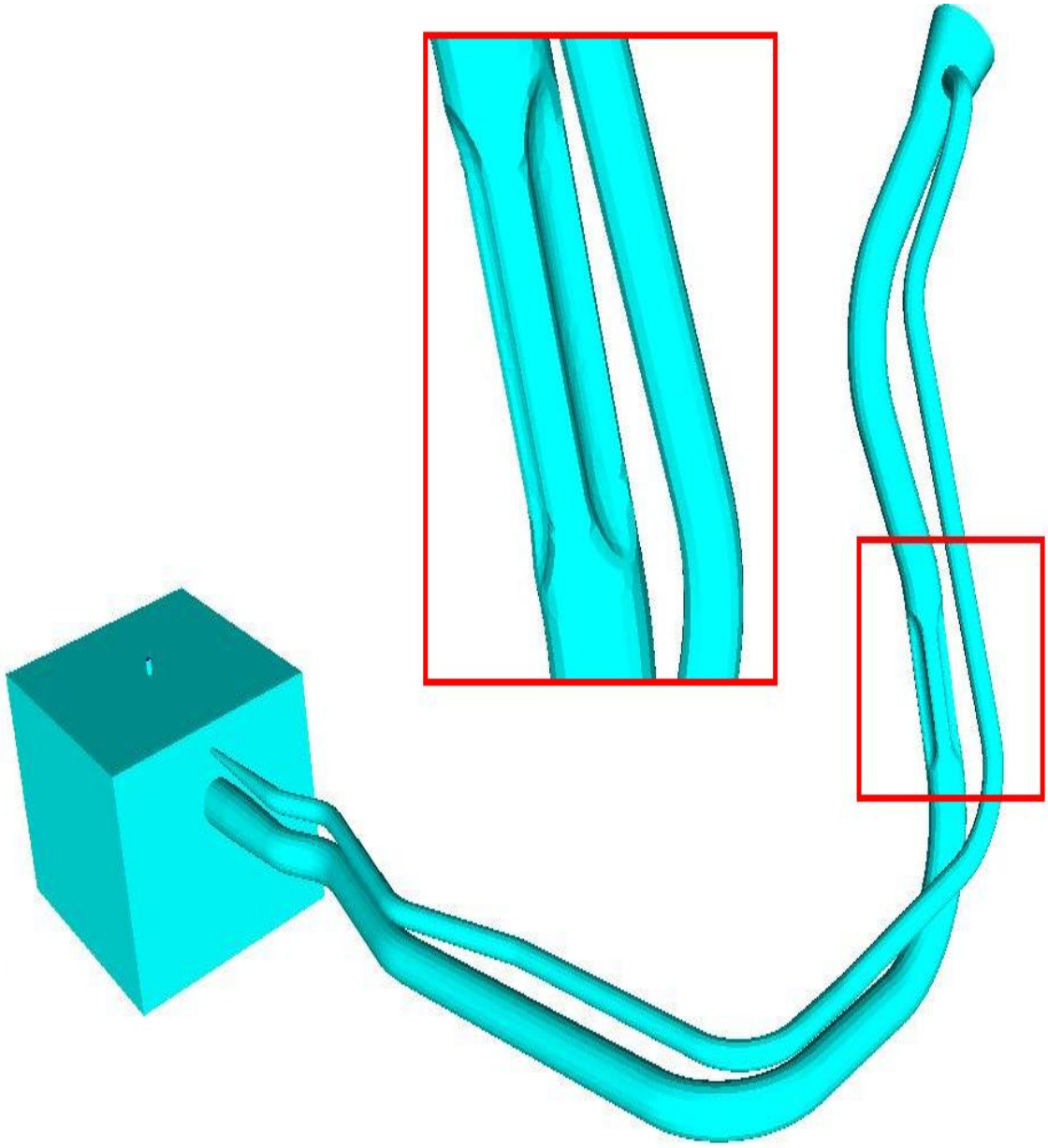

Figure 3-35. Different fill pipe geometry for case 11

It is shown in figure 3-36 below that static pressure in the tank dome is not different significantly for case 11 from the base case. For that reason, it can be said that radius reduction does not have a significant effect on the tank dome static pressure.

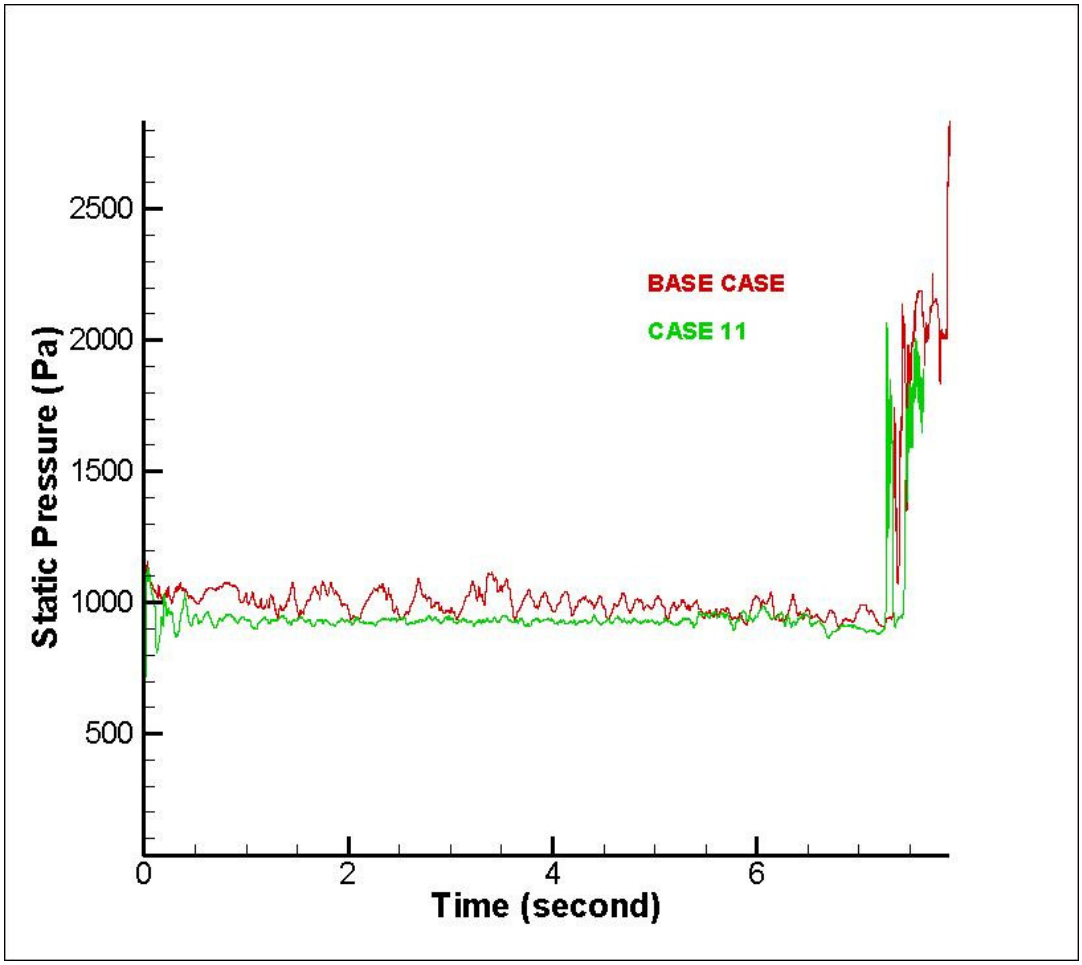

Figure 3-36. Static pressure change in the tank dome for the base case and case 11.

To understand what happens in this radius reduction zone fuel volume fractions at a cross section monitored are shown in figure 3-37 at different times. There is air gap at the center of this radius reduction zone at all times and gasoline coverage does not change significantly. It is also observed that the air at the center of the pipe has higher velocity than gasoline. Velocity magnitude contour plots are shown in figure 3-38 for the base case and case 11. For both cases at after bend 1 velocity magnitude is nearly the same for air and gasoline however after bend 2 it is obvious that velocity magnitude increased for case 11. As we know radius reduction zone is between bend 1 and bend 2, the rise of the velocity magnitude after bend 1 in figure 3-38 is the result of the tightened flow in the radius reduction zone.

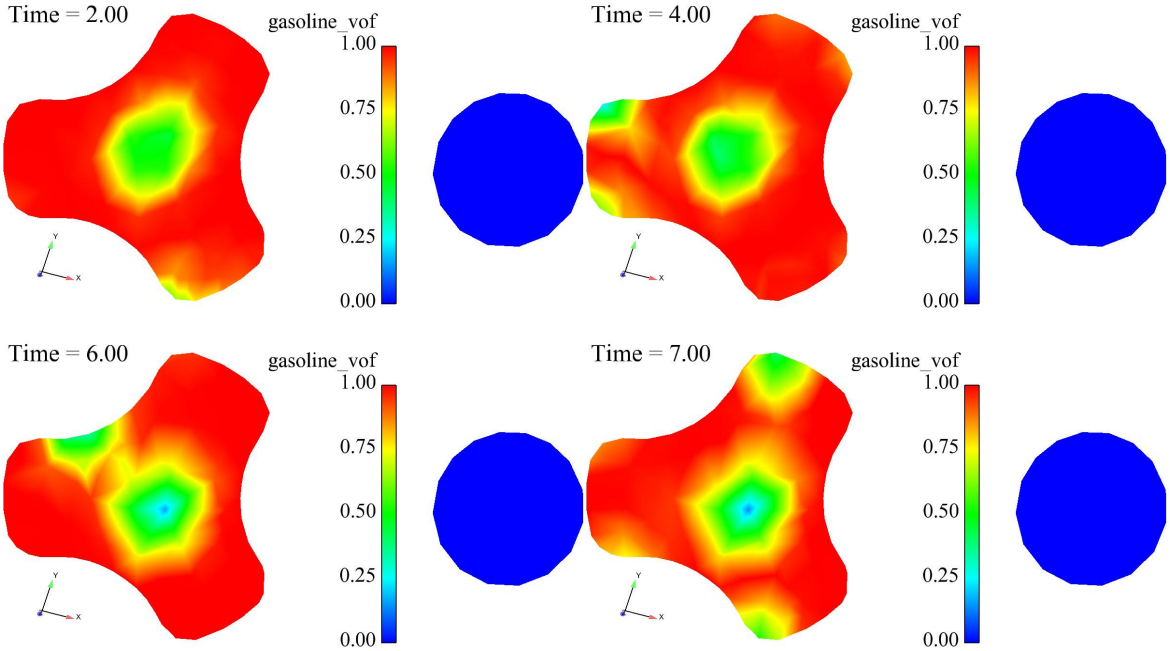

Figure 3-37. Gasoline volume fraction in the radius reduction zone at different times

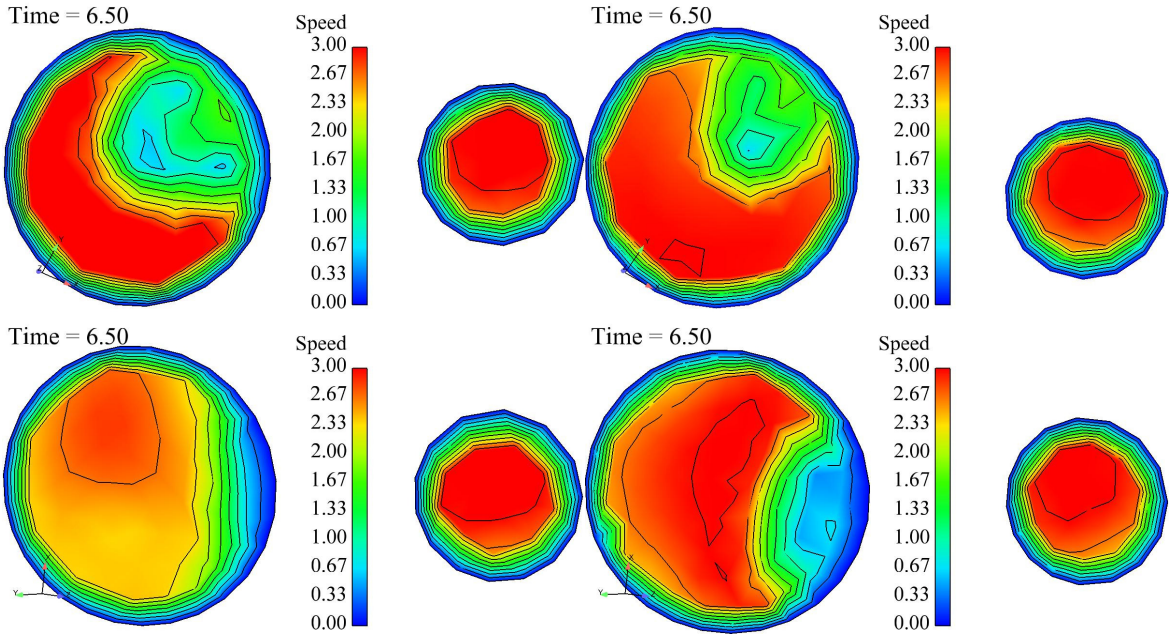

Figure 3-38. Velocity magnitude contours after bend 1 and bend 2 for the base case (left) and for case 11 (right)

4. CONCLUSIONS AND FUTURE WORK

In this study, automotive fuel tank refueling process is modeled and simulated by using abilities of numerical finite volume program FLUENT. In this model; continuity, momentum, turbulence and volume fraction equations are solved.

Static, dynamic pressures in the tank, gasoline volume fractions at different cross-sections of the pipes, mass flow rates of air from the rollover valve and upper part of the fill neck to the atmosphere is observed and monitored to understand the flow in the tank system in detail. Pressure time graph, which is obtained from the past numerical works and experimental results, is seen in all of the cases as a pressure rise at the start of the refueling which then gets a stable character and a pressure peak near the end of the refueling. Nozzle shut of time is assumed with that pressure peak near the end of the refueling process. In such cases with high flow rates when the rollover valve is closed or the fuel dispensing nozzle is in different axial direction premature nozzle shut off happened.

High inlet fuel flow rate of the nozzle increased the tank pressure and air entrainment values in the vent pipe. It is also seen in the results that high fuel flow rate caused more air to vent out from the system. As a volume of fuel starts to flow in the fill pipe, same volume of air is flowing out from the system through the rollover valve and the filler neck. It is also seen that pressure constraints at the top of the tank and the filer neck change the air venting way. When there is a higher pressure value specified at the rollover valve, more air tends to vent out through the filler neck. On the contrary, if there is a pressure boundary defined at the filler pipe neck, more air flows out from the system through the rollover valve. Interesting results are also obtained when the total vent area of the system is reduced by applying a wall boundary condition to the rollover valve and the filler neck. The total pressure in the tank increased to four fold of the base case when the total vent area is reduced to the half of the base case.

Besides, it is seen that in low fuel ratio flows nozzle shut off occurs late however there is less amount of gasoline in the tank dome with respect to the base case when the nozzle shut itself off.

When the nozzle is positioned such that the flow of gasoline hits the filler pipe wall in the filler pipe entrance, it does not significantly alter the tank pressure and the entrainment values. It is seen that in lower flow rates with this nozzle position, gasoline hits the wall after flowing out from the nozzle and volume flow rate can not provide the necessary pressure for gasoline to reach into the tank dome and gasoline starts to flow upwards. Therefore premature nozzle shut-off is seen.

Different fill pipe geometry which has a radius reduction in the fill pipe is also investigated and the effect of this radius reduction is discussed. There is not a significant pressure change in the tank dome, conversely velocities in the fill pipe changed because of the diameter change in the path of the flow.

For future work, this numerical model can be tested with different pipe geometries. Tank volume and tank shape can be made to match the ones used in automotive industry. Rollover valve is modeled here as a pressure boundary condition, more realistic rollover valve model can be generated.

5. APPENDIX A: MESH INDEPENDENCY

Throughout the thesis pressure results were plotted at different places. For that reason a pressure independecy check should be done. Firstly, geometry was meshed with 44782 hexahedral grid elements. In the filler pipe, interval size of hexahedral elements were 4 mm, for the vent pipe interval size of hexahedral elements were 3 mm and in the tank dome it was 15 mm. Total number of 44782 hexahedral elements were used in the whole tank system and 33722 number of them were used in the filler pipe and vent pipe, 11060 number of them were used in the tank dome. After that meshing dependency was checked with 155808 hexahedral grid elements. In that mesh filler pipe has an interval size of 2.8 mm and the vent pipe has 1.8 mm of interval size for the hexahedral meshes. In the tank dome the interval size was 9 mm. For the tank dome 45705 number of hexahedral elements were used and 110103 number of them were used in the pipes. When we check the results of these two different meshes, it is seen that the results are completely different. It is also shown in figure A-1, which is a graph of static pressure change in the tank dome for different cases.

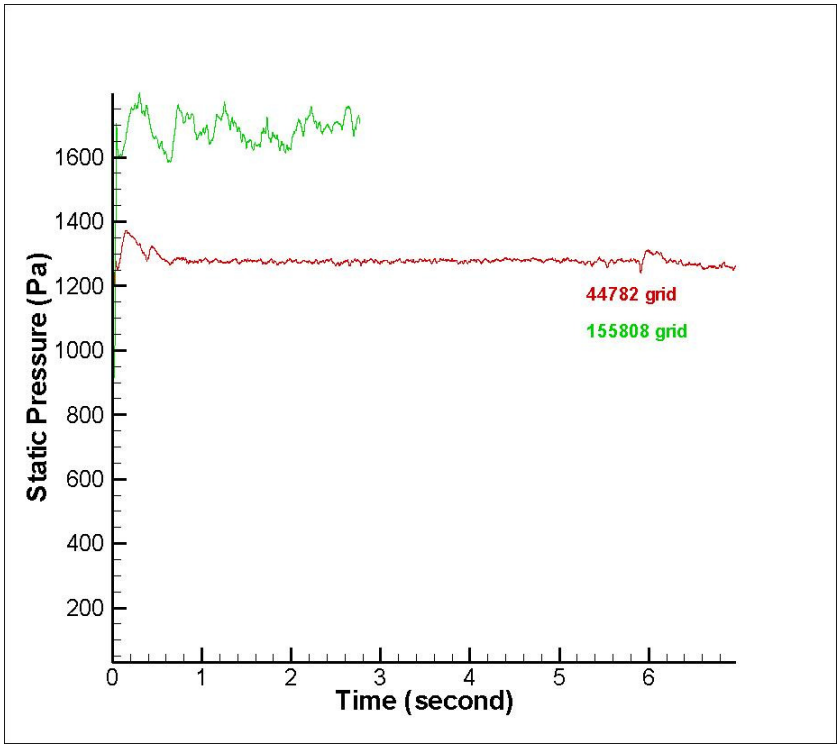

Figure A-1. Static pressure change in the tank dome for different cases

After that total mesh number increased to 233599 hexahedral elements which has 2.5 mm interval size in the fill pipe, 1.5 mm interval size in the vent pipe and 8 mm interval size in the tank dome. Unfortunately, this was also an unsuccessful effort. In figure A-2, the results for the static pressure in the tank dome with different number of grid elements are plotted. Although 233599 mesh number is a very high value for this size of geomety, the results are completely different and the problem should be somewhere else rather than the mesh size.

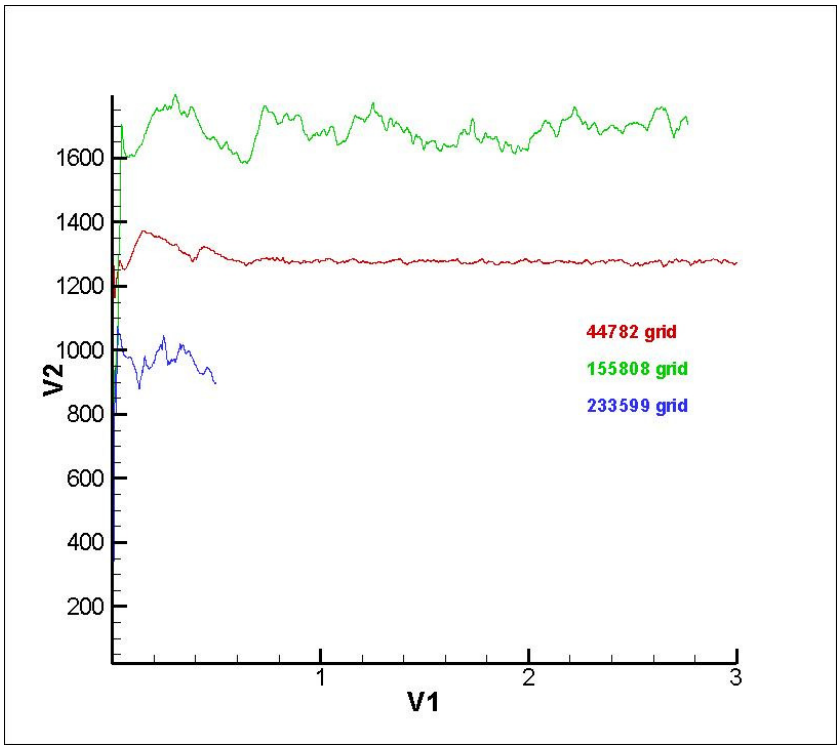

Figure A-2. Static pressure change in the tank dome with different mesh size

After these tries, mesh type was changed from hexahedral to tetrahedral mesh which is seen in figure A-3 in detail. Actually tetrahedral meshes have inherently larger truncation error than hexahedral meshes which are aligned with the flow direction, however for complex flows without dominant flow direction hexahedral meshes loose their advantage over tetrahedral meshes. For that reason, geometray was meshed with all tetrahedral meshes. In the filler pipe and vent pipe interval size of tetrahedral elements were 3 mm and in the tank dome it was 10 mm. Total number of 118784 number of

tetrahedral elements were used in the whole tank system 85395 number of them were used in the filler pipe and vent pipe, 33389 number of them were used in the tank dome.

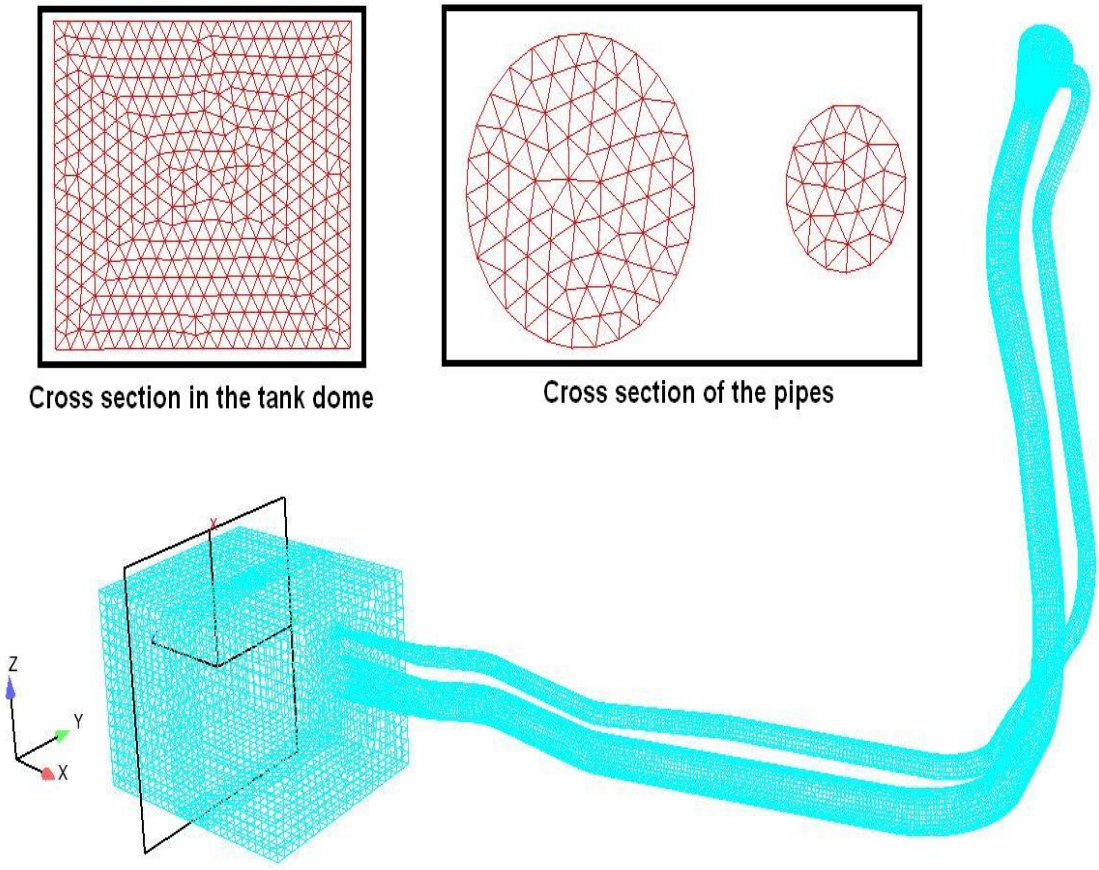

Figure A-3. Mesh of the base case

This geometry which has 118784 grid elements was checked with another meshed geometry (case 15), which has total number of 146970 tetrahedral grid elements. Firstly, static pressure in the tank dome was checked for these two cases and shown in figure A-4. The results were calculated at nine different points and average of them were plotted in the figure below. It is seen that static pressure and the total pressure in the tank dome has very similar values for both of these cases.

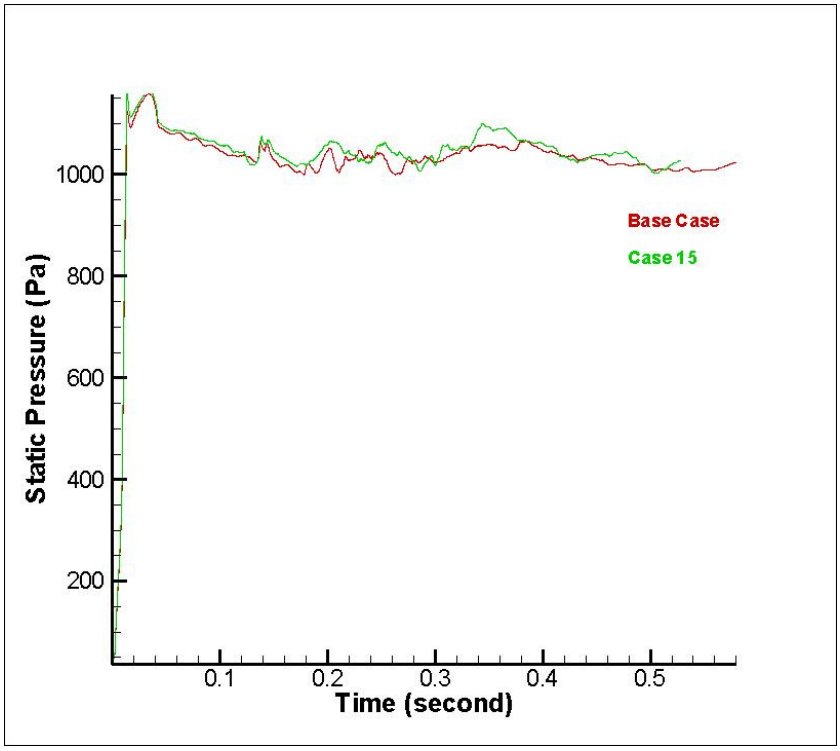

Figure A-4. Static Pressure in the tank dome for case 1 and case 15

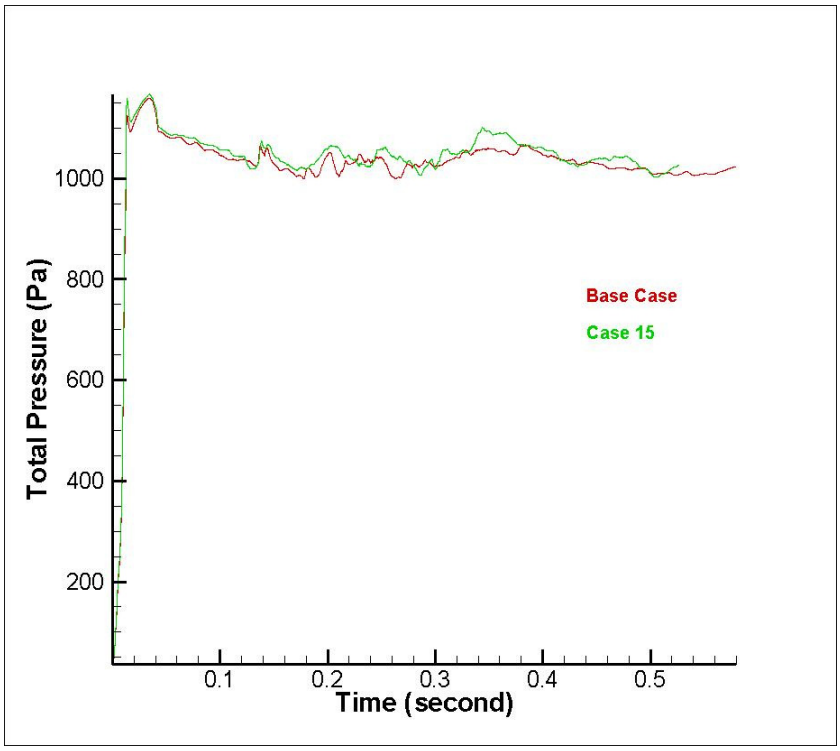

Figure A-5. Total Pressure in the tank dome for the base case and case 15

Furthermore, dynamic pressure values are compared at point fill 1 and fill 4 in figure A-6 and A-7. There is not a significant difference in these pictures. Hence, dynamic

pressure values are also passed the meshing dependency check. For that reason, it can be said that mesh independency is also satisfied for the pressure values.

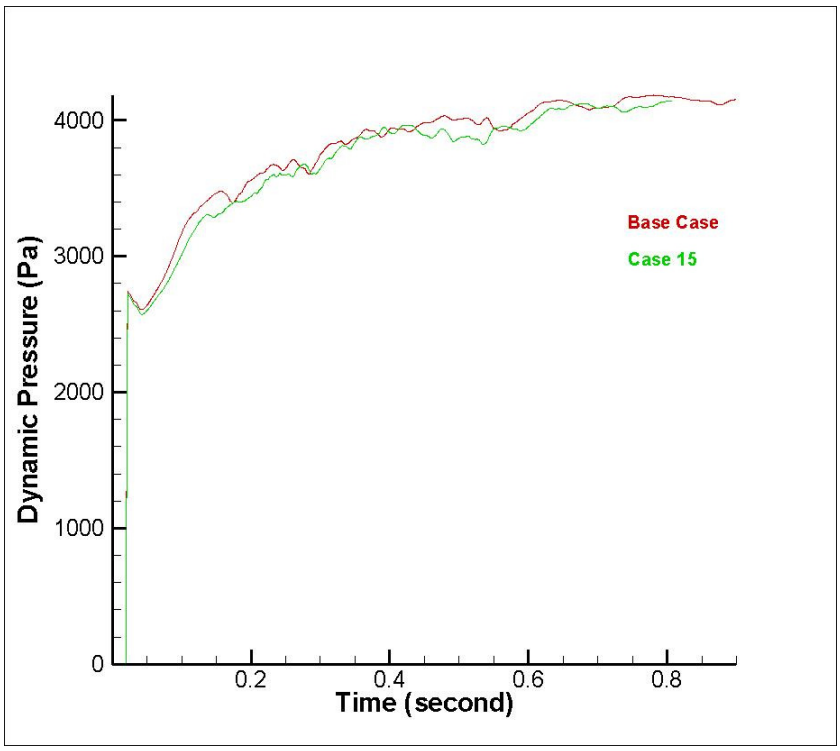

Figure A-6. Dynamic pressure versus time graph at point fill 1

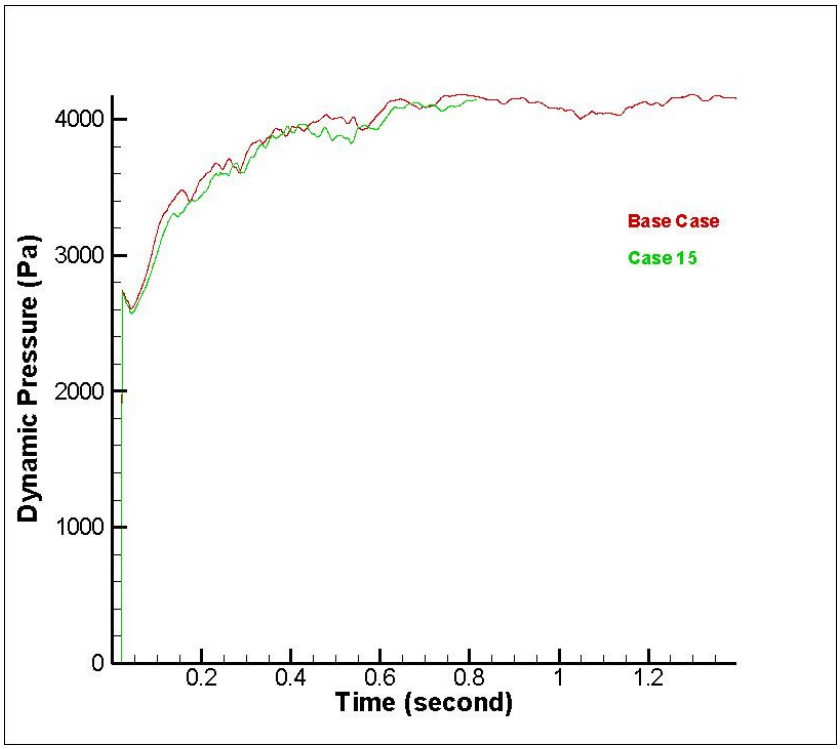

Figure A-7. Dynamic pressure versus time graph at point fill 4

After the pressure validation, gasoline volume fraction in the tank dome was checked with this case and as seen in the figure below, there is not an important difference between these two gasoline volume fractions in the tank dome.

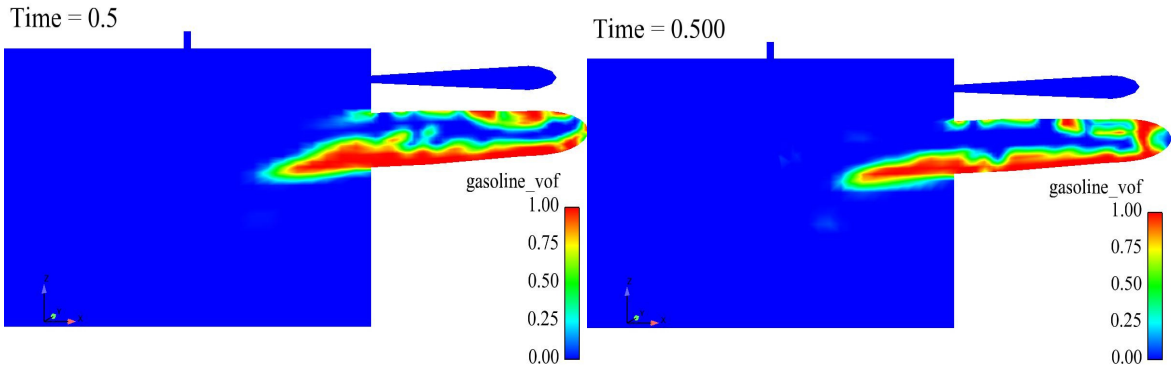

Figure A-8. Gasoline volume fraction for base case and case 15 at time 0.5 seconds

Gasoline volume fractions after different bends was checked for both of these cases. In figure A-9 gasoline volume fractions are near the same for the base case and case 15. There are more gasoline sticked to the wall for the case 15 at the right side of the figure A-9. This difference is only in shape. This time in figure A-10, gasoline volume fractions are totally the same in shape. When we look at in figure A-11, it is seen that there is an air core in the fill pipe in both of the cases. In figure A-12, it is seen that both of the pictures are totally the same. For that reason, it is showed that the grid for the base case is meshing independent for the volume fractions.

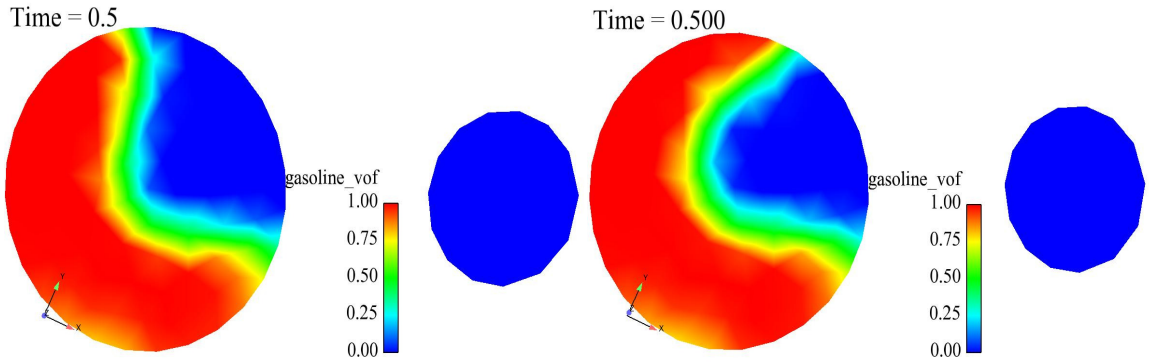

Figure A-9. Gasoline volume fractions after bend 1 at time 0.5 seconds

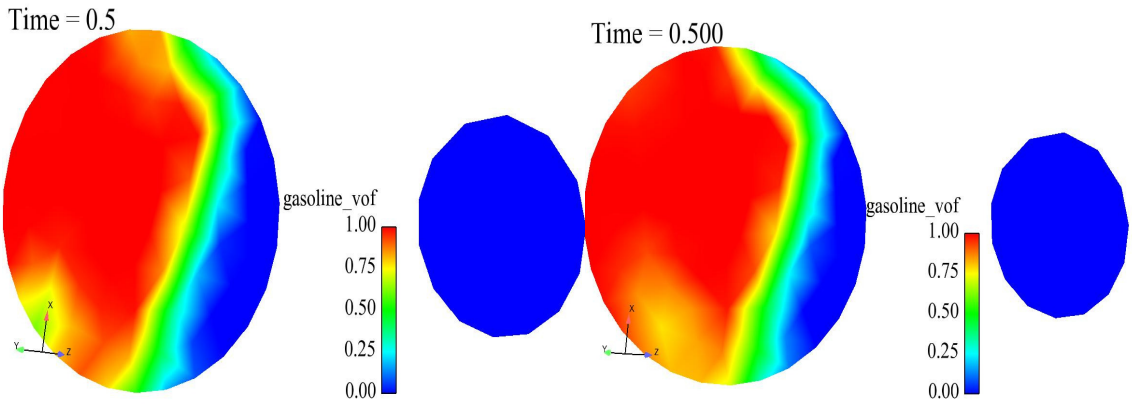

Figure A-10. Gasoline volume fractions after bend 2 at time 0.5 seconds

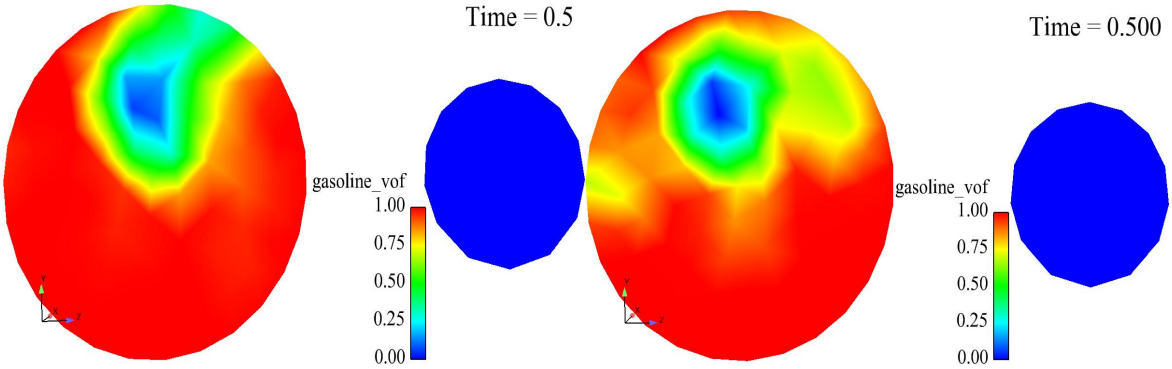

Figure A-11. Gasoline volume fractions after bend 4 at time 0.5 seconds

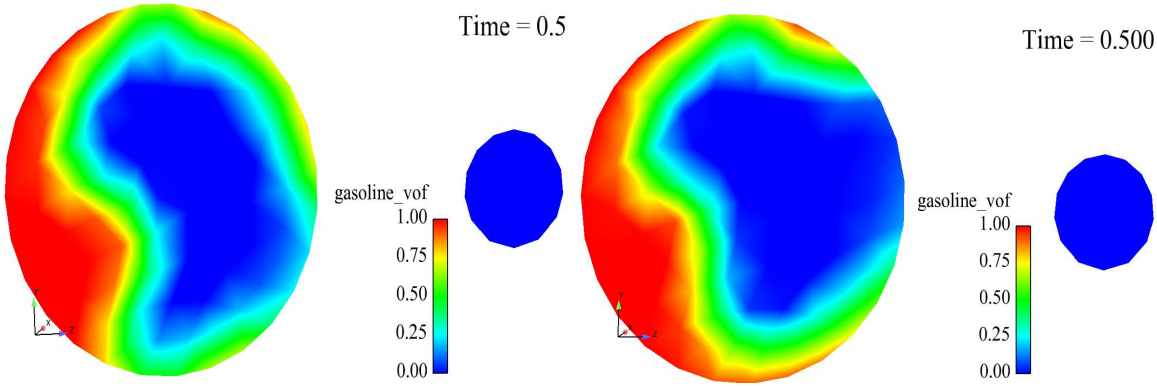

Figure A-12. Gasoline volume fractions after bend 5 at time 0.5 seconds

6. REFERENCES

1. Stoneman, S., 1997, "On the design of automotive fuel filler pipes", *Automotive Engineering,* Vol. 22, pp. 32–36, EBSCO publishing.

2. Sinha, N., R. Thompson, M. Harrigan, 1998, *Computational simulation of fuel shut-off during refueling*, SAE Technical Paper 981377, Michigan.

3. Mastroianni, M., 2000, *Experimental Investigation of Automotive Fuel Tank Filling*, M. S. Thesis, University of Windsor, Canada.

4. Banerjee, R., K. M. Isaac, L. Oliver and W. Breig, "A numerical study of automotive gas tank filler pipe two phase flow", *SAE Technical Paper*, 2001–01–0732.

5. Banerjee, R., X. Bai, D. Pugh, K. M. Isaac, D. Klein, J. Edson, W. Breig and L. Oliver, "CFD Simulations of critical components in fuel filling systems", *SAE Technical Paper*, 2002–01–0573.

6. Banerjee, R., K. M. Isaac, L. Oliver and W. Breig, "Features of automotive gas tank filler pipe two phase flow: experiments and CFD simulations", *ASME J. Gas Turbine Power*, Vol. 124, pp. 412–420, Missouri, 2002.

7. Fackrell, S., M. Mastroianni and G. W. Rankin, *Model of the Filling of an Automotive Fuel Tank*, Ontario, 2003.

8. Wiesche, S., "Simulation of automotive fuel tank filler pipe flows", *Computational Mechanics*, Vol. 30, pp. 139–149, 2004.

9. Ding, P. and A. J. Buifk, *Simulation of Fuel Tank Filling using a Multi-material Euler Solver with Multiple Adaptive Domains,* MSC Software Corporation, 2005.

10. Allan, G. Z., *A Hybrid Numerical Study of Automotive Fuel Tank Filling*, M.S. Thesis, University of Windsor, 2002.

11. Banerjee, R., 2001, *CFD Analyses of two-phase flow with vapor emission for automotive refueling system*, Ph.D. Dissertation, Missouri.

12. *FLUENT 5 User's Guide*, Vol. 1-5, Fluent Inc, 1998.

13. Peric, M., *Computational Methods for Fluid Dynamics*, 2002, 3rd edition, Springer, Berlin, 2002.